Cosimulation of Linear Feedback Postural Sway Model to Explore the Effects of Parkinson's Disease

By

Corbin N. Reagan

Submitted to the graduate degree program in Bioengineering and the Graduate Faculty of the University of Kansas in partial fulfillment of the requirements for the degree of Master of Science.

_____

Chairperson Carl Luchies Ph.D.

_____

Sara Wilson Ph.D.

_____

Terry Faddis D.E.

Date Defended: _____

The Thesis Committee for Corbin N. Reagan

certifies that this is the approved version of the following thesis:

Cosimulation of Linear Feedback Postural Sway Model to Explore the Effects of Parkinson's Disease

_____

Chairperson Carl Luchies Ph.D.

Date approved: _____

Abstract

The focus of this study was to design and develop a postural sway model using cosimulation of ADAMS dynamic modelling software and Simulink as the control system. This model could then be used to study the biomechanics and neuromuscular control of the system through physiological input parameters (controller gains, neuromuscular noise, and feedback time delay) and center of pressure (COP) output parameters. In the first study, we showed the characteristics of the model input parameters and their effect on the model robustness and COP output measures. Finally, we were able to develop a set of input model parameters that validated the model COP measures with experimental COP measures observed in healthy control (HC) subjects during eyes closed stance.

In the second study, the validated HC parameters were used as a baseline for investigation of the effects of the changes of the input model parameters on the model COP measures when related to the experimental COP measures of a HC group and Parkinson's disease (PD) group. This study showed that when the feedback time delay and proportional gain were independently studied and manipulated from the HC base set, no changes in the model COP measures could be related exclusively to either group. When investigating the neuromuscular noise and derivative gain parameters, varying these parameters caused changes in output COP measures that specifically related to PD and HC groups.

This study has shown the possibility of reverse engineering biomechanics measures back to the control system. This allows for more complex models to be investigated and further studies to be carried out on subjects with injury, who are aging, or possess a neurological disease.

Acknowledgements

I would like to thank my advisor and mentor Dr. Carl Luchies for giving me the opportunity to work in the University of Kansas Biodynamics Lab. I will forever be grateful for the opportunity to learn from him how to be an effective learner, teacher, and researcher. Most importantly he has provided support every step of the way in this process. I would like to give thanks to my colleague and friend Annaria Barnds, who has provided me with unmatched support and advice throughout my time at the University of Kansas.

Thank you to my committee members Dr. Sara Wilson and Dr. Terry Faddis for providing guidance throughout this project. I would also like to thank Dr. Paul Cheney for his knowledge and support for this project. Thank you to Sommer Amundsen and Josh Harper for helping and assisting with testing and development.

I would like to finally thank my wonderful wife Erin Reagan, who has been patient with me throughout this process and pushed me to the end. Without your love and support I would not have been able to reach this goal. I would like to give a final thanks to my family and friends for their support and love for me over the years.

TABLE OF CONTENTS

LIST OF FIGURES

LIST OF TABLES

Chapter 1 : Introduction

Background and Motivation

Parkinson's disease (PD) is a neurodegenerative disease with no known cause, that affects over 5 million people worldwide and is the second most common neurodegenerative disease in the world (Dauer & Przedborski, 2003). Pathologically, PD is the death of dopamine-generating cells in the substantia nigra pars compacta. The cause of dopamine-generating cell death is unknown. Dopamine degeneration results in changes in the basal ganglia function and adverse changes to the motor cortex (Centonze, Calabresi, Giacomini, & Bernardi, 1999). These changes cause symptoms such as bradykinseia (slowed movements), rigidity, tremors, and postural instability. Several treatments (e.g. pharmaceutical, surgical, physical therapy) provide relief from these symptoms; however, postural instability has proven to be resistant to the available pharmaceutical treatments. The increased presence of postural instability corresponding to disease progression is a primary cause of falling, fractures, and nursing home placement. Postural instability results in a significant reduction in quality of life. A better understanding of postural instability is needed in order to understand the underlying biological effects of PD.

Modeling human postural sway as a single inverted pendulum with a linear feedback controller has gained popularity with the goal of understanding the control strategies for maintaining upright stance (Masani, Vette, Abe, & Nakazawa, 2014; Maurer & Peterka, 2005). The inverted pendulum model allows for the direct comparison of model data with experimental data acquired in human subject testing of postural sway. For example, the center of pressure (COP) time series can be calculated from the foot-floor reaction forces and moments measured using a force plate during quiet standing. A similar COP time series can be calculated based on

model predictions of the ankle torque required to maintain an upright configuration of the inverted pendulum with the assumption of a stationary foot. Using both the experimental and model data provides an opportunity to improve understanding of the control strategy being used by the central nervous system to maintain upright stance. These models have previously been used to investigate COP patterns of healthy control (HC) subjects (Maurer & Peterka, 2005). However, no such studies have been reported which use these models to investigate the adverse effects on the control system resulting from a neurodegenerative disease such as PD.

This thesis has been broken into two studies that can be found in Chapter 3 and Chapter 4. The objective of the overall study is to develop a postural sway model that provides insight in to the effects of the input parameters on COP output measures relating to human postural sway in HC subjects, as well as in the presence of neurological diseases such as PD.

The objective of the first study is to design, develop, and validate a linear feedback control model used to simulate the active neuromuscular control system which maintains stable balance during quiet standing in humans. The control parameters are tuned to represent the COP data from HC adult subjects during eyes close postural sway. The model is analyzed in order to understand the effects of the input parameters on the output COP measures. Comparison methods are used to validate the model simulation with HC adults during eyes closed stance.

In the second study, the model is related to COP data from a group of patients diagnosed with idiopathic PD and a group of age range matched HC. Information from the second study is used to understand how changes in the parameters will affect the output COP measures that relate to PD. The goal is to use the control parameter changes related to PD to provide insights into the effects that PD has on the neuromuscular control system. This knowledge could provide

the potential for a better understanding of the effects of PD on motor control, the development of improved clinical tools to track the disease progression, and the development of improved treatment strategies.

Specific Aims

The goals of this study requires for the model to first be implemented and validated for HC subjects. The human body is modeled as a single link inverted pendulum with a revolute joint at the ankle, that is balanced upright using a proportional-derivative controller regulating the ankle torque (Masani et al., 2014; Maurer & Peterka, 2005). The foot is assumed stationary. The model COP time series is calculated using the ankle joint reaction forces and torques. The "healthy" model control parameter set is determined by comparing the model COP time series with the experimentally determined COP time series of a HC group of subjects from a previous biomechanical study of postural sway.

The set of measures used to quantify the COP time series that have been found to be related to the development and progression of PD include: total distance, sway range, peak speed, root mean square, and mean velocity in the anterior-posterior direction. The five parameters in the linear feedback control model used to tune the model to simulate realistic COP movements consist of: the neuromuscular time delay, the neural control time delay, proportional and derivate gain constants, and the low pass filter gain of the noise input to the system as disturbance torque.

Specific Aim 1: Implement and validate a linear feedback control model used to simulate the active neuromuscular control system that maintains stable balance during quiet standing in HC adult humans. The five model parameters are tuned so that the model COP

time series is similar to the average experimental COP time series measured in HC subjects. This model parameter set for the HC group is considered the HC model parameter set. A sensitivity analysis and design of experiments is performed to understand the effects of the model input parameters on the COP output measures. A comparison analysis of the COP output measures was performed to validate a set of input model parameters with experimental COP output measures of HC subjects during eyes closed stance.

Specific Aim 2: Determine the PD model input parameters required so that the model COP time series is similar to the average experimental COP time series measured in a group of subjects diagnosed with PD. This step used the model to investigate the changes in motor control introduced by PD. The PD model parameters are varied so the model COP time series is similar to the average experimental COP time series measured in a group of subjects diagnosed with PD. Differences between the HC and PD model parameter set are then compared to investigate the changes in the neuromuscular control system due to PD.

Thesis Content

This document contains five chapters. Chapter 1 is an introduction of the field of study, significance and specific aims. Chapter 2 contains a background of all relevant information of postural sway studies and modeling of postural sway. Chapter 3 consists of a study on the design and development of a postural sway model that is validated with HC subjects during postural sway. Chapter 4 reports the findings of an initial study on the effects of model changes when the COP measures of the mode are related to HC and PD subjects. Chapter 5 is a summary containing the conclusion and future considerations gathered from this overall study.

References

Centonze, D., Calabresi, P., Giacomini, P., & Bernardi, G. (1999). Neurophysiology of Parkinson's disease: from basic research to clinical correlates. *Clinical Neurophysiology, 110*(12), 2006-2013. doi: 10.1016/s1388-2457(99)00173-x

Dauer, W., & Przedborski, S. (2003). Parkinson's disease: Mechanisms and models. *Neuron, 39*(6), 889-909. doi: 10.1016/s0896-6273(03)00568-3

Masani, K., Vette, A. H., Abe, M. O., & Nakazawa, K. (2014). Center of pressure velocity reflects body acceleration rather than body velocity during quiet standing. *Gait & Posture, 39*(3), 946-952. doi: 10.1016/j.gaitpost.2013.12.008

Maurer, C., & Peterka, R. J. (2005). A new interpretation of spontaneous sway measures based on a simple model of human postural control. *Journal of Neurophysiology, 93*(1), 189-200. doi: 10.1152/jn.00221.2004

Chapter 2 : Background

Parkinson's Disease

Parkinson's disease (PD) is an idiopathic neuromuscular disease with many debilitating symptoms and no known causes. PD affects over 5 million people worldwide and is the second most common neurodegenerative disease in the world (Dauer & Przedborski, 2003). Pathologically, PD is the degeneration of dopamine cells in the substantia nigra pars compacta. As a result, dopamine degeneration causes changes in basal ganglia function. The degeneration of dopamine containing cells causes adverse changes to the motor cortex (Centonze, Calabresi, Giacomini, & Bernardi, 1999). When dopamine cells in the substantia nigra pars compacta are reduced to approximately 50% of healthy individuals, symptoms of PD can be clinically observed (Wichmann & DeLong, 2003). Recent studies have identified multiple genetic causes of PD, and suggest the ability of various biomarkers to improve diagnosis, progression, and treatment advancements in PD (Marek, Jennings, Tamagnan, & Seibyl, 2008).The main motor symptoms characterized by PD are bradykinesia, tremor, and rigidity (Centonze et al., 1999). Currently, there is no cure for PD, however several different treatment methods do exist such as pharmaceutical therapies like Levodopa (Salat & Tolosa, 2013) and more invasive therapies like deep brain stimulation (Plessow, Fischer, Volkmann, & Schubert, 2014). Fall risk is an innate danger of PD developed by the aggressive symptoms of the disorder during the later stages of the disease progression.

Postural Instability

Postural instability causes a fear of falling in patients with PD. Biomechanics studies have looked to quantify the effects of postural instability in order to understand the risk of falling

and the progression of disease states. Patients with PD develop postural instability, which increases their risk of falling. A fall can result in devastating injuries, an increased fear of falling, and potentially shorten the life span of the person if a major injury results. Previous studies have assessed the risk of falling and the progression of PD and aging using biomechanical measures of postural, gait, and step initiation (Hageman, Leibowitz, & Blanke, 1995; McVey et al., 2013; Stylianou, McVey, Lyons, Pahwa, & Luchies, 2011). In particular, biomechanics measures of quiet stance have provided valuable information on postural instability and will be discussed further.

Postural Sway

Biomechanics is a sub discipline of mechanics which analyzes human movement. Movement of humans includes large scale movement tasks such as walking, running, and jumping, as well as minimal movement tasks such as quiet sitting, quiet standing, and fine motor control movements. Previous studies have shown the importance of such minimal movement tasks like postural sway and the potential for precise measurement capabilities of parameters used to quantify the movement that would otherwise go undetected. Biomechanical assessment of postural sway control allows for quantitative measurements of human quiet stance. The postural control system facilitates balance, postural equilibrium, and biomechanical support in order to execute movements. Postural sway requires feedback responses from proprioception, visual, and vestibular sensory mechanisms in order for the central nervous system to control postural sway (Massion, 1998). Balance during postural sway is maintained following internal or external perturbation to the stable systems through integrating sensorimotor process to control the center of mass (COM) of the body (Horak, 2006). Commonly in biomechanics, the foot-floor reactions are measured using force plates and the center of pressure (COP) location as a function

of time is calculated. The COP is the point location of the resultant force at which the plate exerts on the bottom of the feet. The COP can be calculated as follows in the anterior-posterior (AP) and medial-lateral (ML) directions respectively:

$$\boldsymbol{COP_{M/L}} = -\left(\frac{\boldsymbol{M_y + F_x * d_z}}{\boldsymbol{F_z}}\right)$$

$$\boldsymbol{COP_{A/P}} = \left(\frac{\boldsymbol{M_x - F_y * d_z}}{\boldsymbol{F_z}}\right)$$

(Lafond, Duarte, & Prince, 2004; Palmieri, Ingersoll, Stone, & Krause, 2002)

It has been shown that the COP and COM in the AP direction typical stay in phase while the COP moves in front of or behind the COM as the ankle torque is used to decelerate the COM and reverse its direction (David A. Winter, 2009). Because of this, the COP can be considered to control the location of the COM towards stability.

Assessments of Postural Sway

The assessment of postural sway can be broken in to three significant testing areas 1) kinematic motion of body segments, 2) muscle activity analysis, and 3) COP movement (Ruhe, Fejer, & Walker, 2010). The assessment of postural sway is most often done utilizing the measured foot-floor reaction forces & moments to calculate the location of the COP, or in some cases, in combination with the other two protocols. These types of assessments have been used extensively in the past to study the effects of aging, neurological diseases, sensory inputs (e.g. visual, vestibular, proprioceptive), and injuries (Palmieri et al., 2002). COP is commonly measured over a limited time to reduce the chance of muscle fatigue. Following data collection, the COP time series is analyzed to extract parameters used to quantify the time series such as

displacement, velocity, and acceleration. Typical COP parameters that are calculated to characterize the COP time series include the root mean square (RMS) of COP, mean velocity, sway area, total distance traveled, and acceleration (Maurer & Peterka, 2005). In addition, the extremes of these calculations can be extracted, as well as separate components in the AP and ML directions. Studies have shown that COP measures accurately reflect postural stability during postural sway tasks (Ruhe et al., 2010). More recent studies have looked at changes in the COP movement parameters as a way to track the progression of neurological diseases that impair motor control and balance (Mancini et al., 2012).

Modeling Postural Sway

The ability to model the biomechanics of human movement allows for increased understanding of areas that cannot be easily assessed. For example, while experimental measurements of postural sway reflect changes in motor control, the underlining pathology in the neuromuscular control system causing these changes is not well understood. However, many theories and ideas have been developed about the control system that allows for postural stability through dynamic modeling. A full scale approach of the human dynamics and neuromuscular control system must be considered in order to understand and validate a proper model. Computer models allow for a large number of tests to be measured and analyzed in a very short amount of time. Simulation models, such as the postural sway model, allow for insight to be gained and for several parameters to be varied, allowing for the model to enhance the knowledge of the researcher in the physical world. Simulations like the inverted pendulum model provide opportunities for many different areas of the neuromuscular system to be reverse engineered.

Dynamics of the Inverted Pendulum Model

The traditional postural sway model typically accounts for movement in the AP direction. This is largely due to the fact that the dorsi and plantar ankle flexors contribute primarily to movements in this direction (Masani, Vette, Kawashima, & Popovic, 2008).The first focus of the development of a postural sway model is the dynamics of the system. The most common dynamic model of postural sway is the inverted pendulum. Previous studies have developed different ways in setting up the inverted pendulum. The most popular of these is the single inverted pendulum, which lumps all body parts above the ankle together to form a single rigid body from the ankle joint to the body COM (Masani, Popovic, Nakazawa, Kouzaki, & Nozaki, 2003; Peterka, 2000; D. A. Winter, Patla, Prince, Ishac, & Gielo-Perczak, 1998). The single inverted pendulum was validated when it was shown that the ankle strategy was predominately used during postural sway (Karlsson & Lanshammar, 1997). Furthermore, many control schemes have been developed for the single inverted pendulum that have allowed for new understandings of quiet stance control (Masani et al., 2003; Masani et al., 2008; Peterka, 2000). In recent years, a more complex version for modeling postural sway has been developed. The double inverted pendulum takes into account both the ankle and hip strategy, while considering the knee locked, and the head and trunk lumped together (Li, Levine, & Loeb, 2012; Suzuki, Nomura, Casadio, & Morasso, 2012). This strategy not only increases complexity in the dynamics of the model, but also the control of the model where the system becomes multi input-multi output (MIMO). Many recent studies have shown that the increased complexity of this model can be advantageous in understanding the control contributions of both the hip and the ankle strategy (Sasagawa, Ushiyama, Kouzaki, & Kanehisa, 2009). Recent experiments have shown that small perturbations to the system are controlled mostly by the ankle, where larger perturbations require

a combination of contributions from both the ankle and the hip (Li et al., 2012). For the current study involving quiet standing, the ankle strategy is dominate, thus the single inverted pendulum has been chosen and will be discussed from this point on. The equations of motion of the single inverted pendulum can be written as follows:

$$I\ddot{\theta} = mghsin\theta + \tau + \epsilon$$

This is the equation of the pendulum with active torques included when τ equals the control torque from the controller and ϵ equals the noise generated torque in the system. When considering the equation of the pendulum and the torque components summed as they are in the feedback control system the following equations can be formed:

$$I\ddot{\theta} = mghsin\theta + \tau$$

The Laplace transform can be performed on the linearized equation to obtain the following transfer function for the inverted pendulum:

$$\frac{\theta(s)}{\tau(s)} = \frac{I}{Is^2 - mgh}$$

When the control system is developed, this equation represents the plant that the control system will work to stabilize. The dynamics of the single inverted pendulum can now be calculated from the input sum of the torques: active, passive, and noise disturbance. The output of the system is the angle θ of the pendulum from the center line vertical through the ankle joint or rotational joint. The angle of the pendulum is zero when the pendulum is vertically upright creating an angle of 90 degrees with the ground and will be positive in one direction and negative in the other. The output of theta and the system is dependent on the parameters of the inverted pendulum.

Dynamic Inverted Pendulum Model Parameters

The single inverted pendulum is typically made up of a rigid body link or rod with a rotational joint constraint at the base of the rigid body, and a rotating COM at the opposite end of the rigid body. The parameters that define the dynamics of the model are based on human measurements and approximations, in most cases where the measurements cannot be obtained, or they have not been recorded. The primary measurements of the single inverted pendulum that have been derived in previous studies are as follows: the moment of inertia about the ankle, the total mass concentrated at the COM, and the distance from the ankle joint to the COM location (Masani et al., 2008; David A. Winter, 2009). The following equations show how model parameters for moment of inertia (I), distance from the center mass to the ankle (h), and the mass (m), concentrated at the COM at the end of the pendulum are calculated:

$$m = .971M$$

$$h = .261l_1 + .945l_2$$

$$I = .678M(.347l_1 + l_2)^2 + .192Ml_2{}^2$$

These equations can be solved when M is equal the total mass of the subject. The equation for the mass of the pendulum accounts for the body mass excluding the mass of the two feet. The variable l_2 is the leg length from the ankle malleolus to the greater trochanter, and l_1 is the trunk length. In some cases the trunk length may need to be approximated if access to this measure is not available. In this case the value for trunk length can be approximated for a female subject and male subject as follows respectively (David A. Winter, 2009):

$$l_{1female} = .825H - .524H$$

$$l_{1male} = .818H - .530H$$

This equation set can be solved when H is equal to the total height of the subject of interest. These equations can be used to design the model so that experimental data from a group set can be related to the model data with an average parameter set from the subjects used.

Passive versus Active Dynamics

The stabilization of the single inverted pendulum is controlled by the torques about the ankle joint, simulated by the rotational joint of the inverted pendulum. This torque can be broken down into two components, passive torque and active torque. Passive torque is created by the stiffness and tension created by the surrounding tissue of the joint (e.g. muscles, skin, tendons, ligaments). The active torque component is generated by the central nervous system in response to the body sway in an effort to keep the body stabilized (Masani et al., 2003). It has been shown through experiments that active torque generation is required in stabilization of quiet stance (Loram & Lakie, 2002; Morasso & Schieppati, 1999). Recent studies have looked at the influence of passive and active torque on the postural sway movement of subjects. One recent study looked at the COP and COM changes over time when the ankle stiffness was increased with an orthotic, and when increased muscle activity was performed while standing. This study showed a decrease in the frequencies and amplitude of the COP and COM when the ankle stiffness increased. Further results showed an overall decrease in the amplitude of the sway, while decreasing COM velocity and increasing COP frequency when muscle activation was increased (Warnica, Weaver, Prentice, & Laing, 2014). Many studies have shown results of passive torque being a major part of postural sway as well as playing a minor role. More research will need to be dedicated to this subject in the future for a better understanding of the effects of passive and active torques during quiet stance.

Dynamic Control of Inverted Pendulum

The input of active torque about the ankle joint of the single inverted pendulum is dictated by a developed control scheme to ensure stability of the system. Many different types of controllers have been studied and proposed for the control of the active torque. The importance of the controller is to not only stabilize the system, but also create a system that simulates the sway patterns that are measured in experimental studies. In an idealized model, the controller would be the neuromuscular control system of the human body. Several types of controllers have been proposed to simulate this control. The two main adoptions by recent research have been the feedforward controller and the feedback controller. When considering physiology it is possible that the neuromuscular control system uses a combination of the two as shown by recent studies. Finley's recent study showed that feedforward co-contraction control increases to compensate for reduced system stability. Furthermore, co-contraction is not energy efficient and is not observed during quiet stance (Finley, Dhaher, & Perreault, 2012).

More common in postural modeling of the single inverted pendulum is the feedback control system. Several types of feedback control systems have been proposed with varying complexity. The earliest feedback control models for the inverted pendulum utilize the proportional-integral-derivative (PID) controller (Maurer & Peterka, 2005; Peterka, 2002). More recent studies have adapted the proportional-derivative controller in an effort to understand the usage of the position information versus the velocity information of the system. These studies have shown that the velocity information is highly used by the system to balance and that the proportional-derivative controller is indeed a robust control system for postural sway stability (Masani et al., 2003; Masani, Vette, & Popovic, 2006). More recent controllers have enhanced controller complexity by including passive torque components into the feedback loop (Masani et

al., 2008). Other models have suggested weighting the values of sensory systems contributions to the control system (i.e. visual, proprioceptive, and vestibular) (Peterka, 2002; van der Kooij & Peterka, 2011). In any case of a control system model, multiple parameters can be added and manipulated in order to better understand the physiological effects on the neuromuscular control system during quiet standing.

Modeling Postural Sway Parameters

Simulating a physiological system requires an understanding of the system to allow for an accurate model to be developed. The progression of the inverted pendulum model through research has worked to simulate the neuromuscular control system more precisely. In doing so, the equation of the system must be developed in a way to mimic the physiological parameters of the system. Such parameters have been discussed previously such as passive and active torque generation, and feed-forward and feedback control schemes. However, other parameters that change the output of the system must be added to capture the true physiology of the neuromuscular system more completely. The choices that are made to simulate these parameters can result in many different outputs, meaning that many of the parameters require further investigation for a better understanding of their make up in the physiological system. The development of mathematical models of postural sway control requires thorough understanding of the neuromuscular control system.

Physiological Time Delays

In order to develop a more realistic model, time delays due to the neural transmission of signals must be considered. The neural transmission velocity and length of the nerve pathway are the main factors that affect the neural transmission delay (Burdet, Franklin, & Milner, 2013). In inverted pendulum models, it is common to consider feedback time delays, control time

delays, and the activation time delay. The feedback time delay is defined as the time it takes for the ankle somatosensory system to send a signal to the brain (Masani et al., 2008). In the inverted pendulum model, the feedback delay is commonly modeled as the delay time from the plant output of the pendulum angle to the controller input of the system. This value has been shown to be around 30-40 ms in previous studies and has been used in models more recently (Applegate, Gandevia, & Burke, 1988; Masani et al., 2008). The control time delay, on the other hand, represents the time it takes for the brain to determine the next input before sending it to the muscle for activation.

The activation time delay is the time loss from the central nervous system (CNS) to the time of activation of the muscle. The time the CNS takes to calculate for the future muscle activation is currently unknown. However, it has been shown the time loss from the CNS signal to the muscle activation in the lower limb is around 27 to 37 ms (Ackermann, Scholz, Koehler, & Dichgans, 1991; Lavoie, Cody, & Capaday, 1995). It should be noted that time loss found in these studies represents the time loss from the lower limb and is of importance because of the distance that signals must travel, especially in adult human subjects. Furthermore, in recent models it has been suggested that the complete time delay lumped together from the computation of the CNS to the input to the muscle may be reasonably modeled as 40 ms (Masani et al., 2008). The values used for this delay have been tested on PID and proportional-derivative models significantly. Past studies have looked at all three of these delays independently, more recently studies have lumped the neural transmission delay of the controller and the ankle torque activation (Masani et al., 2003; Masani et al., 2008). Other studies have looked at the time delays of the inverted pendulum over larger ranges in order to understand the robustness capabilities of the control system (Masani et al., 2006). In more recent studies, the three time delays have been

summed together based on their individual values and considered in the system at some point in the loop before or after the controller block (Masani et al., 2008; Masani et al., 2006; Maurer & Peterka, 2005; Peterka, 2000; van der Kooij, Jacobs, Koopman, & van der Helm, 2001). Researchers have shown an agreement of the transmission time delay time as 80-100 ms. However, studies have shown that the actual physiological neural transmission may be much larger due to the combination of neuromuscular signal and force generation (Masani et al., 2008). Understanding of these time delays in healthy subjects could allow for a greater understanding of the changes induced in neuromuscular diseases.

Noise Disturbance

In addition to physiological time delays it is known that physiological noise contributes to the human biological system as disturbance to the system requiring stabilization during postural sway. This disturbance to the system causes instability, which requires the generation of passive and active torques to stabilize the system. Noise is likely generated in several different areas in the system including the sensory noise, motor noise, and neuro-mechanical noise (Masani, Vette, Abe, & Nakazawa, 2014). Previous studies have suggested that a majority of noise may be attributed to the sensory organs (van der Kooij et al., 2001). However, models have tested the system with different points of interest for noise and shown that this has a similar effect to one site of interest (Maurer & Peterka, 2005). This suggests that the summation of the noises together is a good representation of the overall noise; however, more in depth understanding of characterized noise in the system may require a more detailed approach to the model. These disturbances are commonly modeled as randomly generated Gaussian white noise filtered with a first-order low pass filter with a zero mean and unit variance (Masani et al., 2003; Masani et al., 2014; Masani et al., 2006; Maurer & Peterka, 2005). This noise is directly input as

a torque disturbance that is summed with the torque input by controller. In recent models the torque controller has been the summation of the active torque and the passive torque generated (Masani et al., 2014; Maurer & Peterka, 2005). Most commonly, studies have looked at manipulating the time constant of the filter and the gain (Maurer & Peterka, 2005). Further, previous studies on neurological diseases have suggested that physiological neural noise may be one of the causes of motor control symptoms in diseases such as PD (Berardelli, Rothwell, Thompson, & Hallet, 2001). The next section describes the process of modeling with ADAMS and Simulink.

Cosimulation ADAMS and Simulink

Modeling for the inverted pendulum has traditionally been done using computational software such as Simulink and MATLAB programming environment (MathWorks, Natick, MA). In this set up, the controls system and dynamic model are all contained and solved in the Simulink platform. The ADAMS software developed by MSC is dynamic simulation software that allows for dynamic systems with very complex capabilities to be modeled and created quickly. This allows for changes to be made easily and readily to the dynamic plant of the postural sway model when needed. ADAMS can be coupled with Simulink to perform what is called a cosimulation between the two. Cosimulation allows for the respective programs to handle parts of the mathematical equations separately and then pass the information back as shown in Figure 2-1.

The dynamic model of the inverted pendulum is created with inputs for the torque from Simulink and outputs of the pendulums angle of displacement to Simulink. The Simulink model diagram is created for the control system and also contains the dynamic plant information from ADAMS. Several parameters can be defined such as the step size, and mathematical solver to

define how ADAMS and Simulink solve for the equations of the controller and the dynamic model. The main two computation setups of ADAMS and Simulink are discrete and continuous modes. In the discrete mode, each entity handles calculations separately and proceeds through the time step. It should be noted that MATLAB will compute the values for the Simulink model. Once the calculations are completed the inputs and outputs from each package are passed between one another so they can move to the next time step. In the continuous setup, MATLAB will solve both ADAMS and Simulink solutions; in this case ADAMS will evaluate the function results. The choice of continuous versus discrete is based on the model achieving the best possible results. In most cases cosimulation is usually more robust based on the ability of ADAMS to solve dynamic equations. The combination of the ADAMS cosimulation with Simulink, allows for more robust and complex dynamic models to be achieved and tested in order to better understand complex systems.

Analysis of Postural Sway Model

Further development of the inverted pendulum requires quantitative analysis that provides comparison to the characterization of human postural control. Researchers have taken several different approaches in understanding the effects of the inverted pendulum model and its simulation of postural sway. The ultimate goal of modeling postural sway is to simulate as closely as possible to the sway parameters measured in experimental data and achieve a neuromuscular control system as physiologically comparable to the biological system used in human quiet stance. Studies have looked to further develop the inverted pendulum model to reproduce normal sway patterns in humans while enhancing the control schemes of the simulated model. This research has led to potential insights into how the CNS may react to changes in body sway as a controller.

For example, in 2003, Masani et al. compared cross correlation functions of measured COM displacement versus EMG signals in the lateral gastrocnemius and soleus muscle with modeled COM displacement cross correlated with the torque input of the active controller with similar curves and time shifts (Masani et al., 2003). This study utilized a laser displacement measurement for the experimental measurements of the COM. This research also looked at the different constants for a proportional-derivative controller and found that the measurable results versus the modeled results were more similar with a high derivative constant. This suggests that velocity information is very important to the control of quiet stance. Other studies have looked at methods such as stabilogram diffusion functions that produce a quantitative statistical measure for apparent random changes of the COP. This study by Robert Peterka showed that this measure could be reproduced in an inverted pendulum with a PID controller compared with COP measured in human experiments (Peterka, 2000). Other studies have also focused more on developing particular aspects of the neuromuscular control system being modelled such as passive torque generation and noise. Maurer discovered that parameters for the single inverted pendulum were capable of recreating realistic time series COP measures. Furthermore, this study showed that small increases in stiffness and damping as well as large increases in noise produced sway measures of COP accounted for with aging (Maurer & Peterka, 2005). Despite the recent success in modeling postural sway for healthy and aging groups, no studies have applied the inverted pendulum model to assess COP parameters in HC versus PD. Such analysis would not only provide the foundation for modeling the motor control of neurological disease states, but in the long term could lead to a better understanding of the neurophysiology behind balance deficits in PD (Kim, Horak, Carlson-Kuhta, & Park, 2009).

Design of Experiments

Complex systems such as the human body require analysis that can evaluate input parameter effects on a response. Design of experiments methods are used widely in research to evaluate such systems. These methods allow for the input parameters of complex systems to be evaluated for the effects on the systems response such is the case in sensitivity analysis. Factorial studies allow for the main effects and the interactions of the input parameters to be better understood. Typically the goal of using design of experiments is to optimize the output response in some way. Design of experiments lends itself nicely to both cases where a study is limited by the number of trials being executed or in cases where a large quantity of trials is available. Typically computer models allow for a large number of trials to be executed and use design of experiments to provide a good initial guess to an optimization.

Such is the case in recent studies of human gait models. Recent human gait models have used design of experiments methods with 2200 trials in order to provide initialization of the input parameters for a cost function optimization (Jonkers, Spaepen, Papaioannou, & Stewart, 2002). In other experiments the study may be looking to understand the behavior of the input parameters or have a limited number of trial executions available. In this case it is likely that further statistical methods could be used such as ANOVA and linear regression to test the relationship of the response to the input parameters. In these studies a 2^k factorial design is often used. In this design, 2 levels are chosen for each parameter commonly at outer ranges high and low. This design allows for an understanding of the interactions and main effects of the input parameters in relation to the response.

Significance

The inverted pendulum has been successfully studied and developed in past studies as a viable option for modeling human postural sway during quiet stance. This research looks to validate the COP sway measures for healthy subjects and subjects with PD. The simulations performed in this study could provide insight into the effects of PD on motor control and neurophysiology degeneration. Physiological parameter changes modeled by the inverted pendulum postural sway model could provide significant information about how the disease is affecting the motor control system. This knowledge could provide researchers with methods for developing the model further and advancing the knowledge of the motor control system. Furthermore, this study could serve as a platform in the long term for understanding the progression of neurodegenerative disease such as PD, in hopes of helping develop better therapies and diagnostic methods that prevent the risk of symptoms and undesirable outcomes.

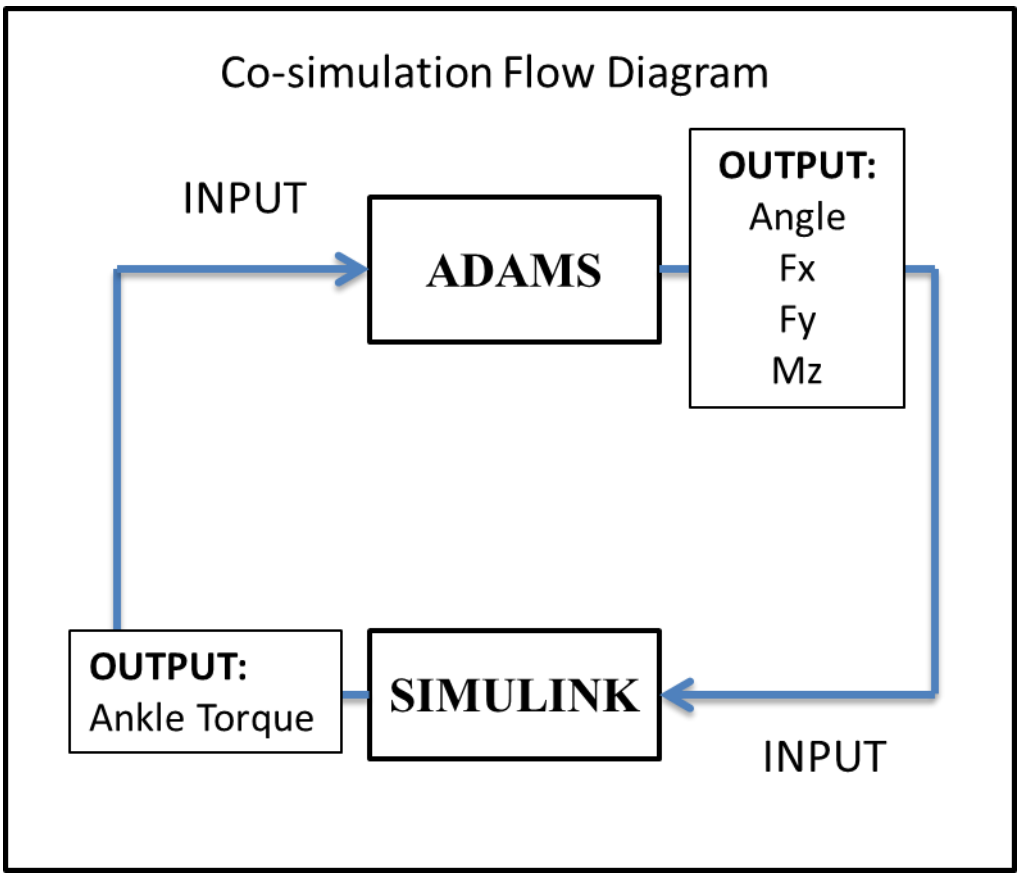

Figure 2-1 - Cosimulation flow diagram between ADAMS MSC and Simulink.

Diagram shows the outputs created by each program and passed on to the other for further calculations of the next time step.

References

Ackermann, H., Scholz, E., Koehler, W., & Dichgans, J. (1991). Influence of Posture and Voluntary Background Contraction Upon Compound Muscle Action-Potentials from Anteriror Tibial and Soleus Muscle Following Transcranial Magnetic Stimulation *Electroencephalography and Clinical Neurophysiology, 81*(1), 71-80. doi: 10.1016/0168-5597(91)90106-8

Applegate, C., Gandevia, S. C., & Burke, D. (1988). Changes in Muscle and Cutaneoous Cerebral Potentials During Standing. *Experimental Brain Research, 71*(1), 183-188.

Berardelli, A., Rothwell, J. C., Thompson, P. D., & Hallet, M. (2001). Pathophysiology of bradykinesia in Parkinson's disease. *Brain, 124*, 2131-2146. doi: 10.1093/brain/124.11.2131

Burdet, E., Franklin, D. W., & Milner, T. E. (2013). *Human Robotics: Neuromechanics and Motor Control* (Vol. 1): The MIT Press.

Centonze, D., Calabresi, P., Giacomini, P., & Bernardi, G. (1999). Neurophysiology of Parkinson's disease: from basic research to clinical correlates. *Clinical Neurophysiology, 110*(12), 2006-2013. doi: 10.1016/s1388-2457(99)00173-x

Dauer, W., & Przedborski, S. (2003). Parkinson's disease: Mechanisms and models. *Neuron, 39*(6), 889-909. doi: 10.1016/s0896-6273(03)00568-3

Finley, J. M., Dhaher, Y. Y., & Perreault, E. J. (2012). Contributions of feed-forward and feedback strategies at the human ankle during control of unstable loads. *Experimental Brain Research, 217*(1), 53-66. doi: 10.1007/s00221-011-2972-9

Hageman, P. A., Leibowitz, J. M., & Blanke, D. (1995). Age and Gender effects on Postural Control. *Archives of Physical Medicine and Rehabilitation, 76*(10), 961-965. doi: 10.1016/s0003-9993(95)80075-1

Horak, F. B. (2006). Postural orientation and equilibrium: what do we need to know about neural control of balance to prevent falls? *Age and Ageing, 35*, 7-11. doi: 10.1093/ageing/afl077

Jonkers, I., Spaepen, A., Papaioannou, G., & Stewart, C. (2002). An EMG-based, muscle driven forward simulation of single support phase of gait. *Journal of Biomechanics, 35*(5), 609-619. doi: 10.1016/s0021-9290(01)00240-8

Karlsson, A., & Lanshammar, H. (1997). Analysis of postural sway strategies using an inverted pendulum model and force plate data. *Gait & Posture, 5*(3), 198-203. doi: 10.1016/s0966-6362(96)01082-x

Kim, S., Horak, F. B., Carlson-Kuhta, P., & Park, S. (2009). Postural Feedback Scaling Deficits in Parkinson's Disease. *Journal of Neurophysiology, 102*(5), 2910-2920. doi: 10.1152/jn.00206.2009

Lafond, D., Duarte, M., & Prince, F. (2004). Comparison of three methods to estimate the center of mass during balance assessment. *Journal of biomechanics, 37*(9), 1421-1426.

Lavoie, B. A., Cody, F. W. J., & Capaday, C. (1995). Cortical Control of Hyman Soleus Muscle During Volitional and Postural Activities Studied Using Focal Magnetic Stimulation. *Experimental Brain Research, 103*(1), 97-107.

Li, Y., Levine, W. S., & Loeb, G. E. (2012). A Two-Joint Human Posture Control Model With Realistic Neural Delays. *Ieee Transactions on Neural Systems and Rehabilitation Engineering, 20*(5), 738-748. doi: 10.1109/tnsre.2012.2199333

Loram, I. D., & Lakie, M. (2002). Direct measurement of human ankle stiffness during quiet standing: the intrinsic mechanical stiffness is insufficient for stability. *Journal of Physiology-London, 545*(3), 1041-1053. doi: 10.1113/jphysiol.2002.025049

Mancini, M., Carlson-Kuhta, P., Zampieri, C., Nutt, J. G., Chiari, L., & Horak, F. B. (2012). Postural sway as a marker of progression in Parkinson's disease: A pilot longitudinal study. *Gait & Posture, 36*(3), 471-476. doi: 10.1016/j.gaitpost.2012.04.010

Marek, K., Jennings, D., Tamagnan, G., & Seibyl, J. (2008). Biomarkers for Parkison's Disease: Tools to Assess Parkinson's Disease Onset and Progression. *Annals of Neurology, 64*(6), S111-S121. doi: 10.1002/ana.21602

Masani, K., Popovic, M. R., Nakazawa, K., Kouzaki, M., & Nozaki, D. (2003). Importance of body sway velocity information in controlling ankle extensor activities during quiet stance. *Journal of Neurophysiology, 90*(6), 3774-3782. doi: 10.1152/jn.00730.2002

Masani, K., Vette, A. H., Abe, M. O., & Nakazawa, K. (2014). Center of pressure velocity reflects body acceleration rather than body velocity during quiet standing. *Gait & Posture, 39*(3), 946-952. doi: 10.1016/j.gaitpost.2013.12.008

Masani, K., Vette, A. H., Kawashima, N., & Popovic, M. R. (2008). Neuromusculoskeletal torque-generation process has a large destabilizing effect on the control mechanism of quiet standing. *Journal of Neurophysiology, 100*(3), 1465-1475. doi: 10.1152/jn.00801.2007

Masani, K., Vette, A. H., & Popovic, M. R. (2006). Controlling balance during quiet standing: Proportional and derivative controller generates preceding motor command to body sway position observed in experiments. *Gait & Posture, 23*(2), 164-172. doi: 10.1016/j.gailpost.2005.01.006

Massion, J. (1998). Postural control systems in developmental perspective. *Neuroscience and Biobehavioral Reviews, 22*(4), 465-472. doi: 10.1016/s0149-7634(97)00031-6

Maurer, C., & Peterka, R. J. (2005). A new interpretation of spontaneous sway measures based on a simple model of human postural control. *Journal of Neurophysiology, 93*(1), 189-200. doi: 10.1152/jn.00221.2004

McVey, M. A., Amundsen, S., Barnds, A., Lyons, K. E., Pahwa, R., Mahnken, J. D., & Luchies, C. W. (2013). The effect of moderate Parkinson's disease on compensatory backwards stepping. *Gait & Posture, 38*(4), 800-805. doi: 10.1016/j.gaitpost.2013.03.028

Morasso, P. G., & Schieppati, M. (1999). Can muscle stiffness alone stabilize upright standing? *Journal of Neurophysiology, 82*(3), 1622-1626.

Palmieri, R. M., Ingersoll, C. D., Stone, M. B., & Krause, B. A. (2002). Center-of-pressure parameters used in the assessment of postural control. *Journal of Sport Rehabilitation, 11*(1), 51-66.

Peterka, R. J. (2000). Postural control model interpretation of stabilogram diffusion analysis. *Biological Cybernetics, 82*(4), 335-343. doi: 10.1007/s004220050587

Peterka, R. J. (2002). Sensorimotor integration in human postural control. *Journal of Neurophysiology, 88*(3), 1097-1118. doi: 10.1152/jn.00605.2001

Plessow, F., Fischer, R., Volkmann, J., & Schubert, T. (2014). Subthalamic deep brain stimulation restores automatic response activation and increases susceptibility to impulsive behavior in patients with Parkinson's disease. *Brain and Cognition, 87*, 16-21. doi: 10.1016/j.bandc.2014.02.009

Ruhe, A., Fejer, R., & Walker, B. (2010). The test-retest reliability of centre of pressure measures in bipedal static task conditions - A systematic review of the literature. *Gait & Posture, 32*(4), 436-445. doi: 10.1016/j.gaitpost.2010.09.012

Salat, D., & Tolosa, E. (2013). Levodopa in the Treatment of Parkinson's Disease: Current Status and New Developments. *Journal of Parkinsons Disease, 3*(3), 255-269. doi: 10.3233/jpd-130186

Sasagawa, S., Ushiyama, J., Kouzaki, M., & Kanehisa, H. (2009). Effect of the hip motion on the body kinematics in the sagittal plane during human quiet standing. *Neuroscience Letters, 450*(1), 27-31. doi: 10.1016/j.neulet.2008.11.027

Stylianou, A. P., McVey, M. A., Lyons, K. E., Pahwa, R., & Luchies, C. W. (2011). Postural Sway in Patients with Mild to Moderate Parkinson's Disease. *International Journal of Neuroscience, 121*(11), 614-621. doi: 10.3109/00207454.2011.602807

Suzuki, Y., Nomura, T., Casadio, M., & Morasso, P. (2012). Intermittent control with ankle, hip, and mixed strategies during quiet standing: A theoretical proposal based on a double inverted pendulum model. *Journal of theoretical Biology, 310*, 55-79. doi: 10.1016/j.jtbi.2012.06.019

van der Kooij, H., Jacobs, R., Koopman, B., & van der Helm, F. (2001). An adaptive model of sensory integration in a dynamic environment applied to human stance control. *Biol Cybern, 84*(2), 103-115.

van der Kooij, H., & Peterka, R. J. (2011). Non-linear stimulus-response behavior of the human stance control system is predicted by optimization of a system with sensory and motor noise. *J Comput Neurosci, 30*(3), 759-778. doi: 10.1007/s10827-010-0291-y

Warnica, M. J., Weaver, T. B., Prentice, S. D., & Laing, A. C. (2014). The influence of ankle muscle activation on postural sway during quiet stance. *Gait & Posture, 39*(4), 1115-1121. doi: 10.1016/j.gaitpost.2014.01.019

Wichmann, T., & DeLong, M. R. (2003). Functional neuroanatomy of the basal ganglia in Parkinson's disease. *Parkinson's Disease, 91*, 9-18.

Winter, D. A. (2009). *Biomechanics and Motor Control of Human Movement* (Vol. 4): Wiley.

Winter, D. A., Patla, A. E., Prince, F., Ishac, M., & Gielo-Perczak, K. (1998). Stiffness control of balance in quiet standing. *Journal of Neurophysiology, 80*(3), 1211-1221.

Chapter 3 : Model Development

Abstract

Background. Postural sway modelling has been studied with the goal to reverse engineer the inputs that affect the measurable biomechanics outcomes such as the center of pressure (COP) time series. The goal of the current study is to develop a powerful cosimulation model of postural sway that consists of physiological related input parameters. These parameters will be used to investigate the model performance and to validate the model COP output measures by comparing them to those measured experimentally in healthy control (HC) participants with their eyes closed during quiet stance.

Methods. Once model development was complete, a stability analysis was performed to understand the robustness of the model. Second, a sensitivity analysis with linear regression was performed to quantify the effect of the model input parameters on the model output COP measures. Third, a design of experiments was performed to understand main effects and interactions between the model input parameters. Finally, a correlation analysis was used to compare the model output COP measures and the HC group COP measures to investigate to validity of the model.

Results. The noise parameter exhibited a linear effect on the output COP measures when the noise was varied for all COP measures except for the COP max, min, and median frequency. The design of experiment for each COP measure response commonly resulted in an interaction between the proportional gain and feedback time delay. The correlation study demonstrated that the model and experimental HC COP measures were similar across a majority of the COP measures.

Conclusions. The proportional-derivative controller proved to be a robust control strategy for the inverted pendulum model. In some cases it may be over controlled in comparison to the human system. The model's base set of parameters were validated using COP measures related to the HC group.

Introduction

Complex systems such as the human body do not lend themselves naturally to large scale controlled studies. Computer models, on the other hand, provide the opportunity to simulate and investigate these complex systems using more easily controlled systematic methods. This approach allows for a large number of trials to be executed with a high amount of control on the system parameters. While initial models generally start out simple, they allow for the use of the crawl-walk-run approach, which systematically increases the complexity of the model one step at a time. In order to ensure the model represents the system's physical behavior, model and experimental results are often compared to establish model validation.

The analysis of the center of pressure (COP) time series, determined based on force plate measures under the feet, has been used to quantify human bipedal stance (Ruhe, Fejer, & Walker, 2010). Abnormalities can be induced into the COP time series through the attenuation of sensory feedback (e.g. visual, vestibular, cutaneous, or proprioceptive) (Palmieri, Ingersoll, Stone, & Krause, 2002). One recent study investigated the idea of monitoring measures used to quantify COP movement as a way to track the progression of neurological diseases (Mancini et al., 2012). With the goal to better understand how the central nervous system controls human stance, models have been created to simulate the controller and the biomechanics of the system during the postural sway task (Masani, Vette, Kawashima, & Popovic, 2008; Maurer & Peterka, 2005; Peterka, 2002; van der Kooij, Jacobs, Koopman, & van der Helm, 2001; van der Kooij & Peterka, 2011).

The COP time series has been studied experimentally through the measurement of the foot-floor forces and moments using force plate measures of human subjects. Quantities used to characterize the COP reflect postural stability during the postural sway tasks (Ruhe et al., 2010).

More recently, the COP time series has been extracted from models of the dynamic control of the inverted pendulum, which is a relatively simple model representing the system dynamics in the anterior-posterior (AP) direction during quiet stance (Masani, Vette, & Popovic, 2006; Maurer & Peterka, 2005; Peterka, 2002). Single inverted pendulum models have been developed to the point that model generated COP time series are comparable to those obtained experimentally for young adults and elderly adults (Maurer & Peterka, 2005). The human subject is modeled in the AP direction as a single inverted pendulum, which is the dynamic plant that is controlled using a linear feedback controller.

Proportional-integral-derivative and proportional-derivative controllers have been investigated to control the upright stabilization of the pendulum, and have achieved realistic COP measures during quiet stance (Masani et al., 2006; Maurer & Peterka, 2005). Physiological noise and time delays are both included in the mathematical equations in order to create a more accurate model (Masani, Vette, Abe, & Nakazawa, 2014; Maurer & Peterka, 2005; Peterka, 2000; van der Kooij & Peterka, 2011). The ability of the model to produce a COP time series with measures that are comparable to those found experimentally in healthy adults increases it's potential to improve our understanding of the impact that injury, aging, and neurodegenerative diseases may have on the operation of the central nervous system.

This study focused on the development, design, implementation, and performance of a single inverted pendulum model controlled by a proportional-derivative controller and allowing for model parameters of control, noise, and system time delays to be varied.

The main goal of this study was to develop a model that simulates bipedal human stance and then to investigate its performance. The human body during quiet stance was modeled as a

noise driven single link inverted pendulum with the ankle torque controlled to maintain balance. This model provides proper simulation of quiet stance (i.e. ankle strategy), whereas a double inverted pendulum model produces hip torque which has been shown to be important only when perturbations occur during postural sway (Li, Levine, & Loeb, 2012) (i.e. ankle and hip strategy). This study utilized several methods to investigate and validate the model. First, a stability analysis was performed on the model input parameters to understand the robustness of the system. Second, a sensitivity analysis was performed to investigate the effects of changes in the model input parameters on the output COP measures. This method was further quantified through a linear regression analysis. Third, a full factorial design was performed to investigate the main effects and interactions of the input model parameters. Finally, the model parameters were tuned so that the model COP time series was comparable to the average experimental COP time series measured in HC subjects. This model input parameter set was labeled the "healthy" base model parameter set.

This is a validation study of a linear feedback control model used to simulate the active neuromuscular control system that maintains stable balance during eyes closed quiet stance in HC adult humans. The methods used to develop the model will allow for future complexity to be added to both the plant and the controller. This model provides a foundation for further growth in studies seeking to reverse engineer measurable biomechanical parameters to the physiological inputs that affect them.

Methods

Experimental Testing

Experimental human subject data previously recorded from 21 HC adults (age 66 ± 8 years, 13males, 8 females) were used in this study. Subjects were asked to stand on a two force plate system (one foot on each force plate) with their hands relaxed at their sides and their eyes closed. Participants self-selected a comfortable and natural stance which was marked and controlled for each trial. Appropriate rest was given as needed between each trial to minimize the potential for muscle fatigue. A total of three 30 second trials were recorded for each subject. Foot-floor reactions were sampled at 1000 Hz using two AMTI (Watertown, MA, USA) force plates. Anthropometric measurements were taken for subject height, total mass, ankle height, foot length, thigh length, and calf length.

Experimental Data Analysis

All force plate experimental data were down sampled to 100 Hz prior to calculate the COP time series for each trial. Force and moment data measured using the force plates were filtered with a zero phase shift, 2^{nd} order Butterworth low pass filter at a 12.5 Hz cutoff frequency. Force plate data were analyzed with MATLAB programming language (MathWorks, Natick, MA, USA). The AP COP time series was derived using the output force and moment data from the force plates. The AP COP time series was analyzed, and measures were extracted that represent frequency, extreme movements, and overall movements of quiet human stance. The COP measures used to compare the model predicted COP time series with the experimental COP time series were: COP total path distance, COP range, median frequency, root mean square (RMS) of the COP displacement, mean velocity, and peak velocity.

Model Design

A cosimulation was performed between a dynamic model and neural feedback controller to simulate the 2-D dynamics of human postural sway. The human body was modeled in the sagittal plane as a single inverted pendulum with a revolute joint representing the net ankle joint (Masani et al., 2014; Maurer & Peterka, 2005; Peterka, 2000). The dynamic model of the inverted pendulum was created and mathematical equations were solved using ADAMS multibody dynamics software (MSC Software, Newport Beach, California). Movement of the inverted pendulum model was only considered in the AP direction. Previous models have assumed the majority of ankle torque in humans is generated in the AP direction (Masani et al., 2008). Anthropometric parameters for the inverted pendulum were selected based on averages of experimental data taken across the subjects. Measurements that were not available from the experimental analysis were calculated as shown by the values found in Table 3-8 and Table 3-9 (Masani et al., 2008; Winter, 2009).

The neural feedback controller was modeled in Simulink (MathWorks, Natick, MA) as a Proportional-Derivative controller with constant values K_P and K_d representing the proportional and derivative constants, respectively (Masani, Popovic, Nakazawa, Kouzaki, & Nozaki, 2003; Masani et al., 2006). The net ankle torque input to the model is the summation of the controller torque developed by the neural controller and the disturbance torque developed by noise in the neuromuscular system and the central nervous system. The disturbance torque was created by a random Gaussian white noise with unit variance and zero mean in MATLAB (MathWorks, Natick, MA). This noise was first-order low pass filtered with a gain value K_n and time constant t_n=100 seconds, in order to create a controller noise component in the system as derived from Maurer (Maurer & Peterka, 2005). Two time delays were included in the model. The neural

muscular time delay T_1, was held constant throughout the study at 40 ms as referenced in previous work (Applegate, Gandevia, & Burke, 1988; Masani et al., 2008). The neural feedback delay T_2 from the sensory system to the controller was varied in the study. Note that the total time delay of the system is $T_{TOT} = T_2 + T_1$. This algebraic equation has been commonly used in previous models to assess the total time delay of the neural transmission (Masani et al., 2006; Maurer & Peterka, 2005; Peterka, 2000; van der Kooij et al., 2001). Recent studies have shown that the neural transmission velocity and length of the nerve pathway are the main factors that affect the neural transmission delay (Burdet, Franklin, & Milner, 2013).

Output of the ADAMS dynamic model included the pendulum's angular displacement of the COM relative to vertical, with 0 degrees used as the neutral configuration. Representations of the model are depicted in Figure 3-7. The ADAMS system block created in Simulink contained a single input from Simulink for the summation of the torque controller and torque disturbance. The ADAMS system block contained four outputs to Simulink which are the reaction forces & moment about the ankle (F_x, F_y, and M_z), as well as the angle of displacement of the pendulum θ. F_x and F_y defined the force component in horizontal AP and vertical direction, respectively. M_z defined the moment about the ankle joint, with an axis perpendicular to the sagittal plane. The center of mass (COM) was measured directly in ADAMS as the displacement of the most vertical point of the pendulum COM. A block diagram representation of the neural control feedback model is provided (Figure 3-1).

Model Simulation

Model testing was performed through a cosimulation of ADAMS multibody dynamics software (MSC Software, Newport Beach, California) and Simulink version 7 of MATLAB (MathWorks, Natick, MA). ADAMS was used to create the virtual model of an inverted

pendulum "plant". The ADAMS solver was used to solve the dynamic equations of motion and algebraic constraint equations at each time step using the net ankle torque, which was provided by the Simulink controller. Simulink was used to build the feedback controller and to provide ADAMS with the controlled ankle torque, which was based on the difference between the desired pendulum angle and the angle θ output from ADAMS virtual plant.

Four controller variables were varied: K_n, K_p, K_d, and T_2 representing physiological noise gain, proportional gain, derivative gain, and feedback time delay, respectively. A baseline set of these input parameters was derived from previous studies and modified to provide model output COP measures similar to those that our laboratory measured previously. The model input parameters were individually varied from the baseline values in order to create new "test sets" for simulation for both stability and sensitivity analyses. Each unique test set of the model parameters was simulated for six 30 second trials, which were different from each other because the system is driven by the disturbance torque produced using random Gaussian white noise. Each trial was simulated with a fixed step-size of 0.01 seconds to correspond to the 100 Hz sampling frequency used from the force plate data in the experiment done previously. The communication interval between ADAMS and Simulink was set to 0.01 seconds. This design was used for all test sets and trials computed.

Model Center of Pressure

The reaction force and moment data at the revolute joint from the ADAMS block of each trial was filtered with a 2nd order Butterworth low pass filter at a 12.5 Hz cutoff frequency, which matches the data processing used on the experimental data. The model COP time series was then calculated using the equations derived from a free body analysis of the foot, which was assumed stationary. The following equation was used to calculate the model COP time series:

$$COP_{A/P} = x_1 + x_0 = \frac{\tau_C - (y_1 R_x) + (-R_y)x_0}{R_y + mg} + x_0$$

(See Appendix A for full derivation)

Where x_1 is the distance of the ground reaction force from the foot COM in AP direction. Furthermore, x_0 is the distance in the AP direction between the foot COM and the ankle joint axis of rotation. The ankle height is depicted by y_1, and the reaction forces in the x and y direction are provided by R_x and R_y, respectively. Finally, the total torque measured by the input to the ankle is t_c.

For each trial the following model COP measures were calculated in the AP direction relative to the starting position: COP total path distance, COP range, COP minimum, COP maximum, median frequency, root mean square of the COP displacement, mean velocity, peak velocity, peak acceleration, and mean acceleration. Mean and standard deviation of the COP measures across the 6 trials for each test set were calculated. A single variable sensitivity analysis was then performed on each of the four model parameters of interest.

Analysis of the Inverted Pendulum Model

Base Value Test Set. A "base" value set of model parameters K_n, T_2, K_d, and K_p were selected as the model parameters that resulted in COP measures similar to COP measures found in the experimental tests of 21 HC adults. These values were determined from a starting set of values from Maurer (Maurer & Peterka, 2005). All parameter values were varied in 0.5% increments until COP measures were within +/- 1 standard deviation of the COP measures of 21 HC subjects in the experimental study. The model COP measures of the base test set being compared to the

experimental COP measures were averaged over 21 thirty second trials. The duration and sample size of trials were chosen to match the experimental data protocol.

Model Stability Range. The model was investigated by creating new test sets through systematically varying the individual model input parameter values. Each model parameter was adjusted above and below its base value while the other model parameters were held constant until the model was unstable or stable outside of the limits of experimentally determined COP behavior in the HC group. The parameters were varied creating 150 test sets, each containing 6 trials, until a full spectrum of the stability ranges of the model were determined. Each trial of a test set was examined for stability through a data quality check. The data quality check consisted of time series plots for the COP displacement, COM displacement, torque disturbance, torque active, each of the raw forces and moments, and the angle of displacement. Instability in the model test set was defined if COP displacement range was greater than 1 meter and the pattern of the plots showed a) resonant oscillation (see Figure 3-6), or b) complete loss of control (see Figure 3-5). Based on the size of the stability ranges, each model parameter was varied below and above their base set parameters by a repeated increment percentage of the base value.

Sensitivity Analysis. Sensitivity graphs were created for each COP measure calculated from the inverted pendulum model. Linear regression analysis was performed on each of the model parameters for all COP measures calculated. For each model parameter, 3 test sets above and below the base set were considered. The mean value for each test set of the COP measure of interest was plotted and linear regression was performed. For each plot the coefficient of determination (R^2) and the equation of the best fit line was recorded.

Design of Experiments. A 2^4 full factorial design of experiments was performed to understand the interactions and main effects of the input model parameters on the COP measures. A factorial table is presented in Table 3-3 that shows the responses of each COP measure during each trial. In Table 3-3, the levels of the model parameters during each of the trials are provided. The levels were chosen as the high and low values from the linear regression plots. Six trials were performed for each set of model parameters. The mean and standard deviation of each COP measure across the six trials was calculated. Two-way interaction plots were recorded for each of the COP measure responses. A four-way ANOVA was performed for each of the responses with $p < .05$ defining significance. ANOVA tables were created for the analysis of the main effect, two-way, and three-way interactions. Four-way interactions are not show in the table because of the number of samples taken. It was concluded from cube plots that there were no significant four-way interactions for each of the responses.

Validation of the Inverted Pendulum Model. A Pearson correlation analysis was performed on the output COP measures of 21 base set model parameter trials. This same analysis was carried out on 21 experimental eyes closed trials from HC subjects. Correlation results observed between COP measures in the experimental results was compared with the observed correlation of the model output COP measures.

Results

Base Value Test Set

The following baseline parameter values were established as parameters that resulted in model COP measures similar to HC subjects found experimentally: K_n= 786.5 Nm, K_p=22.4 Nm·deg^{-1}, K_d=7 Nm·s·deg^{-1}, and T_2= 0.15 seconds. See Figure 3-4 for the data quality check for

the base set. Table 3-4 and Table 3-5 show the experimental and model statistics (mean, standard deviation) for each COP measure.

Model Stability Range

Feedback Time Delay (T_2). The sensory feedback time delay T_2 was varied in 2% increments of its base parameter value 0.147 seconds. The stability range for T_2 was -100% to 2% from the base parameter. The range of values for T_2 was 0 to 0.14994 seconds.

Proportional Gain (K_p). The proportional gain K_p was varied in 5% increments of its base parameter value 22.36 (Nm)/deg. The stability range for K_p was -100% to 0% from the base parameter. The range of values for K_p was 0 to 22.36 (Nm)/deg.

Derivative Gain (K_d). The derivative gain K_d was varied in 2% increments of its base parameter value 7.0143 (Nmsec)/deg. The stability range for K_d was -24% to 10% from the base parameter. The range of values for K_d was 5.190582 to 7.71573 (Nmsec)/deg.

Neuromuscular Noise (K_n). The derivative gain K_n was varied in 20% increments of its base parameter value 786.555 Nm. The stability range for K_n was -100% to 600% from the base parameter. The range of values for K_n was 0 to 5505.885 Nm.

Sensitivity Analysis

Sensitivity plots were developed to show the progression of each independent input parameter change from the base within the stability boundaries. These graphs were used to gain a visual understanding of how the input model parameters affect the output COP measures. The

mean and standard deviations for each parameter forthe measure COP total distance are presented in Figure 3-2.

In Figure 3-3, slope values for total distance AP for T_2, K_p, K_d, and K_n were 562.773, 114,126.866, 19.058, and 3.703 mm respectively. It can be seen from Table 3-2 for every COP measure the slope is largest to smallest for K_p, T_2, K_d, and K_n respectively. The coefficient of determination R^2 for each linear regression of T_2 ranged from 0.500 to 0.609 for all COP output parameters except median frequency. The T_2 coefficient of determination for median frequency was 0.981. The R^2 value for each linear regression of K_p ranged from 0.409 to 0.608 for all COP output parameters. The R^2 value for each linear regression of K_d ranged from 0.307 to 0.737 for all COP output parameters except for maximum displacement AP. The K_d coefficient of determination for maximum displacement was 0.092. The R^2 value for each linear regression of K_n ranged from 0.916 to 0.999 for all COP output parameters except for maximum displacement, minimum displacement, and median frequency. The K_n coefficient of determination for maximum displacement, minimum displacement, and median frequency was 0.832, 0.808, and 0.337 respectively.

Design of Experiments

Responses and level design for each trial of the factorial design can be found in Table 3-3. The three-way ANOVA analysis results showed no significant results or main effects in the ANOVA table for COP total distance, maximum displacement, minimum displacement, velocity mean, acceleration mean, RMS, and median frequency. The ANOVA table for COP range showed significant main effects for all input parameters, and two-way interactions for all combinations except K_d/K_n, and similar finding for three-way interactions that did not include K_d/K_n together. COP peak speed observed significant main effects for T_2 and K_p, and two-way

interactions for T_2/K_p. The COP measure peak acceleration presented main effects for all four input parameters, and two-way interactions for every combination except K_d/K_n, and similar finding for three-way interactions that did not include K_d/K_n together.

Model Validation

Table 3-5 and Table 3-6 show the Pearson correlation tables of the COP measures for the experimental and model data independently. The model and experimental data share p-values <0.0001 for COP measure correlations of COP total distance correlated with mean velocity, COP total distance with peak speed, COP range with RMS, and velocity mean with peak speed. The correlation coefficient for each of these correlated parameters was 0.788 to 1.

The model data provided 9 COP measure pairs that were correlated with a p-value of <0.0001 and was not observed for these parameters in the experimental correlation. The parameter pairs that qualified were COP total distance with acceleration mean, COP total distance with RMS, COP total distance with range, COP minimum with median frequency, COP range with velocity mean, velocity mean with acceleration mean, velocity mean with RMS, peak speed with acceleration mean, and acceleration mean with RMS. The positively correlated pairs possessed correlation coefficients ranging from 0.77 to 0.91 in the model correlation and 0.374 to 0.735 in the experimental correlation. In both the model and experimental, correlation of the COP minimum and median frequency were negatively correlated with a correlation coefficient in the experimental and model data of -0.105 and -0.83649 respectively. The experimental data provided one COP measure pair, COP maximum and minimum, not correlated with a p-value of <0.0001 in the model. This pair possessed a correlation coefficient of 0.983 in the experimental correlation. The model correlation coefficient of these two parameters was also positively correlated with a value of 0.584.

Discussion

In this study an inverted pendulum model was developed and validated as a simulation for a HC adult subject during eyes closed quiet stance. A base set of model input parameters that simulated the average HC subject was determined. This base set was then used in stability and sensitivity analysis of the model input parameters on model output COP measures. Finally, a comparative analysis was performed with the model and experimental COP data measures, with the goal of validating the base set of input parameters.

Input Parameters Effect on Output COP Measures

The base model input parameters were developed to gain an initial starting point that was capable of providing insight to the model parameter effects. These parameters were found to be similar to previous studies. Each model parameter was 13.5% greater than those found previously by Maurer and Peterka (Maurer & Peterka, 2005). Differences in these parameters were likely caused by differences in the "plant" anthropometric measures and the experimental group ages. Although we did not quantify the relationship between the COP and COM, we did observe during data quality checks that the COP overlaid with COM agreed with previous suggestions that the COP works to control the COM displacement as shown in Figure 3-4 (Winter, 2009).

Stability of the model was tested to understand the effects of the outer boundaries of each input parameter on the system. Not all parameters reached instability at the outer boundaries listed. In the case of the K_n, T_2, and K_p the effect of the lower boundary does not cause instability, rather it causes increased stability. In these cases we assume that a value in the lower boundary is unreasonable as it is either unrealistic for the study (negative T_2) or the negative value would cause a mirroring of the effects that are observed. In the upper boundary of K_n,

instability was not reached but stability testing was ended because the COP range measures were well beyond realistic ranges of COP measures observed in experimental data. It should be of interest that normal stability was observed in the data quality checks at this outer boundary with amplified COP measure values. This suggests that the base model parameters K_p and K_d provide a robust control system in the presence of increased noise. This finding is similar to that found by Masani, which suggested that the proportional-derivative controller provides robust characteristics capable of controlling postural balance (Masani et al., 2006). All other stability boundaries reached instability where the model was unable to control balance.

Sensitivity analysis was performed to understand the independent effects of each input parameter on the base set of the model. The sensitivity plots showed that independent changes in T_2 have little effect on any of the COP measures except for median frequency. Similar trends were observed when K_d was independently changed from the base set. The observed effect of changes in the magnitude of K_d resulted in a parabolic trend for all the COP measures, except for median frequency. The proportional gain K_p had a significant effect on values of instantaneous nature (i.e. COP range, maximum, minimum, peak speed, peak acceleration, and RMS) when the gain trended toward 0. This is likely due to the large effect that the proportional gain has on the control of the system. As the gain becomes less effective, the parameters most affected by extreme measurement are highlighted. The K_p and K_d parameters exhibited an interesting trend with a short valley effect before a shallow rise in most of the COP measure responses. This can be seen in the total distance response in Figure 3-2. Instability is reached quickly after the base set for K_p where the system becomes over controlled, with overshoot increasing. The parameter K_n shows a strong linearity through all COP range measures. The largest effects of changes in K_n are observed in mean acceleration and peak acceleration. Similar effects at lesser magnitudes are

seen in mean velocity, peak velocity, and total distance. The overall linear trend of the K_n parameter is observed in all the graphs except for median frequency.

Linear regression analysis of the input parameter T_2 supported the observed effects from the sensitivity plots. The input parameters K_p and T_2 had instability values within the prescribed range for the linear regression. For T_2, the graphs show a relatively rapid change from stability to instability in the model at 2, 4, and 6 % away from the base parameter (T_2 range: 0.14994, 0.15288, and 0.15582 respectively). This instability relates well with the increase in duration of the time delay for the controller to react. Similar effects were also observed for K_p which can be interpreted that the proportional gain creates a system that becomes over controlled. For T_2 linearity holds for the median frequency even with instability which possesses an R^2 value of 0.981. The derivative gain shows an exponentially increasing curve as the input parameter value increases for most COP measures. K_n shows a strong linear change in most of the COP measures which supports the idea of a robust controller at the base set of model parameters, which is not susceptible to instability caused by noise input to the system. Changes in the input parameters when analyzing the COP measures of median frequency, max displacement, and minimum displacement showed trends with high variance and low coefficients of determination. This trend is supported in previous studies that suggest these parameters are not a good measurement of postural stability, especially when comparing to possible instability (Barnds, 2015).

Full factorial analysis demonstrated a significant interaction between T_2 and K_p. From the response data it is shown that when these parameters were both at high levels together, the system trended toward instability. The ANOVA table supports this idea particularly for the COP peak speed, peak acceleration, and range. The data suggests that there exists a main effect for both parameters and an interaction effect between T_2 and K_p when both parameters are at high

levels. This can be interpreted as a large amount of control induced by the proportional gain, which increases overshoot characteristics of the controller. When the proportional gain increases along with the delay time of the controller, the effects of the overshoot are amplified because the controller has less resolution to fix the large amount error that has occurred.

Healthy Control Eyes Closed Model Validation

Correlation analysis showed evidence that the model COP measures and the experimental HC eyes closed COP measures are similar. All trends that were observed with a high correlation in experimental data, except for COP maximum and minimum, were also observed in the model. Despite having a similar relationship, some COP measures that were highly correlated in the model were only moderately correlated in the experimental data. This difference in the correlation coefficients could potentially be explained in several different ways. While only the random noise changed for the model trials (for this comparison), variation within each experimental COP measures resulted from limited sampling from a pool of subjects. Naturally, it is expected that the variation across human subjects would be greater than the changes in variation induced by changes in random noise. In looking at the simple statistics we can see that several COP measures of the model were easily captured within 1 standard deviation of the experimental mean. Furthermore, the variance of the model measures is much lower in several cases. This can be attributed to the model controller likely being more controlled and the fact that the experimental data is recorded from different subjects. A future experimental goal might be to assess the variation in COP measures across a larger number of trials within each subject. A good example of the robustness of the model is in COP total distance. Within the model, the mean total distance traveled is larger, and the mean COP range is smaller compared to the experimental data.

The model assumes a limited number of variables can affect the system, whereas the human body is likely a much more complex system. Limitations of this study are the likely need for additional complexity in the dynamic model and the controller. Further limitations of the study can be attributed to the low number of trials available for each test set. This could be increased in future studies and an optimization could be performed from this initial validation study. However, this study provides similar insight to the variances that are observed in the experimental data despite the lesser complexity in this present model. Nevertheless, the overall relationship and direction of the parameter correlations show that the model COP measures are behaving like that of COP measures from human subjects.

Conclusions

The inverted pendulum model developed in this study has been validated with the COP measures from experimental data of human subjects during eyes closed quiet stance. Furthermore, the model was analyzed to understand the effects of the four input parameters of interest. Validation of the model and an increased understanding of the system will allow for future studies to manipulate the input parameters in order to produce output COP measures similar to those observed in subjects with changes to the neurological system. This model provides a foundation for further model development due to the cosimulation of ADAMS and Simulink. These two tools working together allow for an increased complexity to be added on both the control and dynamics models. This infrastructure provides the ability to increase understanding of the human neuromuscular system.

Future work will look to increase the complexity of the inverted pendulum model by investigating the hip joint and medial-lateral direction during stance where perturbations are involved. It has been shown that these two layers of complexity are likely not a factor in

unperturbed stance (Li et al., 2012; Morasso & Schieppati, 1999). The control scheme for the model could be manipulated to take into account the visual, vestibular and proprioceptive feedback systems. Physiological studies have suggested the importance of feedforward pathways in order to compensate for instability (Finley, Dhaher, & Perreault, 2012). This model could help understand the changes that are occurring in the inputs of the system that cause the effects of such neurological diseases as Parkinson's disease. In summary, we have confirmed the use of a proportional-derivative controlled inverted pendulum as a method of simulating human stance. We have presented a model with input parameters capable of simulating eyes closed stance in HC subjects which provides the opportunity to be built upon and further studied.

References

Applegate, C., Gandevia, S. C., & Burke, D. (1988). Changes in Muscle and Cutaneoous Cerebral Potentials During Standing. *Experimental Brain Research, 71*(1), 183-188.

Barnds, A. N. (2015). *Biomechanical Markers as Indicators of Postural Instability Progression in Parkinson's Disease.* (Dissertation).

Burdet, E., Franklin, D. W., & Milner, T. E. (2013). *Human Robotics: Neuromechanics and Motor Control* (Vol. 1): The MIT Press.

Finley, J. M., Dhaher, Y. Y., & Perreault, E. J. (2012). Contributions of feed-forward and feedback strategies at the human ankle during control of unstable loads. *Experimental Brain Research, 217*(1), 53-66. doi: 10.1007/s00221-011-2972-9

Li, Y., Levine, W. S., & Loeb, G. E. (2012). A Two-Joint Human Posture Control Model With Realistic Neural Delays. *Ieee Transactions on Neural Systems and Rehabilitation Engineering, 20*(5), 738-748. doi: 10.1109/tnsre.2012.2199333

Mancini, M., Carlson-Kuhta, P., Zampieri, C., Nutt, J. G., Chiari, L., & Horak, F. B. (2012). Postural sway as a marker of progression in Parkinson's disease: A pilot longitudinal study. *Gait & Posture, 36*(3), 471-476. doi: 10.1016/j.gaitpost.2012.04.010

Masani, K., Popovic, M. R., Nakazawa, K., Kouzaki, M., & Nozaki, D. (2003). Importance of body sway velocity information in controlling ankle extensor activities during quiet stance. *Journal of Neurophysiology, 90*(6), 3774-3782. doi: 10.1152/jn.00730.2002

Masani, K., Vette, A. H., Abe, M. O., & Nakazawa, K. (2014). Center of pressure velocity reflects body acceleration rather than body velocity during quiet standing. *Gait & Posture, 39*(3), 946-952. doi: 10.1016/j.gaitpost.2013.12.008

Masani, K., Vette, A. H., Kawashima, N., & Popovic, M. R. (2008). Neuromusculoskeletal torque-generation process has a large destabilizing effect on the control mechanism of quiet standing. *Journal of Neurophysiology, 100*(3), 1465-1475. doi: 10.1152/jn.00801.2007

Masani, K., Vette, A. H., & Popovic, M. R. (2006). Controlling balance during quiet standing: Proportional and derivative controller generates preceding motor command to body sway position observed in experiments. *Gait & Posture, 23*(2), 164-172. doi: 10.1016/j.gailpost.2005.01.006

Maurer, C., & Peterka, R. J. (2005). A new interpretation of spontaneous sway measures based on a simple model of human postural control. *Journal of Neurophysiology, 93*(1), 189-200. doi: 10.1152/jn.00221.2004

Morasso, P. G., & Schieppati, M. (1999). Can muscle stiffness alone stabilize upright standing? *Journal of Neurophysiology, 82*(3), 1622-1626.

Palmieri, R. M., Ingersoll, C. D., Stone, M. B., & Krause, B. A. (2002). Center-of-pressure parameters used in the assessment of postural control. *Journal of Sport Rehabilitation, 11*(1), 51-66.

Peterka, R. J. (2000). Postural control model interpretation of stabilogram diffusion analysis. *Biological Cybernetics, 82*(4), 335-343. doi: 10.1007/s004220050587

Peterka, R. J. (2002). Sensorimotor integration in human postural control. *Journal of Neurophysiology, 88*(3), 1097-1118. doi: 10.1152/jn.00605.2001

Ruhe, A., Fejer, R., & Walker, B. (2010). The test-retest reliability of centre of pressure measures in bipedal static task conditions - A systematic review of the literature. *Gait & Posture, 32*(4), 436-445. doi: 10.1016/j.gaitpost.2010.09.012

van der Kooij, H., Jacobs, R., Koopman, B., & van der Helm, F. (2001). An adaptive model of sensory integration in a dynamic environment applied to human stance control. *Biol Cybern, 84*(2), 103-115.
van der Kooij, H., & Peterka, R. J. (2011). Non-linear stimulus-response behavior of the human stance control system is predicted by optimization of a system with sensory and motor noise. *J Comput Neurosci, 30*(3), 759-778. doi: 10.1007/s10827-010-0291-y
Winter, D. A. (2009). *Biomechanics and Motor Control of Human Movement* (Vol. 4): Wiley.

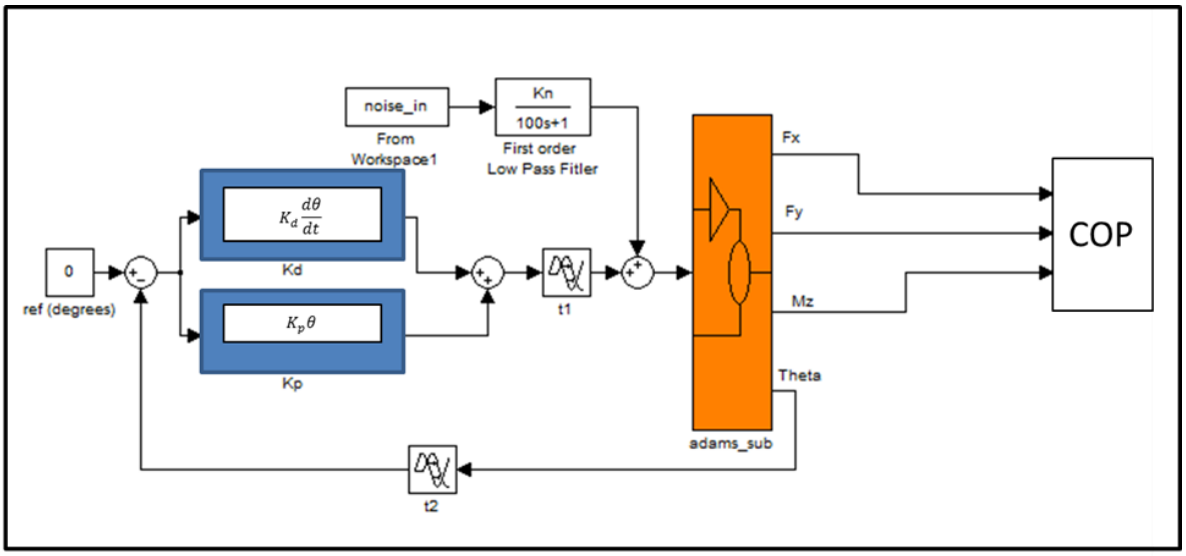

Figure 3-1 - Cosimulation of Postural Sway Inverted Pendulum

Inverted pendulum block diagram. Orange block is the plant connecting to ADAMS. Fx, Fy, and Mz are used in calculation of COP. K_n, T_{tot}, K_d, K_p are model parameters of interest in sensitivity analysis. T_1 represents the neural time delay from the central nervous system to the muscle activation. T_2 represents the feedback time delay.

Stability Ranges					
	Actual Value		% change from base value		
	Min	Max	Min	Max	Increments
T_2	0	0.14994	-100%	2%	2%
K_p	0	22.36	-100%	0%	5%
K_d	5.190582	7.71573	-24%	10%	2%
K_n	0	5505.885	-100%	600%	20%

Table 3-1 - Stability range for each model parameters. Each model parameter is made up of a range of test sets. Each test set is a unique set of model parameters where all parameters are held constant at the base value while the parameter of interest is varied.

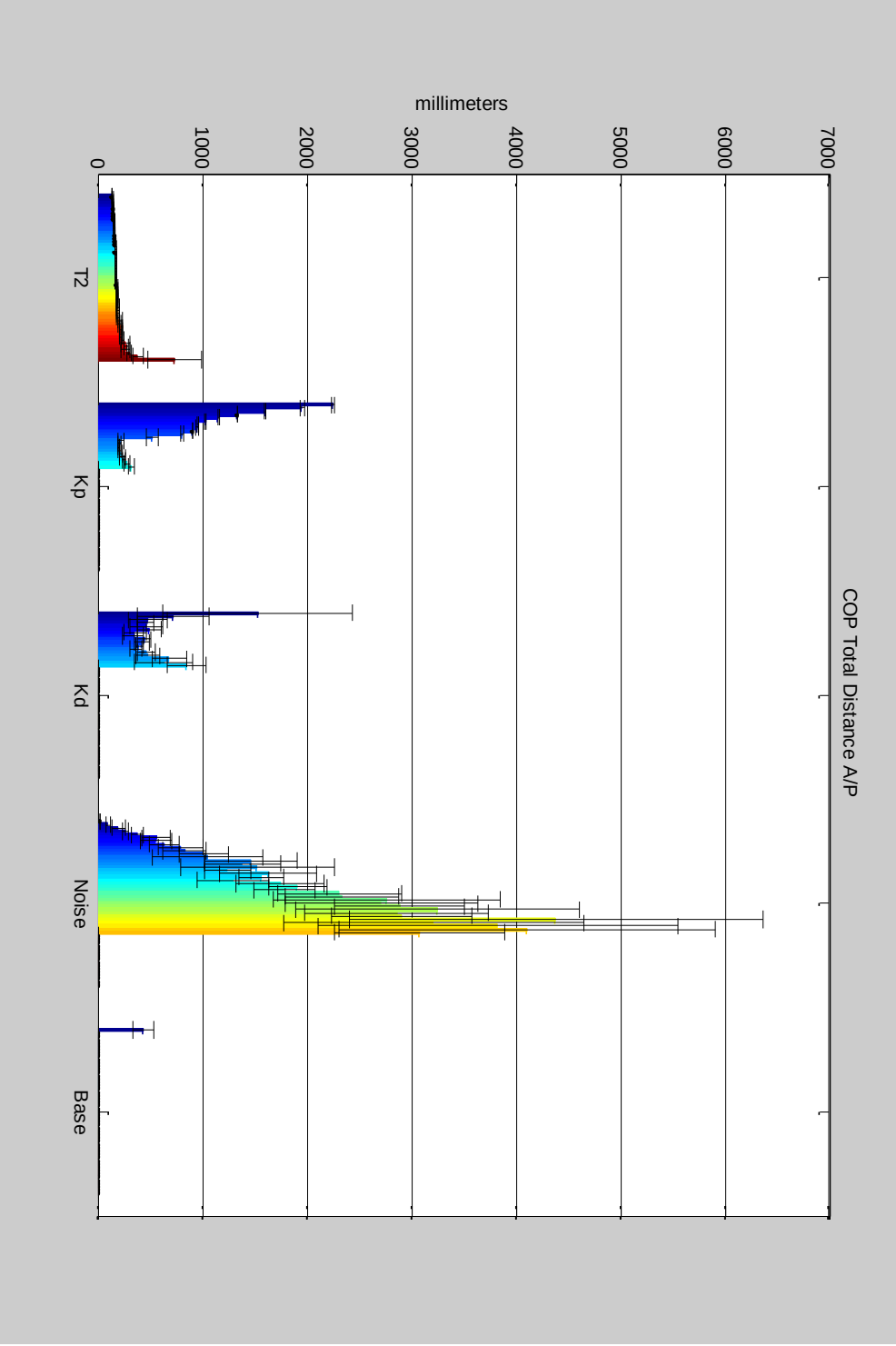

Figure 3-2 - Sensitivity Plots for COP Total Distance. Each bar depicts the mean and standard deviation for each test set for model parameter of interest. See figure Table 3-1 for the range of test sets show for each model parameter of interest.

		Model Parameters											
		T2			Kp			Kd			Kn		
COP Variables A/P	R^2	Slope	Intercept	R^2	Slope	Intercept	R^2	Slope	Intercept	R^2	Slope	Intercept
Total Distance	0.609	562.773	1,998.909	0.461	114,126.866	793,953.934	0.608	19.058	449.481	0.968	3.703	419.334
Maximum Displacement	0.533	24.599	80.012	0.510	12,614.806	89,677.680	0.092	0.171	11.634	0.832	0.083	11.544
Minimum Displacement	0.511	-24.031	-75.219	0.409	-17,155.696	-116,373.134	0.621	-0.357	-8.607	0.808	-0.083	-7.059
Range	0.522	48.629	155.230	0.451	29,770.502	206,050.814	0.456	0.528	20.242	0.958	0.165	18.603
Peak Velocity	0.503	163.283	504.831	0.475	1,428,768.077	9,996,655.070	0.543	1.641	54.021	0.971	0.471	52.517
Mean Velocity	0.608	18.778	66.692	0.468	2,941.814	20,527.080	0.608	0.635	14.990	0.968	0.124	13.985
Peak Acceleration	0.500	723.955	2,882.138	0.460	519,902,868.960	3,613,378,343.222	0.737	8.285	881.502	0.994	8.566	864.323
Mean Acceleration	0.562	96.094	463.751	0.459	923,142.875	6,411,123.863	0.708	2.295	192.675	0.999	1.848	189.382
RMS	0.586	3.566	13.161	0.514	37.702	271.551	0.307	0.071	3.301	0.916	0.025	2.999
Median Frequency	0.981	0.033	0.631	0.608	0.391	3.324	0.647	0.018	0.600	0.337	0.001	0.570

Table 3-2 - Linear Regression Data Table

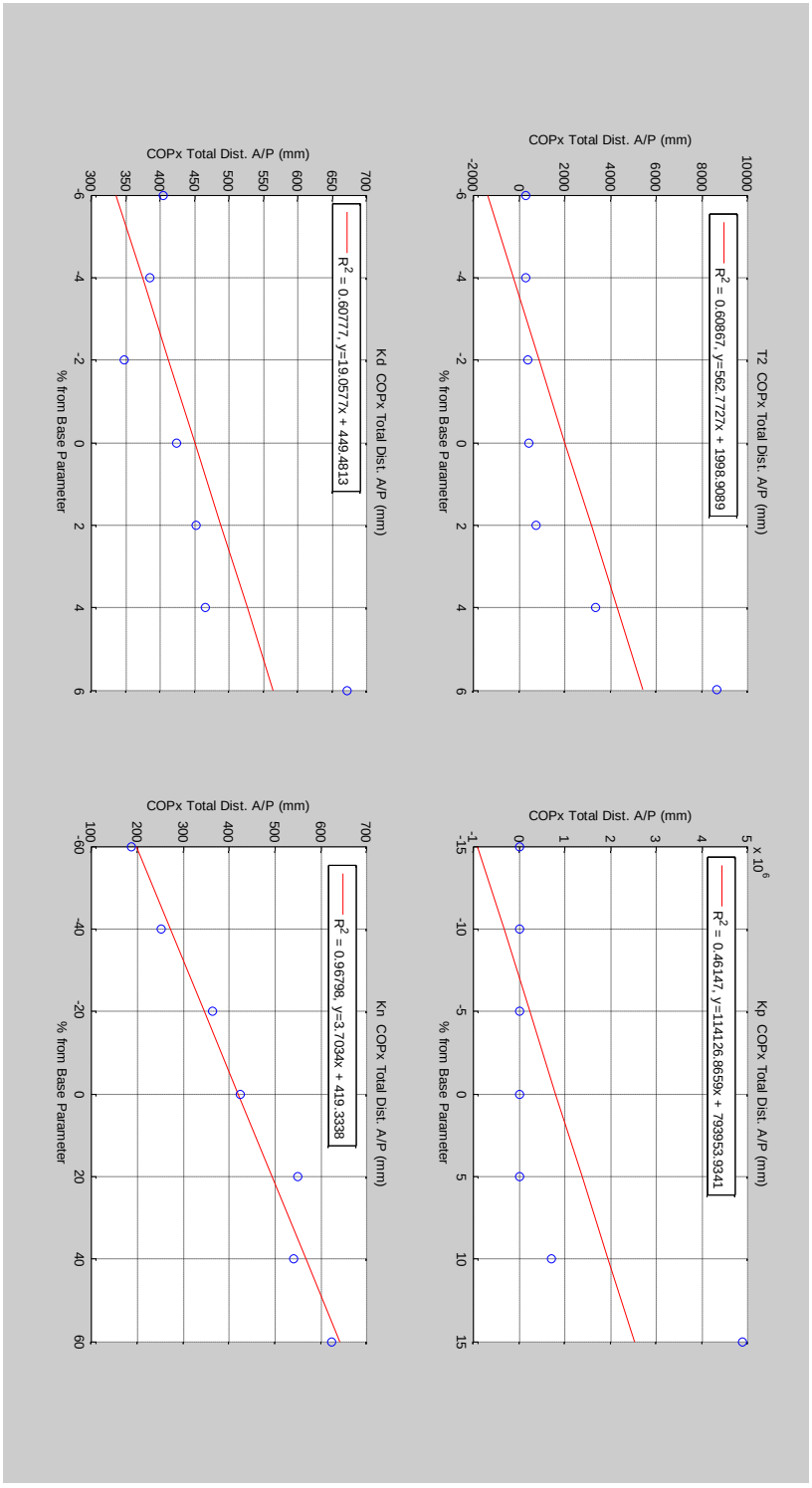

Figure 3-3 - Linear Regression Plots COP Total Distance AP

Trials	COP parameter Response to each Trial											Factorial Design Levels			
	COPx_tot_dist	COPx_max	COPx_min	COP_range_AP	vel_mean_x	peak_COP_speed_x	acc_mean_x	peak_COP_acc_x	RMS_COP_x	MedFREQ	T2	Kp	Kd	Kn
1	81.25505065	4.483919593	-1.310294899	5.794214492	2.714332972	12.5047695	71.47057301	337.8629341	1.063970719	0.285554354	137.5523	158.4304	914.5516	4.663977
2	95.36700397	5.509034144	-0.709295599	6.218329744	3.183171071	12.85061683	71.37194308	314.2638553	1.125716018	0.234196859	12.85062	158.4304	914.5516	4.663977
3	736.7120267	28.39699224	-21.8510088	50.24800104	24.56770381	137.5523048	158.4304156	914.5516208	4.663977022	0.727656664	137.5523	71.37194	914.5516	4.663977
4	6124132.491	299329.0778	-1412287.371	1711616.449	15495.4488	100147715.2	50973635.25	37009504606	1750.773978	16.78902623	12.85062	71.37194	914.5516	4.663977
5	87.14884429	4.445746987	-0.839793729	5.285540716	2.909553752	11.17203917	69.37828601	324.9816607	0.892756345	0.275115837	137.5523	158.4304	314.2639	4.663977
6	124.1542622	5.352284803	-4.309780266	9.662065069	4.141635439	15.98578726	73.51163139	345.6121033	1.67116527	0.28645462	12.85062	158.4304	314.2639	4.663977
7	2055.512013	89.84264676	-93.72537791	183.5680247	68.53983313	553.5306618	431.8798167	3410.701073	11.88216611	0.791183149	137.5523	71.37194	314.2639	4.663977
8	3808359.957	280112.3093	-595994.7643	876107.0736	95045.95955	50014585.9	32074885.62	1860589854	1127.821951	15.19384262	12.85062	71.37194	314.2639	4.663977
9	317.1824883	15.15258677	-14.81519831	29.96778508	10.59415796	46.91941103	280.2158242	1242.916146	6.275514419	0.251495526	137.5523	158.4304	914.5516	1.125716
10	390.5452912	12.41319853	-18.75018591	31.16338445	13.03518077	58.96154054	286.3914734	1330.039565	5.855345016	0.283934399	12.85062	158.4304	914.5516	1.125716
11	5987.159769	275.7151258	-259.1580898	534.8732156	199.6838635	1640.584798	1184.485829	8173.645564	37.99569206	0.829414732	137.5523	71.37194	914.5516	1.125716
12	4744630.955	499968.6009	-473507.8536	973476.4545	116511.5203	50281465.81	39750940.96	18852791208	1265.870201	15.90254774	12.85062	71.37194	914.5516	1.125716
13	355.9721186	14.6293081	-14.92247873	29.55117683	11.8837663	45.83802366	284.9955309	1264.502891	5.652171493	0.276800105	137.5523	158.4304	314.2639	1.125716
14	451.8706979	12.91733474	-17.9978022	30.91513694	15.07416602	65.47120012	295.0095719	1378.90018	5.507940919	0.401132751	12.85062	158.4304	314.2639	1.125716
15	57900.20449	3742.62143	-9344.554248	13087.17568	1659.907716	670721.0073	318744.8563	24211706 5.2	111.9501569	1.412987008	137.5523	71.37194	314.2639	1.125716
16	801619.4513	84004.48289	-80527.20606	164531.689	19735.18416	8492332.946	6678622.784	318248673 7	238.8052512	3.184469455	12.85062	71.37194	314.2639	1.125716

Table 3-3 - Design of Experiments Response Data and Factorial Level Design

Simple Statistics						
Variable	N	Mean	Std Dev	Sum	Minimum	Maximum
COPx_tot_dist	21	335.27903	129.3022	7041	192.72509	685.84465
COPx_max	21	-26.23904	47.23038	-551.01974	-119.01983	55.33674
COPx_min	21	-52.68668	46.42976	-1106	-138.28983	37.28125
COP_range_AP	21	26.44765	8.58197	555.40056	14.06401	43.03448
vel_mean_x	21	11.1934	4.3137	235.06136	6.44478	22.87773
peak_COP_speed_x	21	65.42324	23.76267	1374	30.7014	126.37068
acc_mean_x	21	227.81889	71.63565	4784	124.97204	430.3234
peak_COP_acc_x	21	1635	760.6892	34343	648.29998	3176
RMS_COP_x	21	4.26063	1.57265	89.47318	2.27418	7.67118
MedFREQ	21	0.45315	0.1393	9.51614	0.16586	0.80081

Table 3-4 - Experimental Statistical Data

Simple Statistics						
Variable	N	Mean	Std Dev	Sum	Minimum	Maximum
COPx_tot_dist	21	430.49746	108.86464	9040	319.13501	775.0856
COPx_max	21	12.33966	3.6048	259.1329	6.5051	22.1573
COPx_min	21	-7.00203	3.69745	-147.04266	-12.59497	-0.00361
COP_range_AP	21	19.34169	3.33174	406.17556	14.28069	27.98317
vel_mean_x	21	14.35772	3.62669	301.51203	10.64863	25.83811
peak_COP_speed_x	21	51.36944	11.34146	1079	36.53758	79.52939
acc_mean_x	21	193.02083	10.64192	4053	181.96785	228.09103
peak_COP_acc_x	21	883.79897	89.11377	18560	767.77411	1144
RMS_COP_x	21	3.10393	0.58968	65.18251	2.38201	4.73958
MedFREQ	21	0.57043	0.15732	11.97901	0.2706	0.84191

Table 3-5 - Model Base Set Statistical Data

Pearson Correlation Coefficients, N = 21										
	COPx_tot_dist	COPx_max	COPx_min	COP_range_AP	vel_mean_x	peak_COP_speed_x	acc_mean_x	peak_COP_acc_x	RMS_COP_x	MedFREQ
COPx_tot_dist	1	0.12725	0.01634	0.61191	1	0.89009	0.73462	0.43628	0.39964	0.63993
		0.5826	0.944	0.0032	<.0001	<.0001	0.0001	0.048	0.0727	0.0018
COPx_max	0.12725	1	0.98335	0.18335	0.12647	0.19028	-0.14839	0.22552	0.18718	-0.13389
	0.5826		<.0001	0.4263	0.5849	0.4087	0.5209	0.3256	0.4165	0.5629
COPx_min	0.01634	0.98335	1	0.00168	0.01558	0.08952	-0.23839	0.14969	0.023	-0.10515
	0.944	<.0001		0.9942	0.9466	0.6996	0.298	0.5172	0.9212	0.6501
COP_range_AP	0.61191	0.18335	0.00168	1	0.61173	0.56288	0.47311	0.43128	0.90571	-0.16796
	0.0032	0.4263	0.9942		0.0032	0.0079	0.0303	0.0509	<.0001	0.4668
vel_mean_x	1	0.12647	0.01558	0.61173	1	0.89008	0.7359	0.43721	0.3996	0.6401
	<.0001	0.5849	0.9466	0.0032		<.0001	0.0001	0.0475	0.0727	0.0018
peak_COP_speed_x	0.89009	0.19028	0.08952	0.56288	0.89008	1	0.65448	0.54413	0.3616	0.55335
	<.0001	0.4087	0.6996	0.0079	<.0001		0.0013	0.0108	0.1073	0.0093
acc_mean_x	0.73462	-0.14839	-0.23839	0.47311	0.7359	0.65448	1	0.65265	0.37374	0.4456
	0.0001	0.5209	0.298	0.0303	0.0001	0.0013		0.0013	0.0951	0.0429
peak_COP_acc_x	0.43628	0.22552	0.14969	0.43128	0.43721	0.54413	0.65265	1	0.52262	0.05041
	0.048	0.3256	0.5172	0.0509	0.0475	0.0108	0.0013		0.0151	0.8282
RMS_COP_x	0.39964	0.18718	0.023	0.90571	0.3996	0.3616	0.37374	0.52262	1	-0.40064
	0.0727	0.4165	0.9212	<.0001	0.0727	0.1073	0.0951	0.0151		0.0719
MedFREQ	0.63993	-0.13389	-0.10515	-0.16796	0.6401	0.55335	0.4456	0.05041	-0.40064	1
	0.0018	0.5629	0.6501	0.4668	0.0018	0.0093	0.0429	0.8282	0.0719	

Table 3-6 - Pearson Correlation Experimental Data: For each parameter correlation the upper value is the Pearson correlation coefficient and the lower value is the p-value.

Pearson Correlation Coefficients, N = 21										
	COPx_tot_dist	COPx_max	COPx_min	COP_range_AP	vel_mean_x	peak_COP_speed_x	acc_mean_x	peak_COP_acc_x	RMS_COP_x	MedFREQ
COPx_tot_dist	1	0.34033	-0.36561	0.77396	1	0.78842	0.91049	0.31459	0.86575	0.46804
		0.1312	0.1031	<.0001	<.0001	<.0001	<.0001	0.1649	<.0001	0.0324
COPx_max	0.34033	1	0.5839	0.43396	0.34061	0.18338	0.29408	-0.10826	0.44025	-0.54433
	0.1312		0.0055	0.0494	0.1308	0.4262	0.1957	0.6404	0.0458	0.0107
COPx_min	-0.36561	0.5839	1	-0.47801	-0.36543	-0.47292	-0.3579	-0.12139	-0.34877	-0.83649
	0.1031	0.0055		0.0284	0.1033	0.0304	0.1112	0.6002	0.1213	<.0001
COP_range_AP	0.77396	0.43396	-0.47801	1	0.77406	0.72324	0.71537	0.01758	0.86338	0.33936
	<.0001	0.0494	0.0284		<.0001	0.0002	0.0003	0.9397	<.0001	0.1323
vel_mean_x	1	0.34061	-0.36543	0.77406	1	0.78878	0.91037	0.31474	0.86579	0.46793
	<.0001	0.1308	0.1033	<.0001		<.0001	<.0001	0.1646	<.0001	0.0324
peak_COP_speed_x	0.78842	0.18338	-0.47292	0.72324	0.78878	1	0.79496	0.46653	0.62643	0.57756
	<.0001	0.4262	0.0304	0.0002	<.0001		<.0001	0.033	0.0024	0.0061
acc_mean_x	0.91049	0.29408	-0.3579	0.71537	0.91037	0.79496	1	0.31017	0.76373	0.43087
	<.0001	0.1957	0.1112	0.0003	<.0001	<.0001		0.1712	<.0001	0.0512
peak_COP_acc_x	0.31459	-0.10826	-0.12139	0.01758	0.31474	0.46653	0.31017	1	0.03444	0.28172
	0.1649	0.6404	0.6002	0.9397	0.1646	0.033	0.1712		0.8822	0.216
RMS_COP_x	0.86575	0.44025	-0.34877	0.86338	0.86579	0.62643	0.76373	0.03444	1	0.31563
	<.0001	0.0458	0.1213	<.0001	<.0001	0.0024	<.0001	0.8822		0.1634
MedFREQ	0.46804	-0.54433	-0.83649	0.33936	0.46793	0.57756	0.43087	0.28172	0.31563	1
	0.0324	0.0107	<.0001	0.1323	0.0324	0.0061	0.0512	0.216	0.1634	

Table 3-7 - Pearson Correlation Model Base Set Data: For each parameter correlation the upper value is the Pearson correlation coefficient and the lower value is the p-value

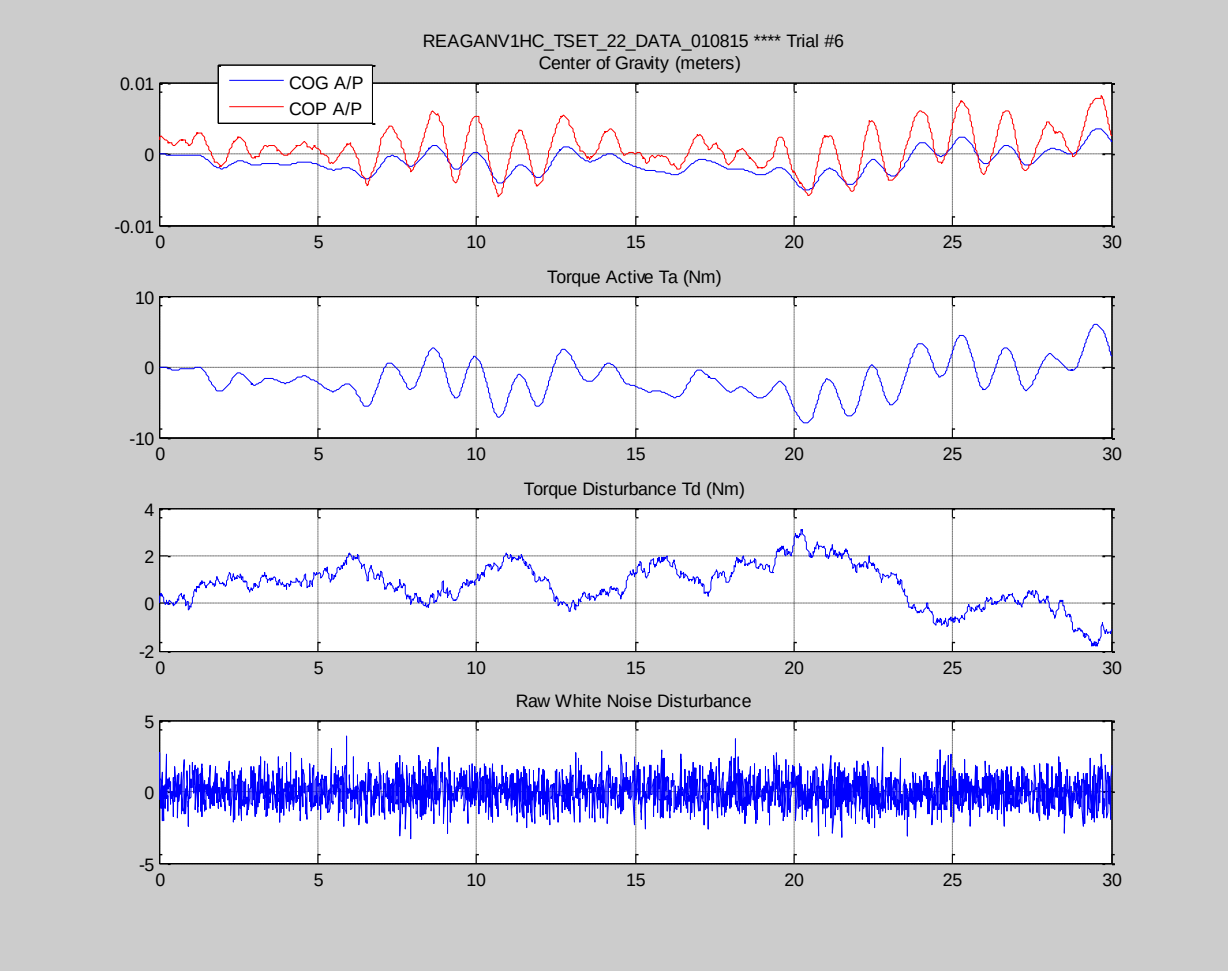

Figure 3-4 - Data Quality Plots / Experiment 301 Test Set 22 / K_n =786.55 K_d =7.0143 K_p =22.36 T_2=0.1470 / Stable Base set

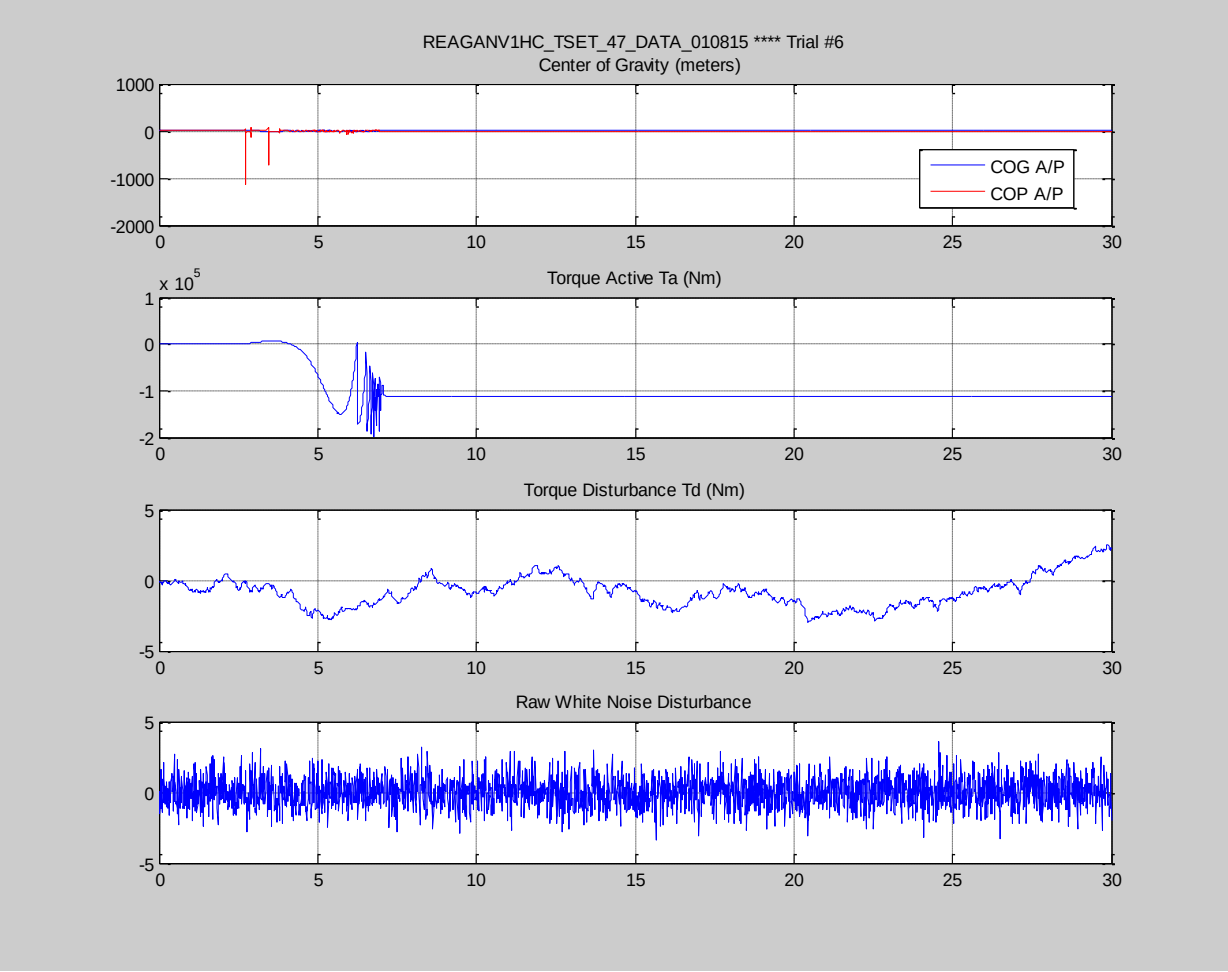

Figure 3-5 - Data Quality Plots / Experiment 303 Test Set 47 / K_d =5.0503 / % from base = -28% / Severe Instability

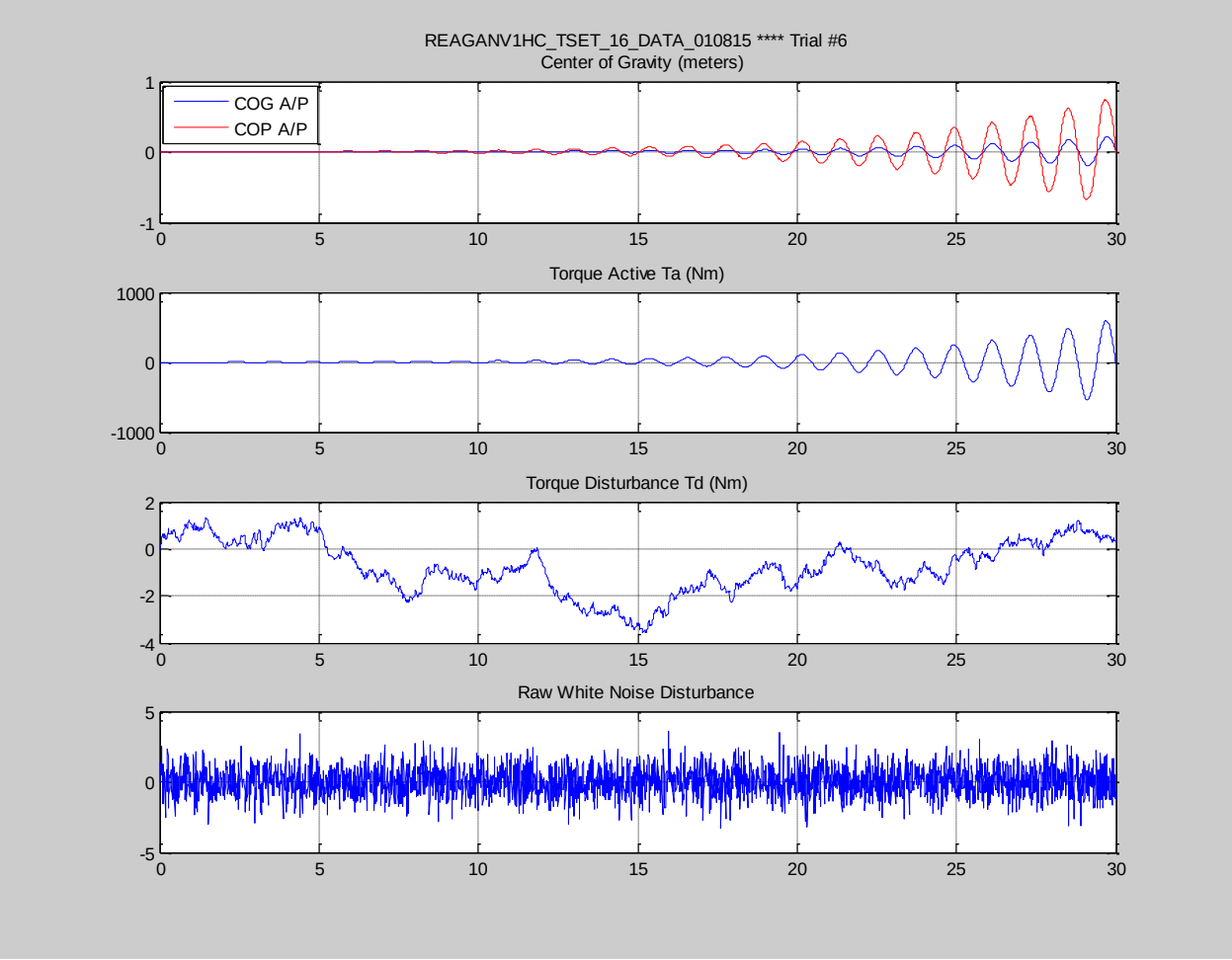

Figure 3-6 - Data Quality Plots / Experiment 301 Test Set 16 / T_2= 0.155 seconds / %change from base=+6%

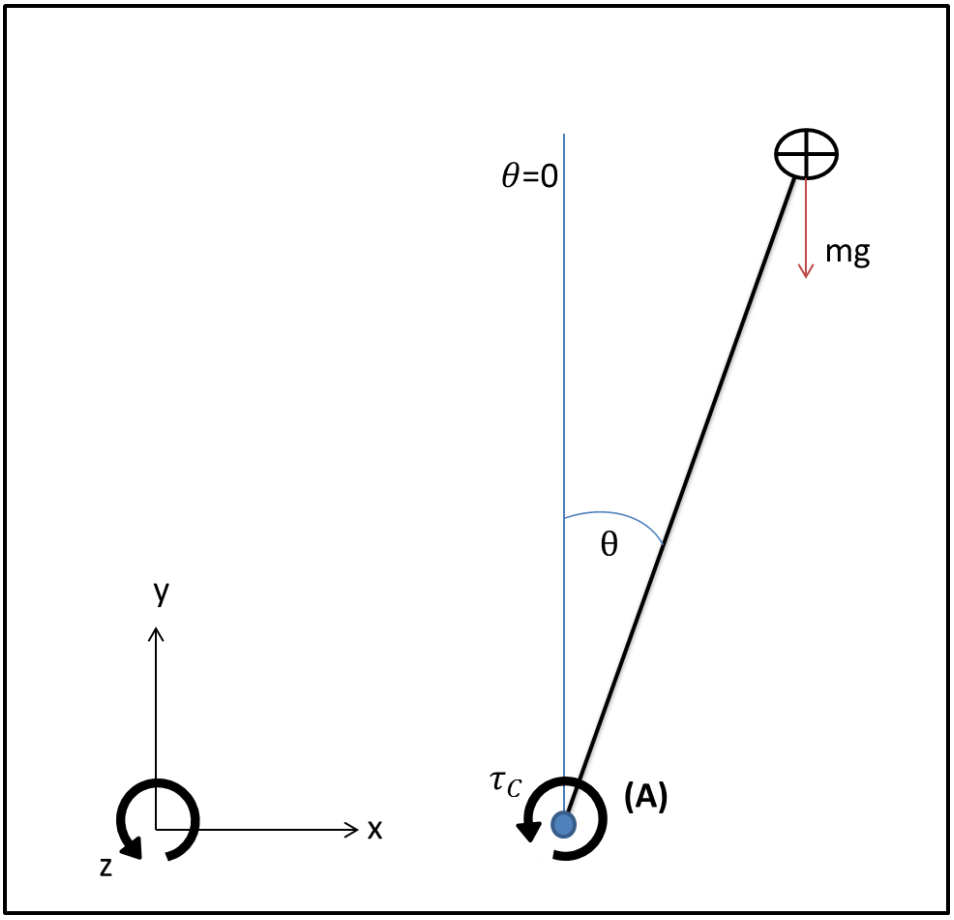

Figure 3-7 - Inverted Pendulum Model Diagram and COP Derivation

The following is a diagram of the classic inverted pendulum model used throughout the study to develop equations of motion and the ADAMS model validation.

Theta = the angle relative to the y- plane

t_c= torque active control

m= mass of the pendulum located at the center of mass

g=acceleration due to gravity

Measured Parameters from Experimental Study	
Total height	H
Thigh length	l_T
Total mass of subject	M
Ankle height	$y1$
Calf length	l_C
Foot length	l_F

Table 3-8. Measured Parameters from Experimental Study

List of parameters measured from experimental study. These parameters were either directly used for model parameters and cop calculations or used in the approximation of other parameters for the inverted pendulum model

Approximated Parameters of Inverted Pendulum	
Trunk length ($\boldsymbol{l_1}$)	$l_1 = .818H + .530(l_1 + l_2 + a)$
Leg length, no ankle($\boldsymbol{l_2}$)	$l_2 = l_T + l_C$
Mass of pendulum, no feet($\boldsymbol{m}$)	$m = .971M$
Length of the pendulum, ankle to COM ($\boldsymbol{h}$)	$h = .261l_1 + .945l_2$
Moment of inertia about ankle joint($\boldsymbol{I}$)	$I = .678M(.347l_1 + l_2)^2 + .192Ml_2^2$
Foot COM anterior-posterior from ankle $\boldsymbol{f_{com}}$	$x_0 = .5l_F$
Foot mass	$m_f = 0.0145l_F$

Table 3-9. Approximated Parameters of Inverted Pendulum

List of parameters approximated from values in measured in experimental study found in table 1. These parameters were either used for the inverted model directly or to calculate the COP parameters of the model.

Chapter 4 : Modelling Parkinson's disease

Abstract

Background. Previous studies have developed and utilized a model of the human body during quiet standing to investigate the effects of aging on the control of postural sway. The current study utilizes a similar model to investigate the effects of Parkinson's disease by determining the range of model parameters that results in model center of pressure (COP) measures similar to those measured experimentally in groups of healthy controls (HC) and Parkinson's disease (PD).

Methods. Robust ranges from the previous study were decomposed in order to obtain limits defined by the outer boundaries of the COP measure of the two groups. Second, a comparative analysis was performed to relate the model COP measures to the COP measure of each group. Finally, a more conservative ANOVA analysis was performed to investigate the significance of each mode COP measure to the measures of the groups independently.

Results. The comparative analysis showed no discernible difference when investigating the proportional gain and feedback time delay. The HC and PD groups were related to different test sets of model parameters driven by the derivative and noise gain parameters. Similar results were observed in the ANOVA technique, with a more conservative bias.

Conclusions. The comparative analysis and ANOVA both showed similar trends for the model parameters of interest. Changes in the neuromuscular noise and derivative gain showed the ability to exclusively result in COP measures related to PD and HC. This study suggests further investigation into the progression of PD groups.

Introduction

The COP time series has been studied extensively with the goal of understanding the dynamics and controls of human bipedal quiet stance. Changes in COP patterns can be induced through the removal of sensory feedback methods (e.g. visual, vestibular, cutaneous, or proprioceptive) (Palmieri, Ingersoll, Stone, & Krause, 2002), or by the presence of a disease, aging, or injury that affects the central nervous system which may impair the ability to control balance. Balance impairments caused by pathological changes are often related to neurodegenerative diseases.

Parkinson's disease (PD) is a neurodegenerative disease that causes symptoms of rigidity, bradykinesia (slowed movements), postural instability, and tremor. These symptoms are known to be caused by dopamine degeneration changes affecting the basal ganglia function. The degeneration of dopamine containing cells results in adverse changes to the motor cortex (Centonze, Calabresi, Giacomini, & Bernardi, 1999). Postural instability is a significant problem for the PD patient and has been quantified through the analysis of the COP time series using biomechanical measures. Differences in the COP time series between HC and PD subjects for COP measures have been observed, and could potentially provide information about the onset and progression of postural instability within PD (Barnds, 2015; Mancini et al., 2012; McVey et al., 2013; Stylianou, McVey, Lyons, Pahwa, & Luchies, 2011).

However, the COP time series is an output of a very complex system, thus this information alone may have limited value in assessing the changes in balance ability related to disease progression. PD is primarily a brain disease, affecting the control of the system. An engineering analysis that includes a simplified model of the "plant" (i.e. the human body) and the actions of the controller (i.e. the brain) may represent an approach that is more sensitive to small

changes in the system due to the adverse effects of PD. Recent studies using control theory coupled with a model of the dynamic system have shown promise in revealing insight into the changes taking place within the central nervous system which result in corresponding changes in postural sway measures.

The COP time series has been studied experimentally through the measurement of the foot-floor forces and moments using force plate measures of human subjects. Quantities such as COP mean velocity appear to accurately reflect postural stability during postural sway tasks (Ruhe, Fejer, & Walker, 2010). During the postural sway task, the subject is asked to simply stand relaxed for a period of time, with eyes open or closed, and with the feet in a prescribed configuration (e.g. comfortable stance, a set stance, feet placed right next to each other side-to-side or front-to-back). One advantage to the postural sway task is that it can be done with subjects with significant balance problems as long as they are able to stand for a short period of time without external support.

More recently, the COP has been extracted from models of the dynamic control of an inverted pendulum representing the human body during quiet stance. Single inverted pendulum models have been developed to the point that model COP time series are comparable to those obtained experimentally for young adults and elderly adults (Maurer & Peterka, 2005). A human subject in the anterior-posterior direction is modeled as a single inverted pendulum, which is the dynamic plant that is controlled using a linear feedback controller. Proportional-integral-derivative and proportional-derivative controllers have both been investigated to control the upright stabilization of the pendulum, and achieve realistic sway measures of COP (Masani, Popovic, Nakazawa, Kouzaki, & Nozaki, 2003; Masani, Vette, & Popovic, 2006; Maurer & Peterka, 2005). Physiological noise and time delays are both added to the mathematical

equations in order to create a more physiologically accurate model (Masani, Vette, Abe, & Nakazawa, 2014; Maurer & Peterka, 2005; Peterka, 2000). The ability of the model to provide COP measures comparable to those found experimentally increases its potential to improve our understanding of the impact that injury, aging, and neurodegenerative diseases have on the operation of the central nervous system.

The effects of PD on the actions of the brain as a controller have not been previously investigated using a single inverted pendulum model. In Chapter 3 a model was developed and COP output measures were validated with experimental data of HC subjects during eyes closed stance. The HC validated model will provide a basis for this study.

The primary goal of this study is to explore how changing the model input parameters effects output COP measures related to HC subjects and PD subjects during eyes close quiet stance. Toward this goal, we first defined the limits of each model parameter when varied independent of the other model parameters. These parameter limits were based on the boundaries of the output COP measures of the previously measured experimental HC and PD groups. Secondly, we explored the effect of model input parameter changes on the model COP measures, and then used two methods to investigate how these model COP measures are related to the experimentally determined COP measures for HC and PD groups. The first method was a comparative analysis that employed boundary conditions defined by the individual experimental groups' standard deviation and mean for each COP measure considered. The second method used a more conservative ANOVA analysis where each experimental group was tested for significant differences when compared to the model output COP measures. The long term goal of this research is to determine the effect that PD has on actions of the brain as the controller during motor control tasks.

Methods

Experimental data previously recorded in the University of Kansas Biodynamics Laboratory was used in this study. This data was recorded from 21 HC subjects (66 ± 8 years, 13 males, and 8 females) and 23 PD subjects (65 ± 7 years, 15 males, 8 females) during eyes closed postural sway. A subset of these participants (n = 12 HC and n = 11 PD) were from a previous postural sway study looking at the effects of visual conditions on COP measures (Stylianou et al., 2011). The following explains the methods used to determine the model parameters and the statistical methods used for the comparison.

For each model parameter, a range of test sets was created by varying the model parameter of interest while holding the other parameters at the base set of values validated as the "healthy test set" as described in Chapter 3. Each change in the model parameters used to define a new test set is calculated as the percentage difference from the model parameter's base value. The percentage that each parameter was incremented from the base value was determined by the effect on the model stability reported in Chapter 3.

Each test set from the stability ranges of the model parameters previously mentioned in Chapter 3 was used in this study. An example of the test set and ranges can be seen in Figure 4-1. A test set is defined by the unique values of the model parameters that result in the six COP measures that are listed in the figure. Each test set shows the averages of the COP measures recorded over 6 simulations of the model. Differences in model simulations from one test to the next are the result of the random noise added to the applied ankle torque which represents neuromuscular noise. The six COP parameters investigated were A/P COP: total distance, range, peak speed, mean velocity, median frequency, and RMS. These parameters were chosen because

they were found to be significantly different between HC and PD in previous studies (Barnds, 2015).

Limits for Center of Pressure within the Subject Groups

For each COP measure, a lower boundary was defined by subtracting one standard deviation from the mean of the experimental HC group in the eyes closed condition. The upper boundary for each group was defined by adding one standard deviation to the mean of the experimental PD group in the eyes closed condition. For each test set, data was collected to show the COP measures that were within these defined boundaries. Test sets that had at least 3 model COP measures within these boundaries were retained. For each model parameter, a range of test sets were retained based on this systematic approach to create a limit of the realistic COP model measures corresponding to the COP measures in the experimental groups. This was used as a starting point for the comparative analysis.

Comparative Analysis

A comparative analysis was used to relate the model COP measures to the COP measures of HC and PD groups. This analysis was performed similar to the approach used to define the limits of realistic COP measures for each test set. In the comparative analysis, boundaries were defined by the COP measures from each experimental group. The HC group boundary was defined by one standard deviation above and below the mean for each COP measure. The PD group boundary was defined in the same way for the corresponding COP measure. These two boundary ranges were applied to the COP measures for each test set of the model parameter ranges that were defined in the previous section. Test sets that resulted in at least 3 COP measures that were comparable to the HC or PD groups (within one standard deviation of the group mean) were considered similar to the respective group.

ANOVA

An analysis of variance (ANOVA), with a $p \leq 0.05$ defined as significant, was performed on each subject group, HC and PD independently. The model COP measures for each test were tested for significant differences compared to the experimental group of interest. Each model COP measure that was not found to be significantly different compared to the COP group measure was recorded (considered similar to the group compared to the model test set). A set of tables were created to show the test sets that were found to be significantly different from the group of interest (i.e. HC versus PD) by the ANOVA.

Results

Limits for Center of Pressure of the Group

Feedback Time Delay (T_2). The stability range previously observed in Chapter 3 for the feedback time delay was -100% to 2% from the base model parameter value of 0.147 seconds. Each test set was developed in 2% increments. This range corresponds to time delays of 0 to 0.150 seconds. This range was further decomposed by the limit analysis of the COP measures. The range derived from the limit analysis for the feedback time delay was -14 % to 2%. This range corresponds to time delays of 0.126 to 0.150 seconds.

Proportional Gain (K_p). The stability range previously observed in Chapter 3 for the proportional gain was -100% to 2% from the base model parameter value of 22.36 $\frac{N*m}{deg}$. Each test set was developed in 5% increments. This range corresponds to gain values of 0 to 22.36 $\frac{N*m}{deg}$. This range was further decomposed by the limit analysis of the COP measures. The range derived from the limit analysis for the proportional gain was -30 % to 0%. This range corresponds to gain values of 15.65 to 22.36 $\frac{N*m}{deg}$.

Derivative Gain (K_d). The stability range previously observed in Chapter 3 for derivative gain was -24% to 10% from the base model parameter value of 7.01 $\frac{N*m*sec}{deg}$. Each test set was developed in 2% increments. This range corresponds to gain values of 5.19 to 7.72 $\frac{N*m*sec}{deg}$. This range was further decomposed by the limit analysis of the COP measures. The range derived from the limit analysis for the derivative gain was -22 % to 10%. This range corresponds to gain values of 5.47 to 7.72 $\frac{N*m*sec}{deg}$.

Noise (K_n). The stability range previously observed in Chapter 3 for the noise gain was -100% to 600% from the base model parameter value of 786.56 $N * m$. Each test set was developed in 20% increments. This range corresponds to gain values of 0 to 5505.89 $\frac{N*m*sec}{deg}$. This range was further decomposed by the limit analysis of the COP measures. The range derived from the limit analysis for the noise gain was -20 % to 140%. This range corresponds to gain values of 629.24 to 1101.20 $\frac{N*m*sec}{deg}$.

Comparative Analysis

Feedback Time Delay (T_2). The comparative analysis of the time delay (T_2) model parameter showed COP mean velocity, median frequency, and total distance measures were consistently comparable to the experimental HC group. For both the HC and PD groups, COP range and peak speed were not comparatively different across the test sets. The test sets with T_2 0% and 2% above the base set recorded the greatest number of COP measures (best aligned with the experimental data) for both PD and HC. Table 4-1 and Table 4-2 show the graphs for both PD and HC standard deviation boundaries.

Proportional Gain (K_p). The K_p model parameter comparative analysis showed similar results to T_2. For COP mean velocity, 5 out of the 7 test sets were related to both PD and HC groups. For COP total distance 6 out of the 7 test sets were related to both PD and HC groups. The model COP peak speed was found to be not significantly different in only the base set of parameters for both groups. Both groups, organized by boundaries for HC and PD, are shown in Table 4-3 and Table 4-4.

Proportional Gain (K_d). The K_d comparative analysis produced several test sets for each PD and HC group, that had all COP measures of interest within the prescribe group boundaries. For HC this occurred at -18%, -16%, -4%, and -2%. For PD all COP measures were within the boundaries at 6%, 8%, 10%, -18%, and -22%. Note that -18% was shared at full capture of the COP measures by both standard deviation boundaries for groups PD and HC. Furthermore, from -16% to 4% COP range and COP RMS modeled COP measures were not within the boundaries for PD but were shown within the boundaries of the HC groups in a majority of the test sets. This can be described visually in Table 4-5 and Table 4-6.

Noise (K_n). For K_n all model COP measures were within the boundaries of the PD limits at 60% to 140%. No test sets had all COP measures capture by HC, but -20%, 0% and 60% each caught 4 COP measures. Furthermore, HC only caught 1 COP measure for 100%, 120%, and 140%, which was Median Frequency. The group results can be seen visually in Table 4-7 and Table 4-8.

ANOVA

Feedback Time Delay (T_2). For the ANOVA analysis model COP measure were investigate to be either found significantly different or not significantly different from the experimental group of interest, PD or HC. For T_2, no model COP measures were found significantly different for either the PD or HC group.

Proportional Gain (K_p). For the ANOVA of the K_p model COP measures, -20% to 0% found at least 5 COP measures for a given test set not significantly different from HC. All but one test set for COP peak speed was found significantly different from both experimental groups PD an HC. For the PD group all test sets model COP measures of peak speed and COP range averages were found significantly different. No test set for PD found more than 4 COP measures that were not significantly different from the PD experimental group

Proportional Gain (K_d). The ANOVA analysis for K_d test sets investigated the relationship of the modeled COP measures with the experimental COP measures of the PD and HC groups. For test sets from -20% to 4%, all COP measures were shown to be not significantly different from the HC group. This was the case for the PD group from -22%, 6%, and 10%. For the PD ANOVA, model COP range measures from -20% to 4% for mode were found to be significantly different. Furthermore, the PD ground ANOVA of the model RMS measure significance from -20 to 4%, except for the 18% test set of the RMS measure.

Noise (K_n). The K_n ANOVA of the COP model measures showed that the test sets from 20 to 140% were not significantly different from the PD groups. Furthermore, from -20 to 60% the HC group showed no significant difference for any of the COP model measures except for one case of the median frequency at the 20% test set. The test sets of K_n from 120% and 140% were found to be significantly different from the HC group for all model parameters except for median frequency. For the PD group the peak speed, COP range, and RMS model parameters for the -20% and 0% test sets were found to be significantly different.

Discussion

The primary goal of this study was to use a postural sway model developed in Chapter 3 to investigate how PD affects the neuromuscular system. The system components investigated were the brain as a controller, the neuromuscular noise induced in the system, and the feedback time delay from the sensory system to the brain. In this study the experimental groups that were taken into consideration were HC and PD subjects during eyes closed quiet stance. The first part of this investigation used the known boundaries of the two groups to limit the quantity of the data to test sets with realistic COP measures. In the second half of this study we looked at how the model COP measures could be related to the experimental COP measures that would provide insight to the changes of the model parameters that simulate physiological components.

Comparative Analysis of Model COP measures versus Experimental groups

In the comparative analysis we were able to see similar trends for both groups in the T_2 ranges. In detail, the COP total distance and velocity mean were found within the boundaries of both groups for a majority of the test sets and the COP range and RMS were found to be outside of the boundaries for both groups for a majority of the test sets. Both groups found the most COP measures within the 0, -2, and 2 % test sets. A clear difference between the groups is hard to see

from the test sets. This was similarly found in the K_p COP model measures when compared with the two groups. These findings show that there was not a noticeable difference in the changes of the K_p and T_2 model parameters effects on the COP model measures when comparing to the two groups. In other words, there was no distinct change in the COP measures that related specifically to one of the two groups. This suggests that PD does not cause changes in the proportional gain and feedback time delay when related using the comparative analysis technique.

In performing this same technique on the derivative gain control and the noise gain we found very different results. Table 4-5 and Table 4-6 demonstrate that there are test sets uniquely comparable to the two groups. The COP measures, COP range, and COP RMS are left definably outside of the boundaries for a large range of the PD group, where they are not in the HC group. This is a trend that was not observed in the previous two model parameters. Furthermore, we see that COP total distance, velocity mean, and median frequency each have a range of test sets where they are found outside the HC boundaries, but not in the PD boundaries. This similar trend is seen in the noise gain model parameter. One can easily observe the test sets that are strongly comparable to the two groups with the information for each of the COP model measures that are found within the boundaries. This suggests that noise and derivative gain changes could be the cause of COP changes observed between HC and PD groups.

ANOVA Analysis of Model COP measures versus Experimental Groups

The ANOVA analysis was used as an alternative method, to investigate how the COP group measures compared to the model COP measures. No differences were found when comparing the test ranges for K_p and T_2 to the two groups. The results for K_n and K_d show test

sets comparable to the PD only and HC only. This finding suggests that PD may cause changes to the derivative gain and neuromuscular noise.

Effects of model parameter changes on COP measures related to HC and PD

Both analysis techniques presented similar results when the group comparisons are visually represented. It is clear from the ANOVA and comparative analysis tables for the feedback time delay and the proportional gain that these parameters do not produce COP measures related specifically to the PD or HC group. For the derivative gain it is easier to represent test cases where more COP measures are related to one group or the other. However, when comparing to the ANOVA and comparative analysis tables for the model parameter K_n, the distinction between test sets related to PD and HC groups is more defined. The results of the ANOVA and comparative analysis suggest that the neuromuscular noise and the derivative gain could be a factor in the progression of PD.

The results for the comparison methods for K_n and K_d show similar trends for the individual COP measures when related to the specific groups. The measures COP Range and RMS were related to the HC group when it is not related to the PD group for a range of test sets. The measures for COP total distance and velocity mean are related to PD when not related to the HC group for a separate range of test sets. This is caused by the variance of the COP measure for the specified group. This suggests that the HC group controls a smaller range for continuous measures of COP total distance and velocity mean in contrast to the large range of the PD group. This further suggests that a strong indication of PD could be COP total distance and velocity mean and is supported in other threshold studies on PD versus HC group COP measures (Barnds, 2015).

The large variances of the experimental data for each group's COP measures causes overlap of the test sets that fall within the boundaries. Furthermore, this inability to have a clear cutoff between the groups can be attributed to the variance caused by having subjects being different ages and body types. Another factor relating to this overlap is that the PD subjects are from a mixture of mild and moderate progression. It is very likely that some of these subjects exhibit COP measures that are closer to HC subjects than more progressive stages of PD. This could be a potential area of study in the future. It is important to determine if the methods used in this study are capable of differentiating between HC and mild PD (i.e. detecting early onset of changes in the controller) as well as between mild and moderate PD (i.e. tracking disease progression).

This study was limited by being an initial study into the effects of PD on our model control parameters. The study does not include any changes to the "plant" that PD may introduce such as bradykinesia, rigidity, and involuntary tremors. This study investigated the effects of independently changing one model parameter while holding the other parameters at a base value. Future studies are planned to investigate changes in multiple parameters and likely will involve optimization to best fit a set of COP measures. Furthermore, this study limited the complexity of the "plant" and "control" models, providing a good first step, but both models will be increased in complexity in the future. Even so, this model approach has the capabilities of being manipulated easily in order to understand the dynamics and control during postural sway.

Conclusions

This study provided insight into the effects of model parameter changes that simulate the neuromuscular control system on the output COP measures. The comparative analysis and ANOVA analysis provided two different techniques for comparing the COP model measures to

those observed experimentally in the HC and PD groups. The results demonstrate that the model parameters for the derivative gain K_p and feedback time delay T_2, when varied from the base set of model parameters, did not simulate output COP measures that were comparable to one group over the other. However, the model parameters for the input noise K_n and the derivative gain of the controller K_d, both showed when independently changed from the base model parameters, the ability to identify test sets that were unique to a particular group. Overall this study suggests that the changes to the model parameters that represent the neuromuscular noise and the derivative controller can be related to COP measures that are found in PD subjects.

References

Barnds, A. N. (2015). *Biomechanical Markers as Indicators of Postural Instability Progression in Parkinson's Disease.* (Dissertation).

Centonze, D., Calabresi, P., Giacomini, P., & Bernardi, G. (1999). Neurophysiology of Parkinson's disease: from basic research to clinical correlates. *Clinical Neurophysiology, 110*(12), 2006-2013. doi: 10.1016/s1388-2457(99)00173-x

Mancini, M., Carlson-Kuhta, P., Zampieri, C., Nutt, J. G., Chiari, L., & Horak, F. B. (2012). Postural sway as a marker of progression in Parkinson's disease: A pilot longitudinal study. *Gait & Posture, 36*(3), 471-476. doi: 10.1016/j.gaitpost.2012.04.010

Masani, K., Popovic, M. R., Nakazawa, K., Kouzaki, M., & Nozaki, D. (2003). Importance of body sway velocity information in controlling ankle extensor activities during quiet stance. *Journal of Neurophysiology, 90*(6), 3774-3782. doi: 10.1152/jn.00730.2002

Masani, K., Vette, A. H., Abe, M. O., & Nakazawa, K. (2014). Center of pressure velocity reflects body acceleration rather than body velocity during quiet standing. *Gait & Posture, 39*(3), 946-952. doi: 10.1016/j.gaitpost.2013.12.008

Masani, K., Vette, A. H., & Popovic, M. R. (2006). Controlling balance during quiet standing: Proportional and derivative controller generates preceding motor command to body sway position observed in experiments. *Gait & Posture, 23*(2), 164-172. doi: 10.1016/j.gailpost.2005.01.006

Maurer, C., & Peterka, R. J. (2005). A new interpretation of spontaneous sway measures based on a simple model of human postural control. *Journal of Neurophysiology, 93*(1), 189-200. doi: 10.1152/jn.00221.2004

McVey, M. A., Amundsen, S., Barnds, A., Lyons, K. E., Pahwa, R., Mahnken, J. D., & Luchies, C. W. (2013). The effect of moderate Parkinson's disease on compensatory backwards stepping. *Gait & Posture, 38*(4), 800-805. doi: 10.1016/j.gaitpost.2013.03.028

Palmieri, R. M., Ingersoll, C. D., Stone, M. B., & Krause, B. A. (2002). Center-of-pressure parameters used in the assessment of postural control. *Journal of Sport Rehabilitation, 11*(1), 51-66.

Peterka, R. J. (2000). Postural control model interpretation of stabilogram diffusion analysis. *Biological Cybernetics, 82*(4), 335-343. doi: 10.1007/s004220050587

Ruhe, A., Fejer, R., & Walker, B. (2010). The test-retest reliability of centre of pressure measures in bipedal static task conditions - A systematic review of the literature. *Gait & Posture, 32*(4), 436-445. doi: 10.1016/j.gaitpost.2010.09.012

Stylianou, A. P., McVey, M. A., Lyons, K. E., Pahwa, R., & Luchies, C. W. (2011). Postural Sway in Patients with Mild to Moderate Parkinson's Disease. *International Journal of Neuroscience, 121*(11), 614-621. doi: 10.3109/00207454.2011.602807

Base Test Set

Test set Kn 80% greater than base set Kn

Mean Responses - Kn									
% Change from Base	-20	0	20	40	60	80	100	120	140
COPx_tot_dist	363.2997	423.1563	549.264	540.9071	621.799	778.9071	818.9337	998.3606	1036.325
COP_range_AP	17.41499	17.30562	24.04563	24.00907	28.17428	34.78331	38.31037	47.41199	44.13937
vel_mean_x	12.11514	14.11126	18.31621	18.03672	20.74128	25.9732	27.31583	33.29254	34.5607
peak_COP_speed_x	46.57029	50.16382	68.38665	68.3609	79.17955	95.59689	105.7955	113.6312	113.2787
RMS_COP_x	3.114523	2.818765	3.778058	3.73018	4.474135	5.720114	6.23339	8.001278	7.620637
MedFREQ	0.478722	0.670027	0.701821	0.618097	0.55501	0.545376	0.493926	0.538785	0.562963

Figure 4-1 Example of Test set where the model parameter is changed by a certain percentage from the base set. The value for K_n is the only model parameter that is changed. The other values remain at the base set values.

Mean Responses - T2									
% Change from Base	-14	-12	-10	-8	-6	-4	-2	0	2
COPx_tot_dist	208.1251	224.5715	253.9983	260.4249	249.7762	288.7569	370.8584	423.1563	722.1128
COP_range_AP	15.13357	13.85478	16.26791	15.29809	14.94051	15.42241	16.20374	17.30562	26.64811
vel_mean_x	6.951156	7.498191	8.477778	8.689972	8.337087	9.633892	12.36862	14.11126	24.07706
peak_COP_speed_x	31.68969	31.90908	35.11235	32.70827	32.92307	40.8459	45.77526	50.16382	73.99716
RMS_COP_x	3.060136	2.518515	2.972054	2.577389	2.554628	2.581164	2.465494	2.818765	4.671869
MedFREQ	0.33893	0.385456	0.309671	0.475774	0.418156	0.511464	0.551112	0.670027	0.6831

Table 4-1- Healthy Control standard deviation comparative analysis for T_2. Yellow shows COP model measures within the healthy control boundaries.

Mean responses - T2									
% Change from Base	-14	-12	-10	-8	-6	-4	-2	0	2
COPx_tot_dist	208.1251	224.5715	253.9983	260.4249	249.7762	288.7569	370.8584	423.1563	722.1128
COP_range_AP	15.13357	13.85478	16.26791	15.29809	14.94051	15.42241	16.20374	17.30562	26.64811
vel_mean_x	6.951156	7.498191	8.477778	8.689972	8.337087	9.633892	12.36862	14.11126	24.07706
peak_COP_speed_x	31.68969	31.90908	35.11235	32.70827	32.92307	40.8459	45.77526	50.16382	73.99716
RMS_COP_x	3.060136	2.518515	2.972054	2.577389	2.554628	2.581164	2.465494	2.818765	4.671869
MedFREQ	0.33893	0.385456	0.309671	0.475774	0.418156	0.511464	0.551112	0.670027	0.6831

Table 4-2- Parkinson's disease standard deviation comparative analysis for T_2. Yellow shows COP model measures within the PD boundaries.

Mean Responses - Kp							
% Change from Base	-30	-25	-20	-15	-10	-5	0
COPx_tot_dist	196.9182	207.9197	221.4098	237.558	268.9184	310.2241	423.1563
COP_range_AP	22.19892	18.79538	16.82534	15.98013	13.84801	18.00883	17.30562
vel_mean_x	6.577301	6.941394	7.392608	7.930273	8.976166	10.34992	14.11126
peak_COP_speed_x	31.00551	30.94845	29.97112	33.89045	34.86773	40.97956	50.16382
RMS_COP_x	5.000829	3.492239	3.302433	2.80522	2.299126	2.916659	2.818765
MedFREQ	0.204029	0.209657	0.261418	0.307657	0.395423	0.410547	0.670027

Table 4-3- Healthy control standard deviation comparative analysis for K_p. Yellow shows COP model measures within the healthy control boundaries.

Mean Responses -Kp							
% Change from Base	-30	-25	-20	-15	-10	-5	0
COPx_tot_dist	196.9182	207.9197	221.4098	237.558	268.9184	310.2241	423.1563
COP_range_AP	22.19892	18.79538	16.82534	15.98013	13.84801	18.00883	17.30562
vel_mean_x	6.577301	6.941394	7.392608	7.930273	8.976166	10.34992	14.11126
peak_COP_speed_x	31.00551	30.94845	29.97112	33.89045	34.86773	40.97956	50.16382
RMS_COP_x	5.000829	3.492239	3.302433	2.80522	2.299126	2.916659	2.818765
MedFREQ	0.204029	0.209657	0.261418	0.307657	0.395423	0.410547	0.670027

Table 4-4- Parkinson's disease standard deviation comparative analysis for K_p. Yellow shows COP model measures within the PD boundaries.

Mean Responses - Kd																	
% Change from Base	-22	-20	-18	-16	-14	-12	-10	-8	-6	-4	-2	0	2	4	6	8	10
COPx_tot_dist	710.6392	462.9235	443.7713	451.6464	473.2519	341.9627	321.9697	431.2593	404.0572	384.209	347.2363	423.1563	451.7099	464.6545	671.3459	619.8931	837.8731
COP_range_AP	33.5716	22.82567	23.71229	22.88474	22.23703	17.30951	17.32457	19.96397	17.59103	21.05666	18.19221	17.30562	19.54866	20.89516	27.10286	24.41521	31.32888
vel_mean_x	23.69286	15.43965	14.79859	15.0589	15.78059	11.40807	10.74015	14.38086	13.47458	12.81678	11.58238	14.11126	15.06377	15.49683	22.38425	20.67236	27.93545
peak_COP_speed_x	77.33103	56.03319	51.84074	54.46686	55.17699	47.74448	43.57515	52.40624	50.56433	50.48444	42.65488	50.16382	54.93463	55.75039	73.59197	66.37702	93.71924
RMS_COP_x	5.720197	3.673234	4.293734	3.679272	3.563977	2.631628	2.877989	3.259366	3.008044	3.506951	2.987007	2.818765	2.986446	3.358773	4.439147	4.550711	5.126685
MedFREQ	0.622712	0.618933	0.451886	0.532632	0.652962	0.550747	0.435194	0.656636	0.560982	0.446301	0.511757	0.670027	0.63709	0.680433	0.694621	0.595423	0.720804

Table 4-5- Healthy control standard deviation comparative analysis for K_d. Yellow shows COP model measures within the healthy control boundaries.

Mean Responses - Kd																	
% Change from Base	-22	-20	-18	-16	-14	-12	-10	-8	-6	-4	-2	0	2	4	6	8	10
COPx_tot_dist	710.6392	462.9235	443.7713	451.6464	473.2519	341.9627	321.9697	431.2593	404.0572	384.209	347.2363	423.1563	451.7099	464.6545	671.3459	619.8931	837.8731
COP_range_AP	33.5716	22.82567	23.71229	22.88474	22.23703	17.30951	17.32457	19.96397	17.59103	21.05666	18.19221	17.30562	19.54866	20.89516	27.10286	24.41521	31.32888
vel_mean_x	23.69286	15.43965	14.79859	15.0589	15.78059	11.40807	10.74015	14.38086	13.47458	12.81678	11.58238	14.11126	15.06377	15.49683	22.38425	20.67236	27.93545
peak_COP_speed_x	77.33103	56.03319	51.84074	54.46686	55.17699	47.74448	43.57515	52.40624	50.56433	50.48444	42.65488	50.16382	54.93463	55.75039	73.59197	66.37702	93.71924
RMS_COP_x	5.720197	3.673234	4.293734	3.679272	3.563977	2.631628	2.877989	3.259366	3.008044	3.506951	2.987007	2.818765	2.986446	3.358773	4.439147	4.550711	5.126685
MedFREQ	0.622712	0.618933	0.451886	0.532632	0.652962	0.550747	0.435194	0.656636	0.560982	0.446301	0.511757	0.670027	0.63709	0.680433	0.694621	0.595423	0.720804

Table 4-6- Parkinson's disease standard deviation comparative analysis for K_d. Yellow shows COP model measures within the PD boundaries.

Mean Responses - Kn									
% Change from Base	-20	0	20	40	60	80	100	120	140
COPx_tot_dist	363.2997	423.1563	549.264	540.9071	621.799	778.9071	818.9337	998.3606	1036.325
COP_range_AP	17.41499	17.30562	24.04563	24.00907	28.17428	34.78331	38.31037	47.41199	44.13937
vel_mean_x	12.11514	14.11126	18.31621	18.03672	20.74128	25.9732	27.31583	33.29254	34.5607
peak_COP_speed_x	46.57029	50.16382	68.38665	68.3609	79.17955	95.59689	105.7955	113.6312	113.2787
RMS_COP_x	3.114523	2.818765	3.778058	3.73018	4.474135	5.720114	6.23339	8.001278	7.620637
MedFREQ	0.478722	0.670027	0.701821	0.618097	0.55501	0.545376	0.493926	0.538785	0.562963

Table 4-7- Healthy control standard deviation comparative analysis for K_n. Yellow shows the COP model measures within the healthy control boundaries.

Mean Responses - Kn									
% Change	-20	0	20	40	60	80	100	120	140
COPx_tot_dist	363.2997	423.1563	549.264	540.9071	621.799	778.9071	818.9337	998.3606	1036.325
COP_range_AP	17.41499	17.30562	24.04563	24.00907	28.17428	34.78331	38.31037	47.41199	44.13937
vel_mean_x	12.11514	14.11126	18.31621	18.03672	20.74128	25.9732	27.31583	33.29254	34.5607
peak_COP_speed_x	46.57029	50.16382	68.38665	68.3609	79.17955	95.59689	105.7955	113.6312	113.2787
RMS_COP_x	3.114523	2.818765	3.778058	3.73018	4.474135	5.720114	6.23339	8.001278	7.620637
MedFREQ	0.478722	0.670027	0.701821	0.618097	0.55501	0.545376	0.493926	0.538785	0.562963

Table 4-8 - Parkinson's disease standard deviation comparative analysis for K_n. Yellow shows the COP model measures within the PD boundaries

Mean Responses - Kd																	
% Change frome Base	-22	-20	-18	-16	-14	-12	-10	-8	-6	-4	-2	0	2	4	6	8	10
COPx_tot_dist	710.6392	462.9235	443.7713	451.6464	473.2519	341.9627	321.9697	431.2593	404.0572	384.209	347.2363	423.1563	451.7099	464.6545	671.3459	619.8931	837.8731
COP_range_AP	33.5716	22.82567	23.71229	22.88474	22.23703	17.30951	17.32457	19.96397	17.59103	21.05666	18.19221	17.30562	19.54866	20.89516	27.10286	24.41521	31.32888
vel_mean_x	23.69286	15.43965	14.79859	15.0589	15.78059	11.40807	10.74015	14.38086	13.47458	12.81678	11.58238	14.11126	15.06377	15.49683	22.38425	20.67236	27.93545
peak_COP_speed_x	77.33103	56.03319	51.84074	54.46686	55.17699	47.74448	43.57515	52.40624	50.56433	50.48444	42.65488	50.16382	54.93463	55.75039	73.59197	66.37702	93.71924
RMS_COP_x	5.720197	3.673234	4.293734	3.679272	3.563977	2.631628	2.877989	3.259366	3.008044	3.506951	2.987007	2.818765	2.986446	3.358773	4.439147	4.550711	5.126685
MedFREQ	0.622712	0.618933	0.451886	0.532632	0.652962	0.550747	0.435194	0.656636	0.560982	0.446301	0.511757	0.670027	0.63709	0.680433	0.694621	0.595423	0.720804

Table 4-9 - Healthy control ANOVA analysis for K_d. Yellow shows COP model measures not significantly different from the HC group.

Mean Responses - Kd																	
% Change from base	-22	-20	-18	-16	-14	-12	-10	-8	-6	-4	-2	0	2	4	6	8	10
COPx_tot_dist	710.6392	462.9235	443.7713	451.6464	473.2519	341.9627	321.9697	431.2593	404.0572	384.209	347.2363	423.1563	451.7099	464.6545	671.3459	619.8931	837.8731
COP_range_AP	33.5716	22.82567	23.71229	22.88474	22.23703	17.30951	17.32457	19.96397	17.59103	21.05666	18.19221	17.30562	19.54866	20.89516	27.10286	24.41521	31.32888
vel_mean_x	23.69286	15.43965	14.79859	15.0589	15.78059	11.40807	10.74015	14.38086	13.47458	12.81678	11.58238	14.11126	15.06377	15.49683	22.38425	20.67236	27.93545
peak_COP_speed_x	77.33103	56.03319	51.84074	54.46686	55.17699	47.74448	43.57515	52.40624	50.56433	50.48444	42.65488	50.16382	54.93463	55.75039	73.59197	66.37702	93.71924
RMS_COP_x	5.720197	3.673234	4.293734	3.679272	3.563977	2.631628	2.877989	3.259366	3.008044	3.506951	2.987007	2.818765	2.986446	3.358773	4.439147	4.550711	5.126685
MedFREQ	0.622712	0.618933	0.451886	0.532632	0.652962	0.550747	0.435194	0.656636	0.560982	0.446301	0.511757	0.670027	0.63709	0.680433	0.694621	0.595423	0.720804

Table 4-10 - Parkinson's disease ANOVA analysis for K_d. Yellow shows COP model measures not significantly different from the PD group.

Mean Responses - Kn									
% Change from Base	-20	0	20	40	60	80	100	120	140
COPx_tot_dist	363.2997	423.1563	549.264	540.9071	621.799	778.9071	818.9337	998.3606	1036.325
COP_range_AP	17.41499	17.30562	24.04563	24.00907	28.17428	34.78331	38.31037	47.41199	44.13937
vel_mean_x	12.11514	14.11126	18.31621	18.03672	20.74128	25.9732	27.31583	33.29254	34.5607
peak_COP_speed_x	46.57029	50.16382	68.38665	68.3609	79.17955	95.59689	105.7955	113.6312	113.2787
RMS_COP_x	3.114523	2.818765	3.778058	3.73018	4.474135	5.720114	6.23339	8.001278	7.620637
MedFREQ	0.478722	0.670027	0.701821	0.618097	0.55501	0.545376	0.493926	0.538785	0.562963

Table 4-11 - Healthy control ANOVA analysis for K_n. Yellow shows COP model measures not significantly different from the HC group.

Mean Responses - Kn									
% Change from Base	-20	0	20	40	60	80	100	120	140
COPx_tot_dist	363.2997	423.1563	549.264	540.9071	621.799	778.9071	818.9337	998.3606	1036.325
COP_range_AP	17.41499	17.30562	24.04563	24.00907	28.17428	34.78331	38.31037	47.41199	44.13937
vel_mean_x	12.11514	14.11126	18.31621	18.03672	20.74128	25.9732	27.31583	33.29254	34.5607
peak_COP_speed_x	46.57029	50.16382	68.38665	68.3609	79.17955	95.59689	105.7955	113.6312	113.2787
RMS_COP_x	3.114523	2.818765	3.778058	3.73018	4.474135	5.720114	6.23339	8.001278	7.620637
MedFREQ	0.478722	0.670027	0.701821	0.618097	0.55501	0.545376	0.493926	0.538785	0.562963

Table 4-12- Parkinson's disease ANOVA analysis for K_n. Yellow shows COP model measures not significantly different from the PD group

Chapter 5 : Summary

Summary of Study

This thesis consists of a set of studies that developed, implemented, validated, and applied a computational model used to investigate the human motor control system during a quiet standing task. Using cosimulation, ADAMS was used to model the human body as an inverted pendulum and Simulink was used to model the actions of the brain as the controller. Using this approach we have developed a model that includes several physiologically meaningful parameters. The model has been used to investigate the relationship between the model parameters, the model COP measures, and COP measures measured in a group of healthy controls and a group diagnosed with PD.

In the first study, we sought to develop a model that was capable of being validated with healthy controlled (HC) subjects during postural sway. The model was initially investigated to fully understand the relationship between the model input parameters on the resulting COP output measures. We were able to understand the effects of each model parameter on the COP measures and develop a thorough understanding of the robustness and characteristics of the system. For instance, it was perceived that the model is very robust due to the fact that when the controller gains were held constant and the noise was adjusted, the model controlled the system well outside of realistic sway parameters. Furthermore, we used a correlation method to validate the model with a set of parameters that simulate COP measures that were observed in experimental studies of HC subjects during eyes closed quiet stance.

In the second study, experimental COP data from HC and Parkinson's disease (PD) groups were used to investigate the corresponding model parameters for each group. To do this,

we employed techniques used to decompose the range of a robust test set into a range of realistic test sets with COP measures comparable to those observed in the experimental data previously collected in groups of HC and PD groups. Two methods were used to compare the model COP measures with the experimentally determined HC and PD group COP measures. Both methods produced similar trends in relating to the group measures. Overall findings showed that neither group was strongly related to a unique test set when the feedback time delay and the proportional gain model parameters were varied. However, when the derivative gain and neuromuscular noise model parameters were varied independently, a test set or range of test sets could be identified as exclusive to the PD and HC groups. These relationships suggest that the neuromuscular noise and derivative gain could cause changes observed in the COP measure of subjects with PD.

Conclusions and Recommendation

This study concludes that a proportional-derivative controller provides a reasonable controller for postural sway modelling. This does not mean that the human control system is based on a proportional-derivative controller, but that this is a good method for comparing and understanding the inputs that affect the measurable outputs commonly measured in experimental research laboratory. We believe that the strength of the cosimulation model provides future studies with a foundation on which to build more complex dynamics systems and controls. This development provides researchers with the ability to creatively design experiments while advancing the complexity of the model one piece at a time.

When comparing the first study and second study, it is evident that the first study likely provides an improvement upon the base set of HC model parameters. This is acknowledged by the author, as the first study is meant to understand the model and then perform a novel method for validating the model measures with experimental measures.

In the second study it can be seen in the relationships to the HC and PD groups that there is a large overlap in some of the HC and PD model parameter changes of K_n. This is likely caused by collapsing the mild and moderate PD participants into a single group. Future studies should increase the number of participants within the two PD groups, treat them as separate groups and repeat the methods used in this study to investigate the efficacy of differentiating between HC, mild PD, and moderate PD. This idea is limited at this point by the number of subjects available in the current study, but would be an interesting investigation into the early development of balance impairments in PD and in the progression of the neurological disease.

Study Limitations

This study was limited in both the experimental and modelling area by a low number of samples. Within the model, we chose to use a low number of samples in order to compare to the variation and trial number that were tested on the experimental groups. Furthermore, the PD groups were limited in number and consisted of both mild and moderate PD subjects, which likely increased the variation of the PD group and caused an overlap in the findings.

The model utilized in this study is limited by the use of a single link inverted pendulum, a limited number of model parameters, and only investigating the control of body sway in the AP direction. However, we believe that these are good simplifying assumption due to the majority of the COP displacement during postural sway to be in the AP direction and the documented lack of hip torque generation during unperturbed postural sway.

Finally, this study focused mainly on the effects of the model parameters varying independently while the other parameters remained constant at the base set. This method was used to allow an investigation into the effects of the individual parameters and due to the low

number of test sets available from model measures. However, the cosimulation model offers the opportunity to overcome the limitations of this current model in future studies.

Further Study

The cosimulation of ADAMS and Simulink allows for this model to increase in complexity very effectively in order to reduce the limitations mentioned above. The crawl-walk-run approach allows us to further develop the current model by adding layers of complexity to both the plant and the controller. The control model will allow for changes to be made to better simulate the physiological system. This could be done by adding components of passive torque, sensory pathways, or feedforward mechanisms. Future models could be changed to allow for a double pendulum system, in which the ankle and hip joint torques are controlled synergistically to react to balance disturbances. Another level of complexity could allow for the simultaneous control medial-lateral sway. In addition, the model could be further developed to allow for a simulation of a step to be taken in response to a balance disturbance or for the initiation of gait.

Increasing the number of trials and performing an optimization study should be performed in the future to provide a more accurate estimation of model parameters when comparing across subject groups. Future studies could look more deeply into this idea, utilizing different groups of subjects to investigate such things as healthy aging, injury, and other neurological diseases such as Huntington's disease. The cosimulation model developed in this study allows for a number of possibilities for the future of biomechanics modelling.

Appendix A : Experimental Methods

Measured Parameters from Experimental Study	
Total height	H
Thigh length	l_T
Total mass of subject	M
Ankle height	$y1$
Calf length	l_C
Foot length	l_F

Table A-1. Measured Parameters from Experimental Study

List of parameters measured from experimental study. These parameters were either directly used for model parameters and cop calculations or used in the approximation of other parameters for the inverted pendulum model

Approximated Parameters of Inverted Pendulum	
Trunk length ($\boldsymbol{l_1}$)	$l_1 = .818H + .530(l_1 + l_2 + a)$
Leg length, no ankle($\boldsymbol{l_2}$)	$l_2 = l_T + l_C$
Mass of pendulum, no feet($\boldsymbol{m}$)	$m = .971M$
Length of the pendulum, ankle to COM ($\boldsymbol{h}$)	$h = .261l_1 + .945l_2$
Moment of inertia about ankle joint($\boldsymbol{I}$)	$I = .678M(.347l_1 + l_2)^2 + .192Ml_2^2$
Foot COM anterior-posterior from ankle $\boldsymbol{f_{com}}$	$x_0 = .5l_F$
Foot mass	$m_f = 0.0145l_F$

Table A-2. Approximated Parameters of Inverted Pendulum

List of parameters approximated from values in measured in experimental study found in table 1. These parameters were either used for the inverted model directly or to calculate the COP parameters of the model.

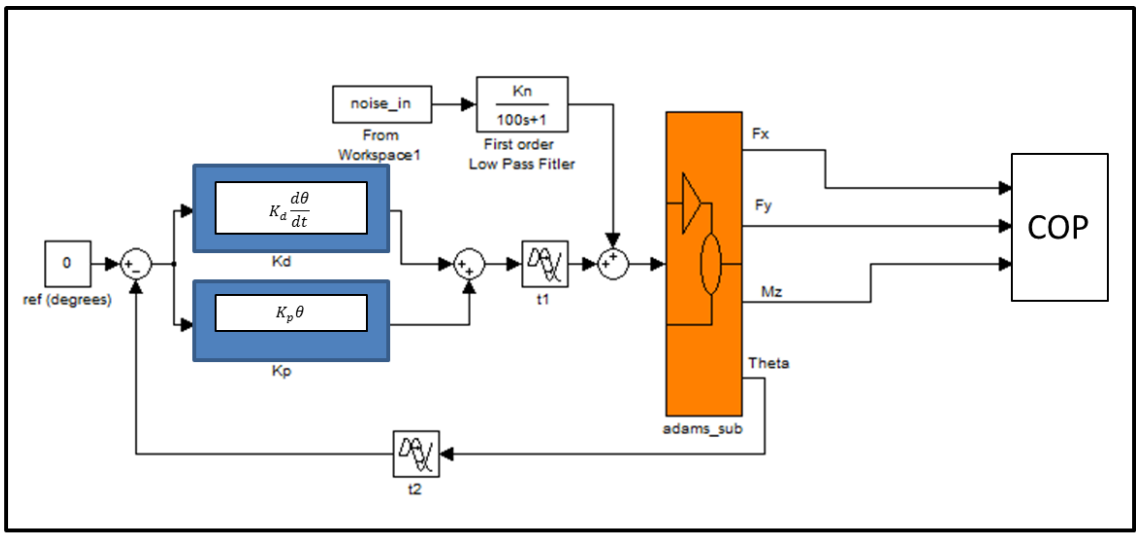

Figure A-1 - Cosimulation of Postural Sway Inverted Pendulum

Inverted pendulum block diagram. Orange block is the plant connecting to ADAMS. Fx, Fy, and Mz are used in calculation of COP. K_n, tf, K_d, K_p are model parameters of interest in sensitivity analysis. T1 represents the neural time delay from the central nervous system to the muscle activation.

ADAMS Representation of Inverted Pendulum Model

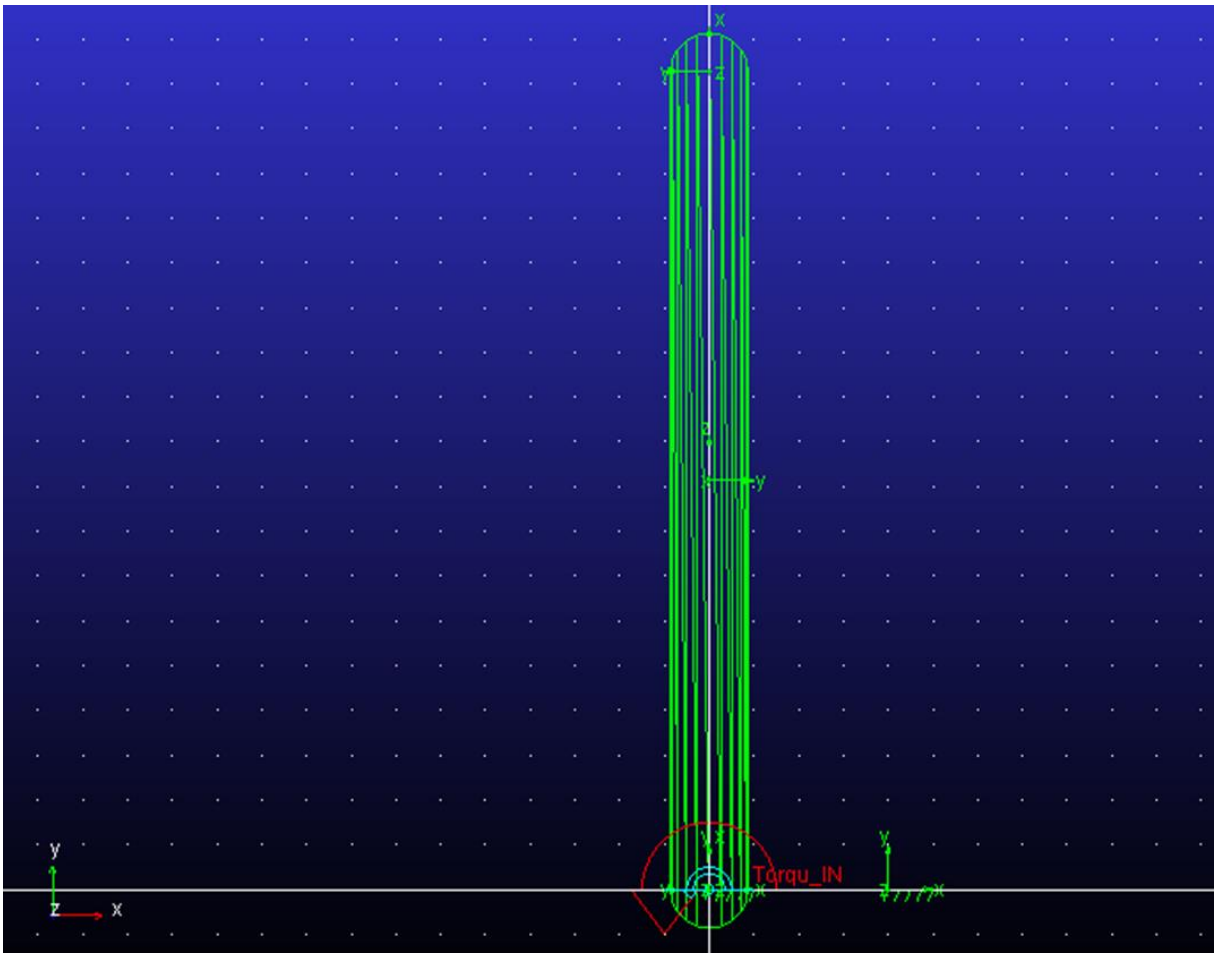

Figure A-2 - ADAMS Representation of Inverted Pendulum Model

Shows the ADAMS model representation of the inverted pendulum. The inverted pendulum model shows the torque of the model that is input from Simulink at the ankle join in by a red arrow. The green marker on the bottom right is a marker used to measure the angle of the pendulum. The pendulum is shown at an angle of 0 degrees. The small blue arrow represents the rotational joint constraint between the ground and the pendulum.

Inverted Pendulum Model Diagram

Figure A-3 - Inverted Pendulum Model Diagram and COP Derivation

The following is a diagram of the classic inverted pendulum model used throughout the study to develop equations of motion and the ADAMS model validation.

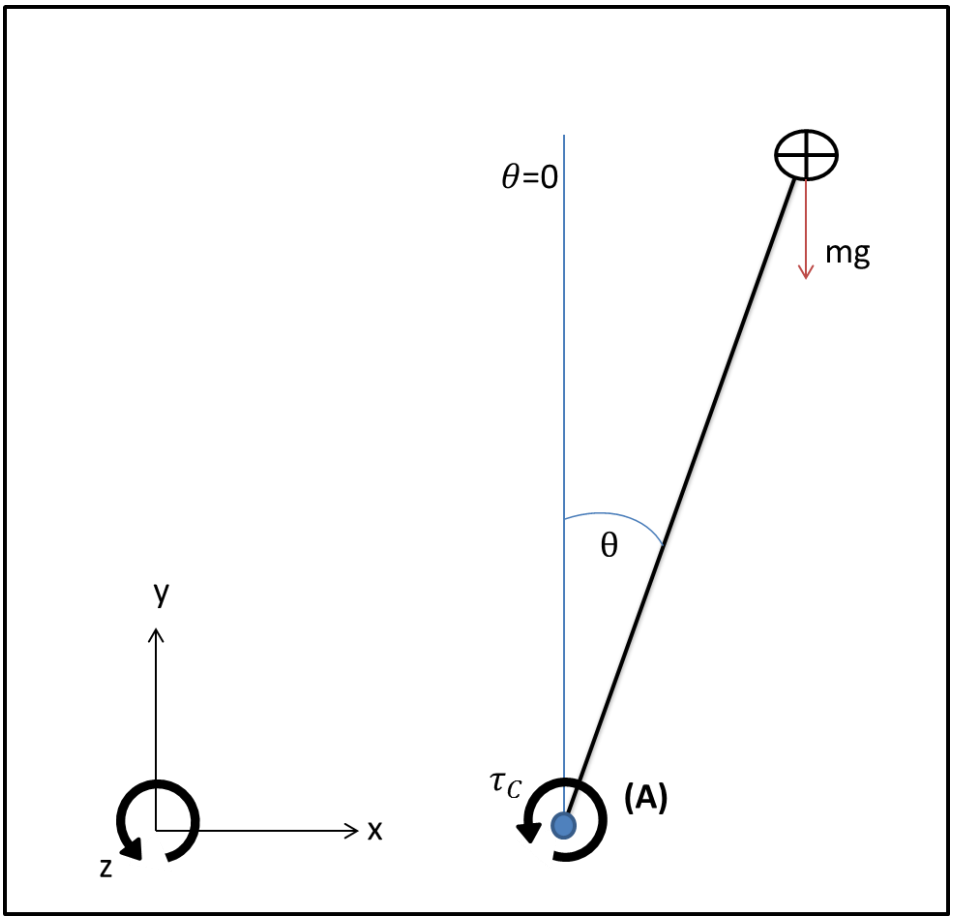

COP Derivation for Inverted Pendulum Model

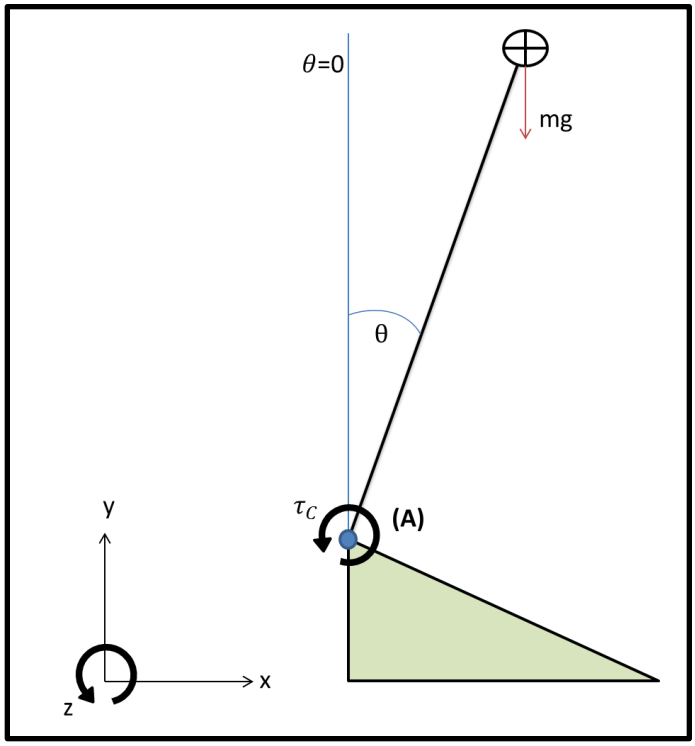

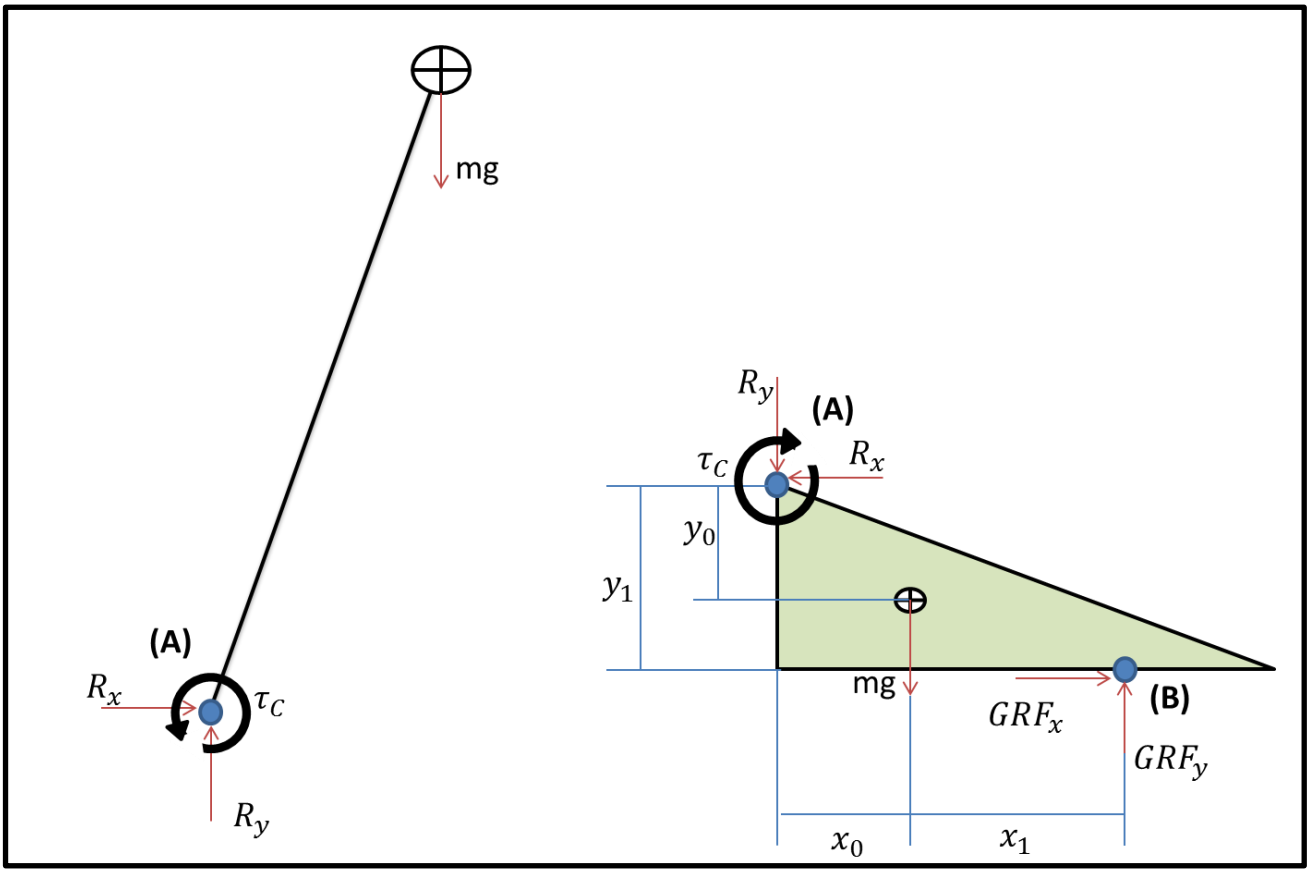

Assumptions:

-Foot is stationary $\boldsymbol{\alpha = 0, a = 0}$

-No force couple between the foot and the ground, which implies that the foot is not attached to the floor

-Intrinsic muscle, tendon, and ligament forces at ankle joint (A) are assumed small compared to the applied muscle moment and are therefore assumed to be zero.

-T_C is the torque input exerted about the ankle joint by the proportional-derivative controller. It represents the summation of the noise and control toque about the ankle joint (A).

Known:

x_0=anterior-posterior distance of COM (COM) from the ankle joint (A)

x_1= anterior-posterior distance of GRF from the COM

y_1= ankle height from floor to ankle joint (A)

(A)=ankle joint

(B)=Point of application of GRF

Find:

GRF_Y, GRF_X, COP_X

Calculations:

$\overrightarrow{\boldsymbol{W}} = -\boldsymbol{mg}\,\hat{\boldsymbol{j}}$ The foot weight vector

$$\vec{R} = -(R_x\, i + R_y\, \hat{j})$$

$$\overrightarrow{GRF} = (GRF_x\, \hat{\imath} + GRF_y\, \hat{j})$$

$$\overrightarrow{\tau_C} = -\tau_C\, \hat{k}$$

$$\vec{r}_{A\_COM} = x_0\, \hat{\imath} - y_0\, \hat{j}$$

$$\vec{r}_{A\_B} = (x_0 + x_1)\hat{\imath} - y_1\, \hat{j}$$

Sum of the forces

$$\sum \vec{F} = m\vec{a}$$

-COM of the foot has no acceleration in the x or y direction, therefore:

$$\sum \vec{F} = \vec{0}$$

$$\sum \vec{F} = \overrightarrow{GRF} + \vec{W} + \vec{R} = \vec{0}$$

$$-(R_x\, i + R_y\, \hat{j}) + (GRF_x\, \hat{\imath} + GRF_y\, \hat{j}) - mg\, \hat{j} = \vec{0}$$

Separating the two scalar equations provided the following two equations:

$\hat{\imath}\ direction$: $-R_x + GRF_x = 0$, which gives:

$$\boldsymbol{GRF_x = R_x} \qquad (1)$$

$\boldsymbol{\hat{j}\ direction}$: $\boldsymbol{-R_y + GRF_y - mg = 0}$, which gives:

$$\boldsymbol{GRF_y = R_y + mg} \qquad (2)$$

$$\sum \boldsymbol{\vec{M} = I\vec{\alpha} + \vec{r} \times m\vec{a}_{COM}}$$

Sum of the moments about point (A):

$$\sum \boldsymbol{\vec{M}_A = I_A\vec{\alpha}}$$

Since the foot is stationary, COM has no acceleration; therefore the angular acceleration is zero, which gives:

$$\sum \boldsymbol{\vec{M}_A = \vec{0}}$$

$$\sum \boldsymbol{\vec{M}_A = \vec{\tau_C} + (\vec{r}_{A\_COM} \times \vec{W}) + (\vec{r}_{A\_B} \times \vec{GRF}) = \vec{0}}$$

$$= \boldsymbol{-\tau_C\,\hat{k} + (x_0\,\hat{\imath} - y_0\,\hat{\jmath}) \times -(mg\,\hat{\jmath}) + ((x_0 + x_1)\hat{\imath} - y_1\,\hat{\jmath}) \times (GRF_x\,\hat{\imath} + GRF_y\,\hat{\jmath}) = \vec{0}}$$

$$= \boldsymbol{-\tau_C\,\hat{k} + (-x_0\,mg)(\hat{\imath} \times \hat{\jmath}) + (x_0 + x_1)GRF_y(\hat{\imath} \times \hat{\jmath}) + (-y_1\,GRF_x)(\hat{\jmath} \times \hat{\imath}) = \vec{0}}$$

$$= -\tau_C\,\hat{k} + (-x_0\,mg)\,\hat{k} + ((x_0 + x_1)GRF_y)\,\hat{k} + (y_1\,GRF_x)\,\hat{k} = \vec{0}$$

$$x_1 = \frac{\tau_C - (y_1\, GRF_x) + (mg - GRF_y)x_0}{GRF_y}$$

Substitute in equation (1) and (2) in to the above equation:

$$x_1 = \frac{\tau_C - (y_1 R_x) + (mg - R_y + mg)x_0}{R_y + mg}$$

$$= \frac{\tau_C - (y_1 R_x) + (-R_y)x_0}{R_y + mg}$$

$$COP_x = x_1 + x_0 = \frac{\tau_C - (y_1\, R_x) + (-R_y)x_0}{R_y + mg} + x_0$$

Postural Sway Testing Script

"For this set of tests you will stand here with your hands to your sides and have either your eyes focused on the target in front of you or have them closed. We will do several trials with rest in between. I will tell you when to begin each trial and I will tell you when to relax."

EO:

Instructions to subject:

"For this test, you will stand as still as possible. Focus your gaze at the target in front of you"

EC:

Instructions to subject:

"For this test, you will stand as still as possible with your eyes closed. Keep your eyes closed until the end of the trial."

Figure A-4 - Postural Sway Testing Script

Set of instructions given to each subject during experimental trials for each particular test.

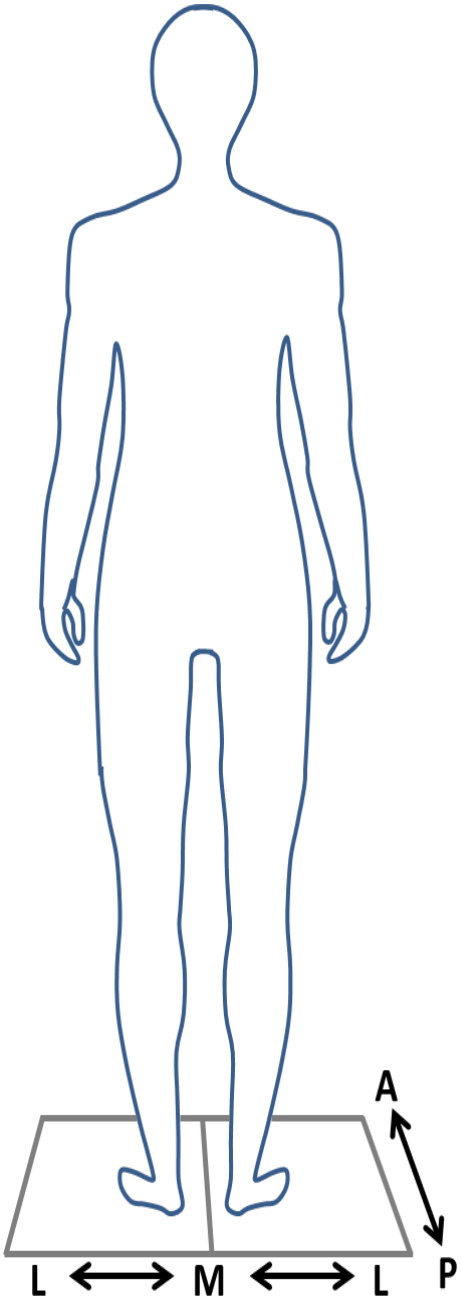

Figure A-5 - Postural Sway Experimental Diagram

Courtesy of Annaria Barnds

Appendix B : Model Development

Base Model Parameter Set		
	Values	Units
T_1 (constant)	0.04	seconds
T_2	0.147	seconds
K_p	22.36	(N*m)/deg
K_d	7.0143	(N*m*sec)/deg
K_n	786.555	N*m

Table B-1 - Base Model Parameter Set

Stability Ranges					
	Actual Value		% change from base value		
	Min	Max	Min	Max	Increments
T_2	0	0.14994	-100%	2%	2%
K_p	0	22.36	-100%	0%	5%
K_d	5.190582	7.71573	-24%	10%	2%
K_n	0	5505.885	-100%	600%	20%

Table B-2 - Stability Ranges

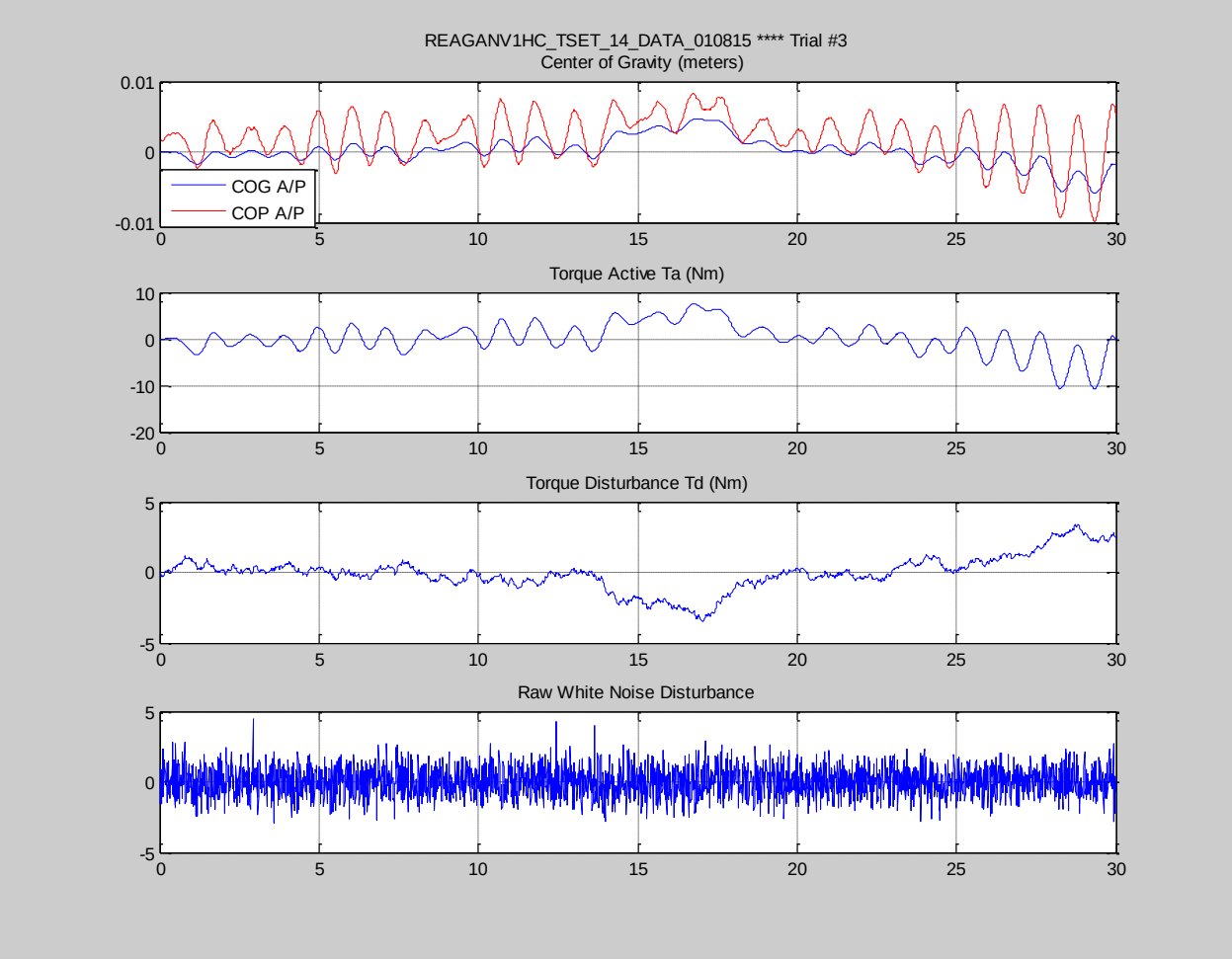

Figure B-1 - Data Quality Plots / Boundary for T_2 / Experiment 301 Test set 14 / T_2 = 0.14994 seconds / % change from base = 2%

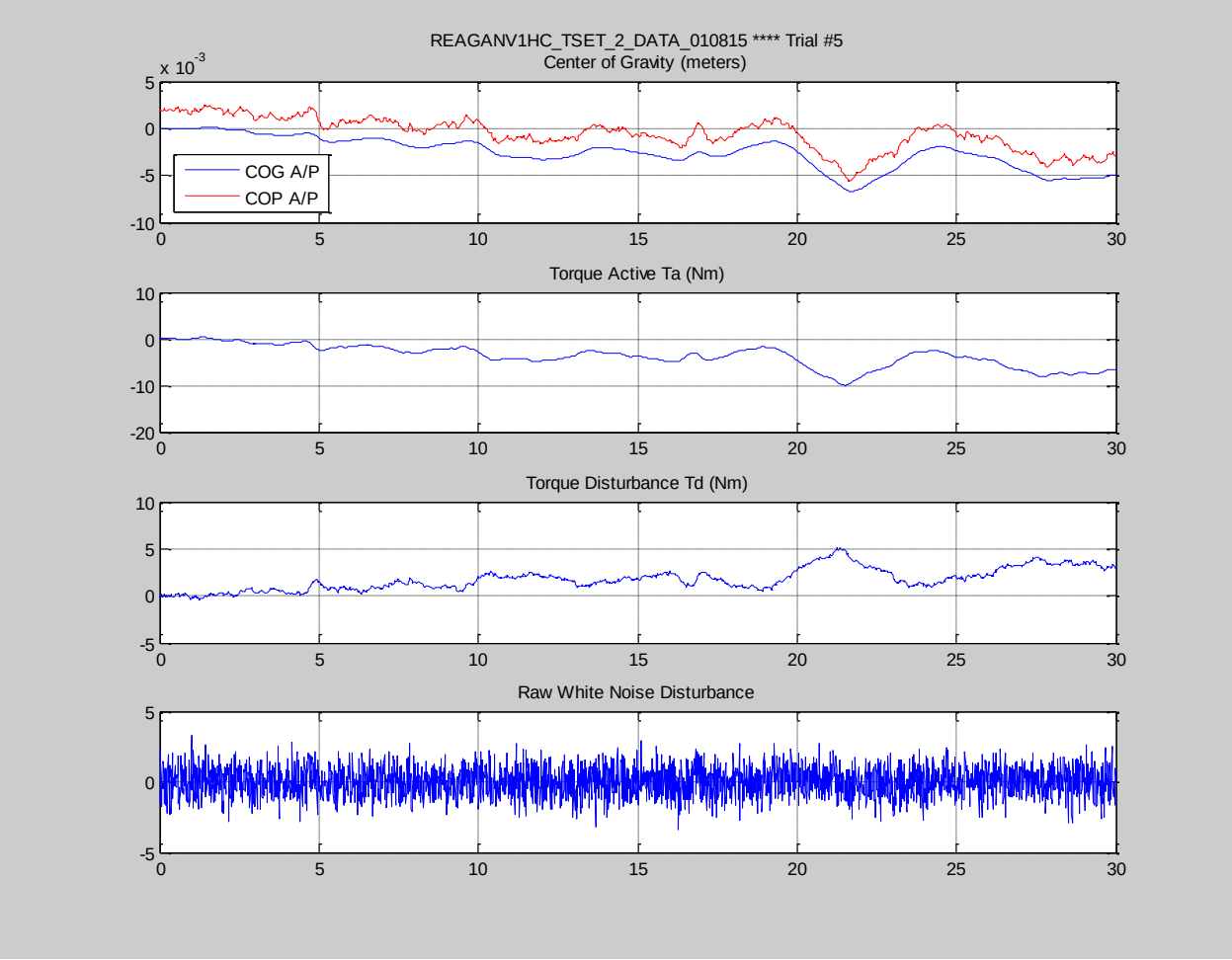

Figure B-2 - Data Quality Plots / Boundary for T_2 / Experiment 303 Test set 2 / T_2 = 0 / % change from base = -100%

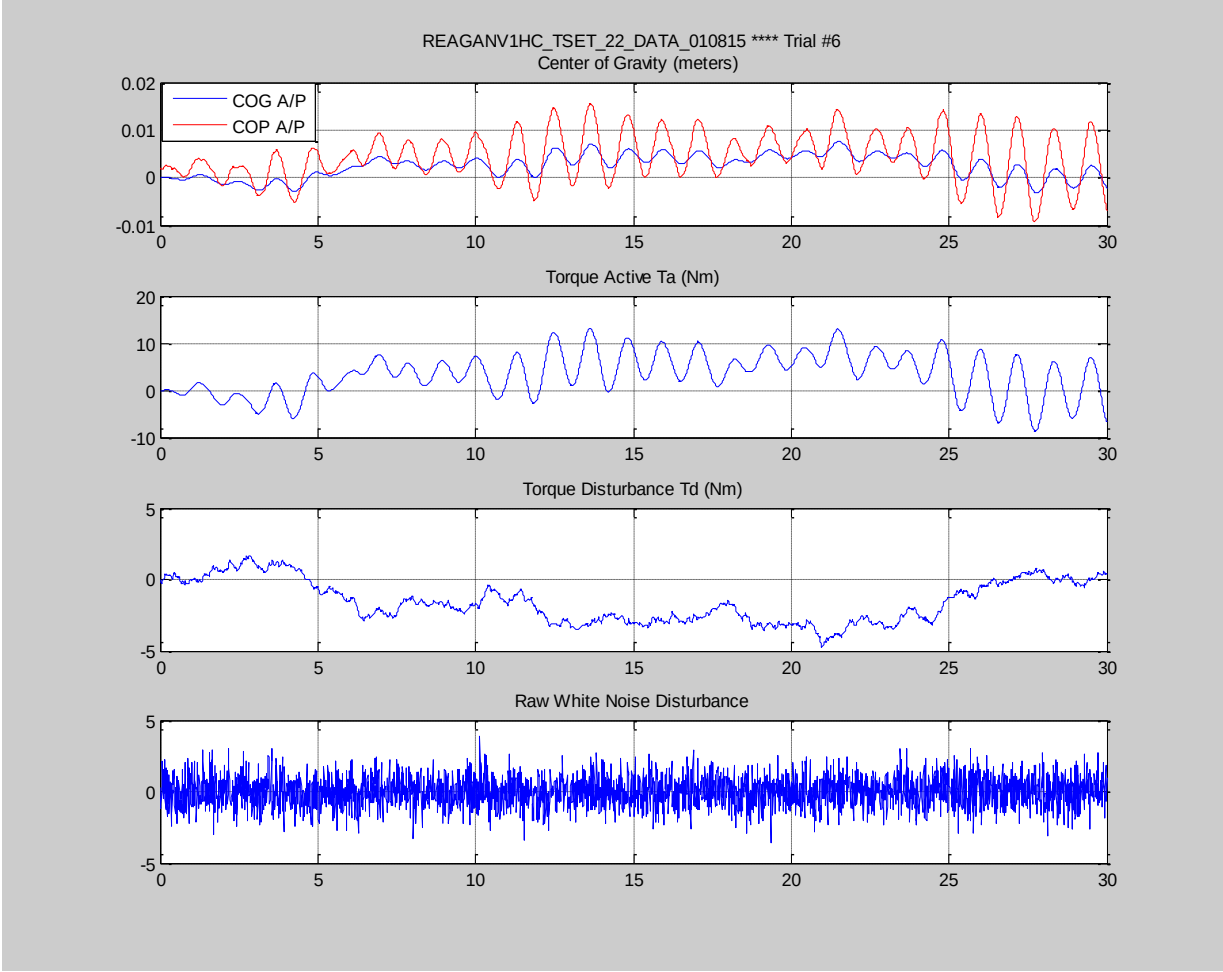

Figure B-3 - Data Quality Plots / Boundary for K_p / Experiment 302 Test set 22 / K_d = 22.36 / % change from base = 0% / Base set Value

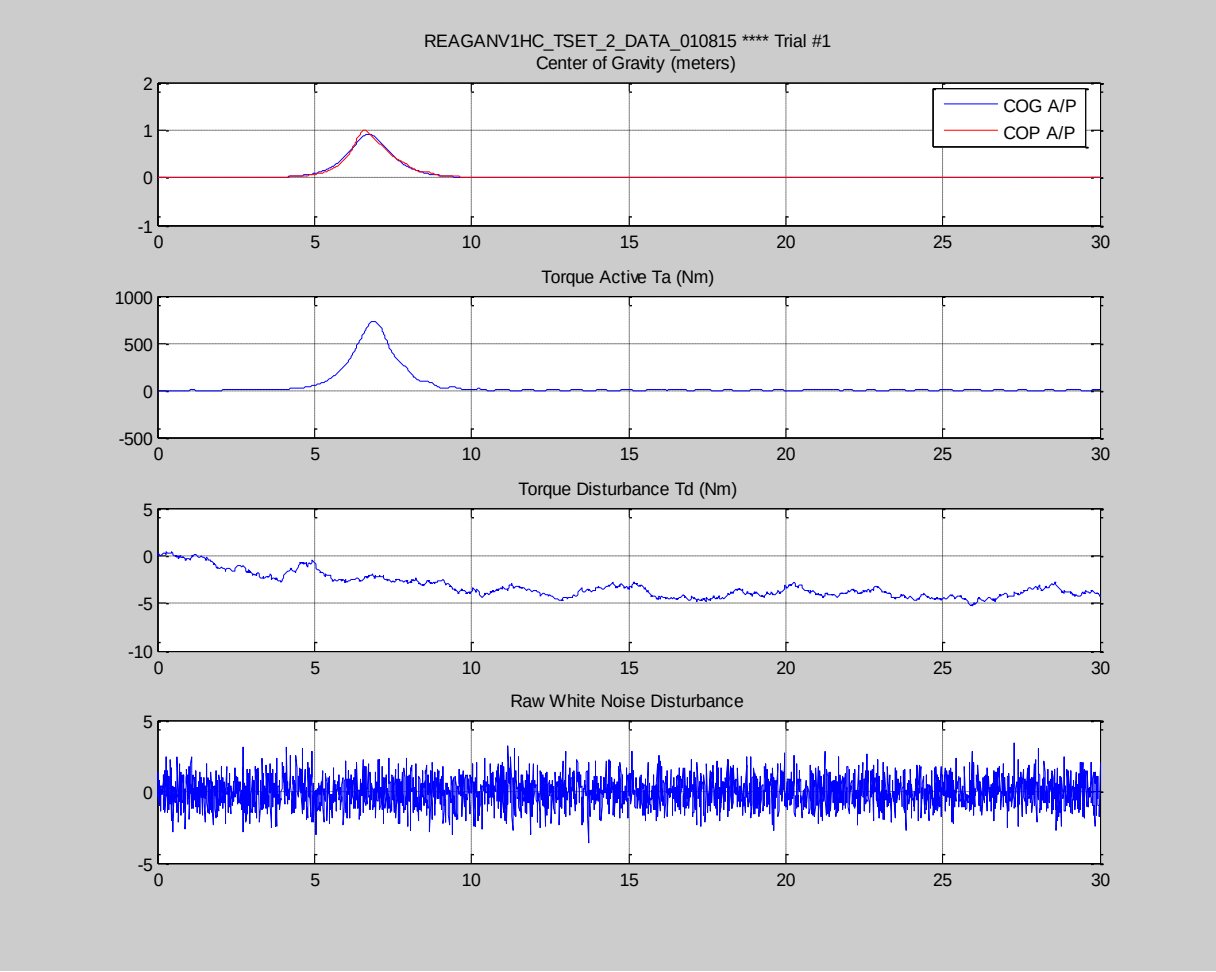

Figure B-4 - Data Quality Plots / Boundary for K_p / Experiment 302 Test set 2 / K_d = 0 / % change from base = -100%

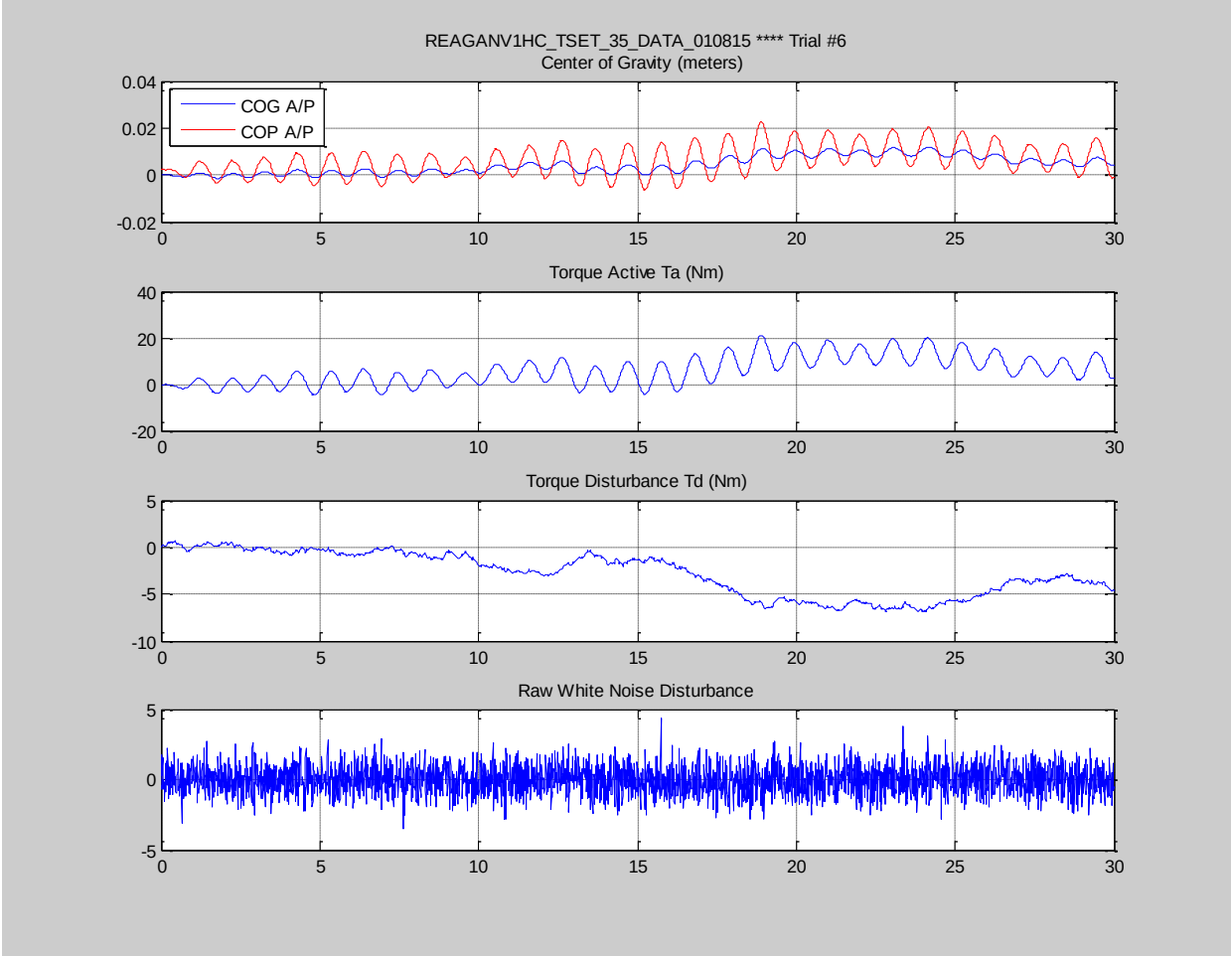

Figure B-5 - Data Quality Plots / Boundary for K_d / Experiment 301 Test set 35 / K_d = 7.716 / % change from base = 10%

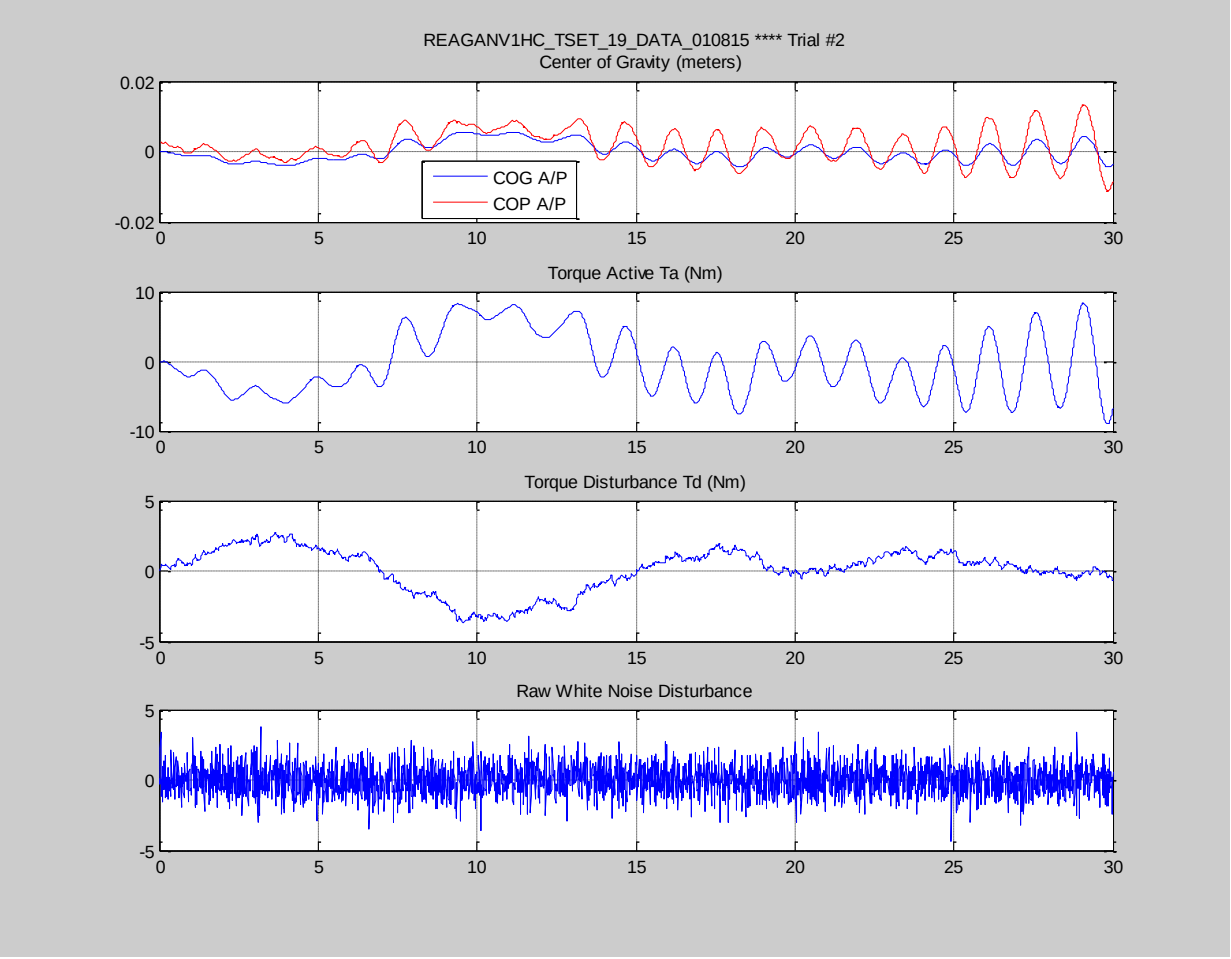

Figure B-6 - Data Quality Plots / Boundary for K_d / Experiment 301 Test set 19 / K_d = 5.33 / % change from base = -24%

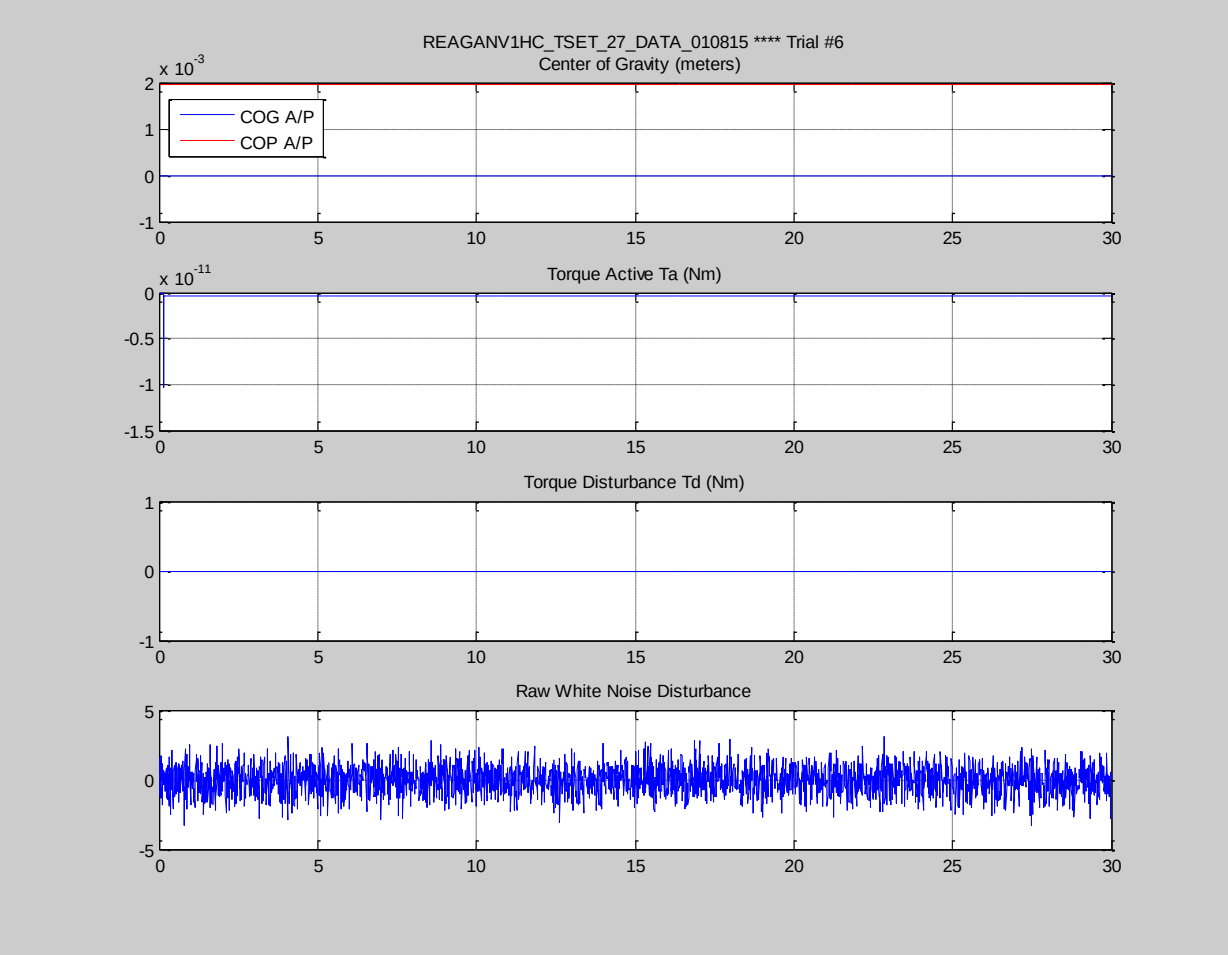

Figure B-7 - Data Quality Plots / Boundary for K_n / Experiment 302 Test set 27 / K_n = 0 / % change from base = -100%

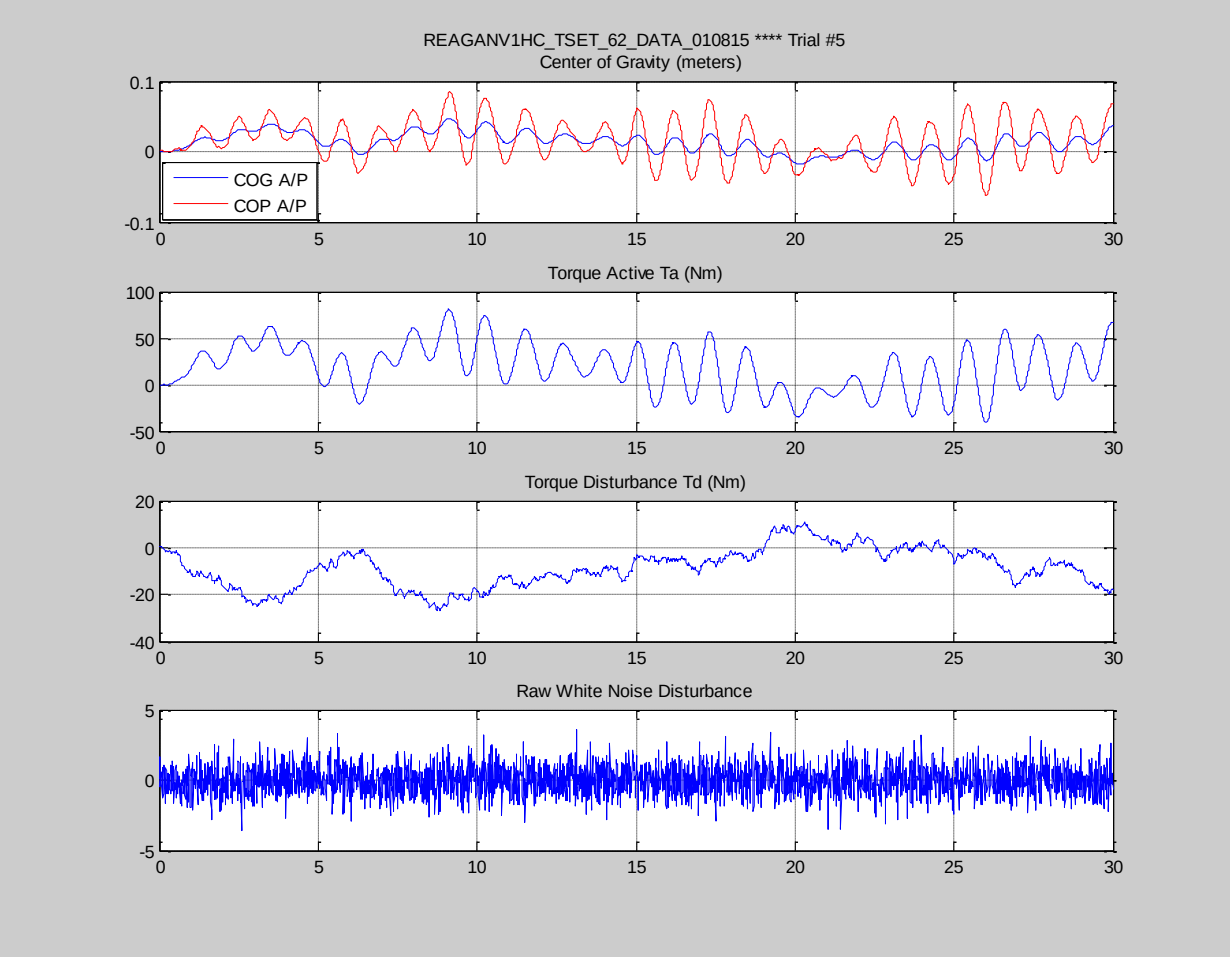

Figure B-8 - Data Quality Plots / Boundary for K_n / Experiment 302 Test set 62 / K_n = 5505.885 / % change from base = 600%

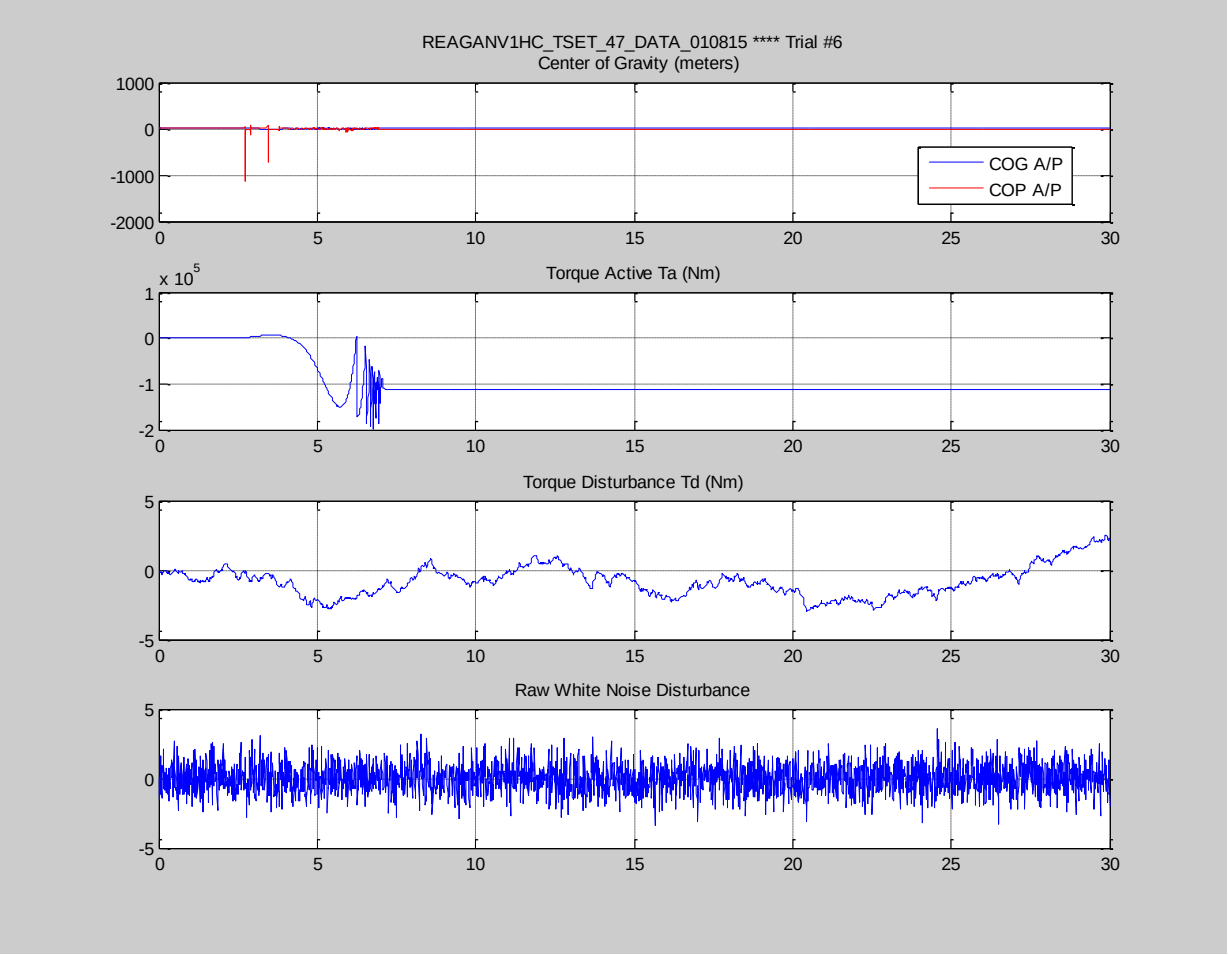

Figure B-9 - Data Quality Plots / Experiment 303 Test Set 47 / K_d =5.0503 / % from base = -28% / Severe Instability

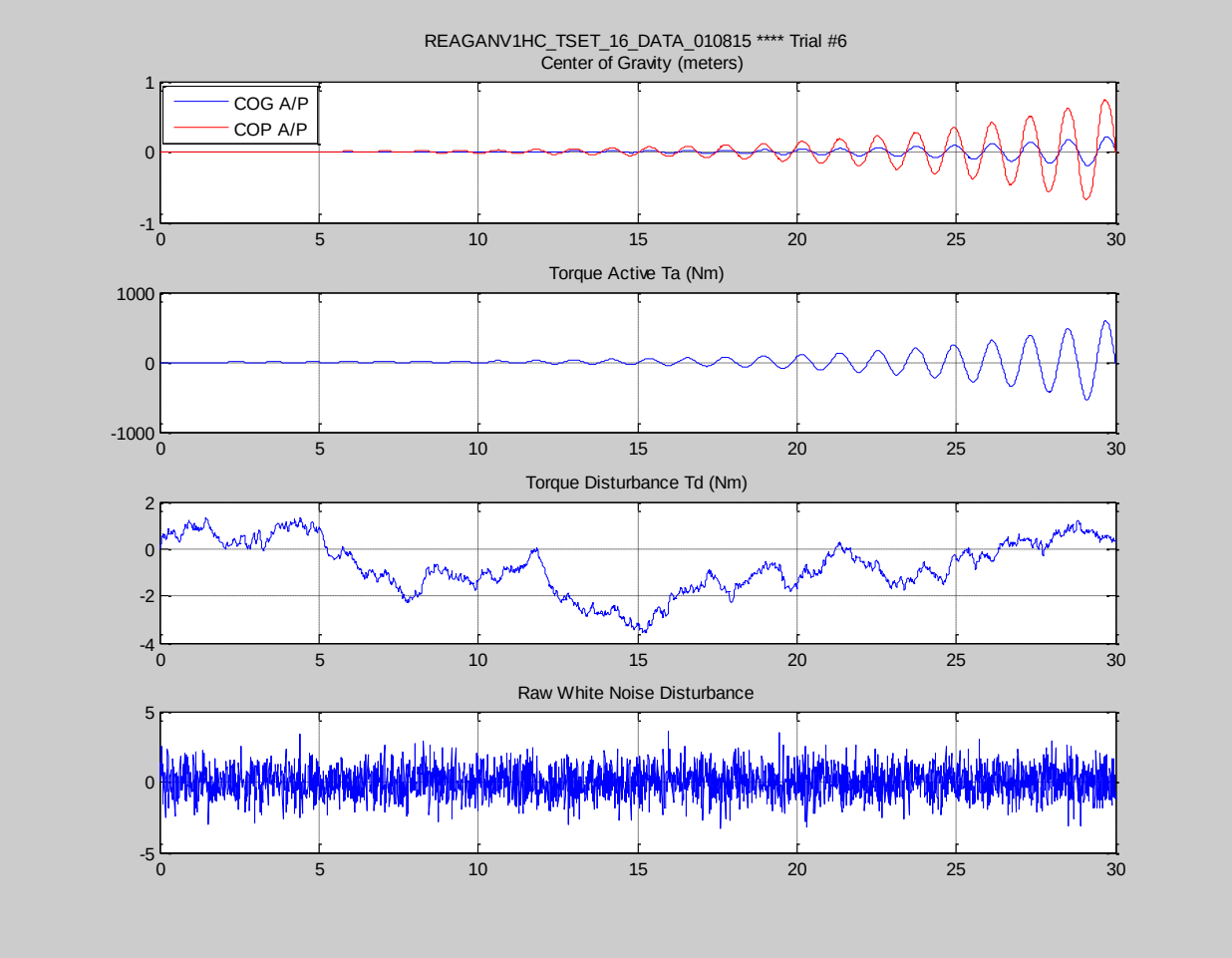

Figure B-10 - Data Quality Plots / Experiment 301 Test Set 16 / T_2= 0.155 seconds / %change from base=+6%

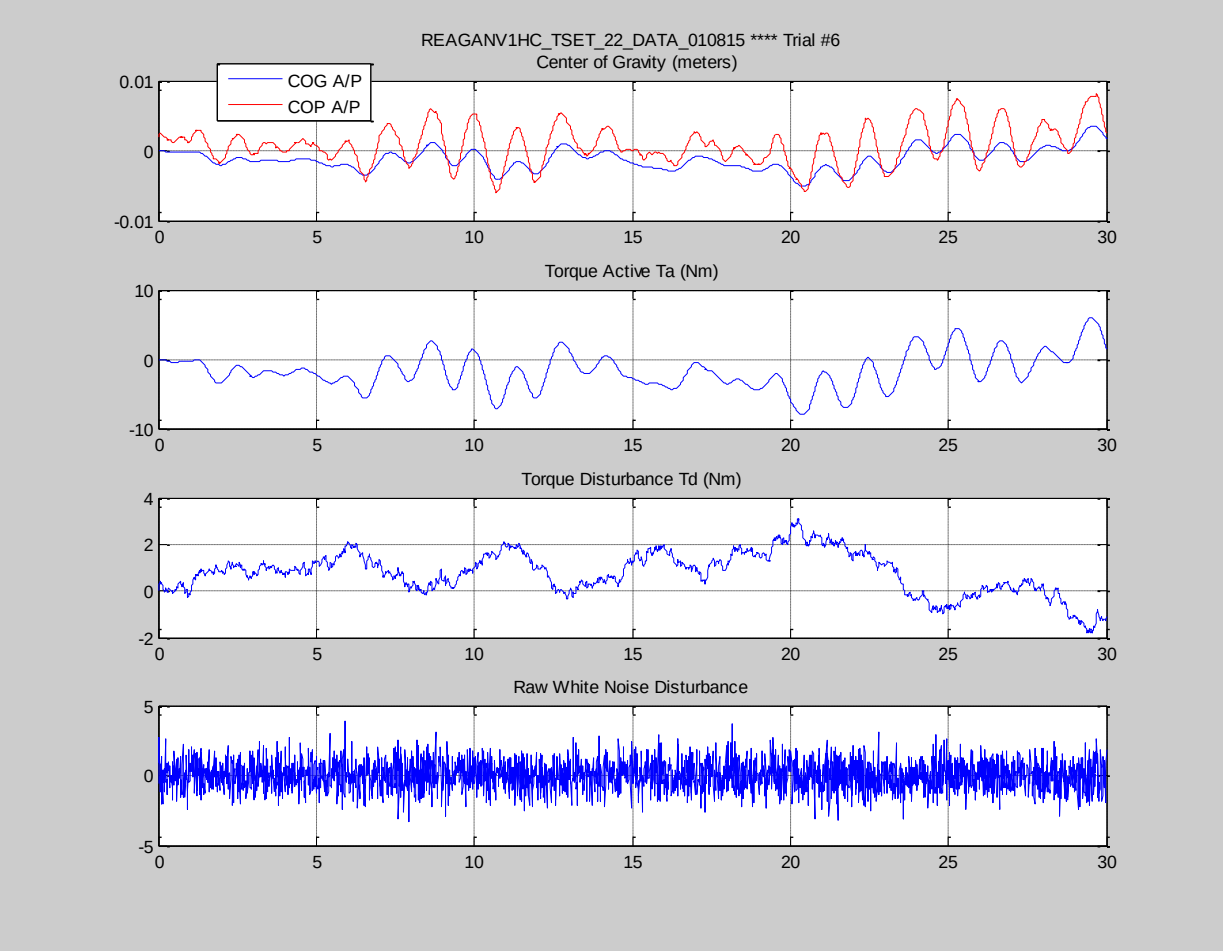

Figure B-11 - Data Quality Plots / Experiment 301 Test Set 22 / K_n =786.55 K_d =7.0143 K_p=22.36 T_2=0.1470 / Stable Base set

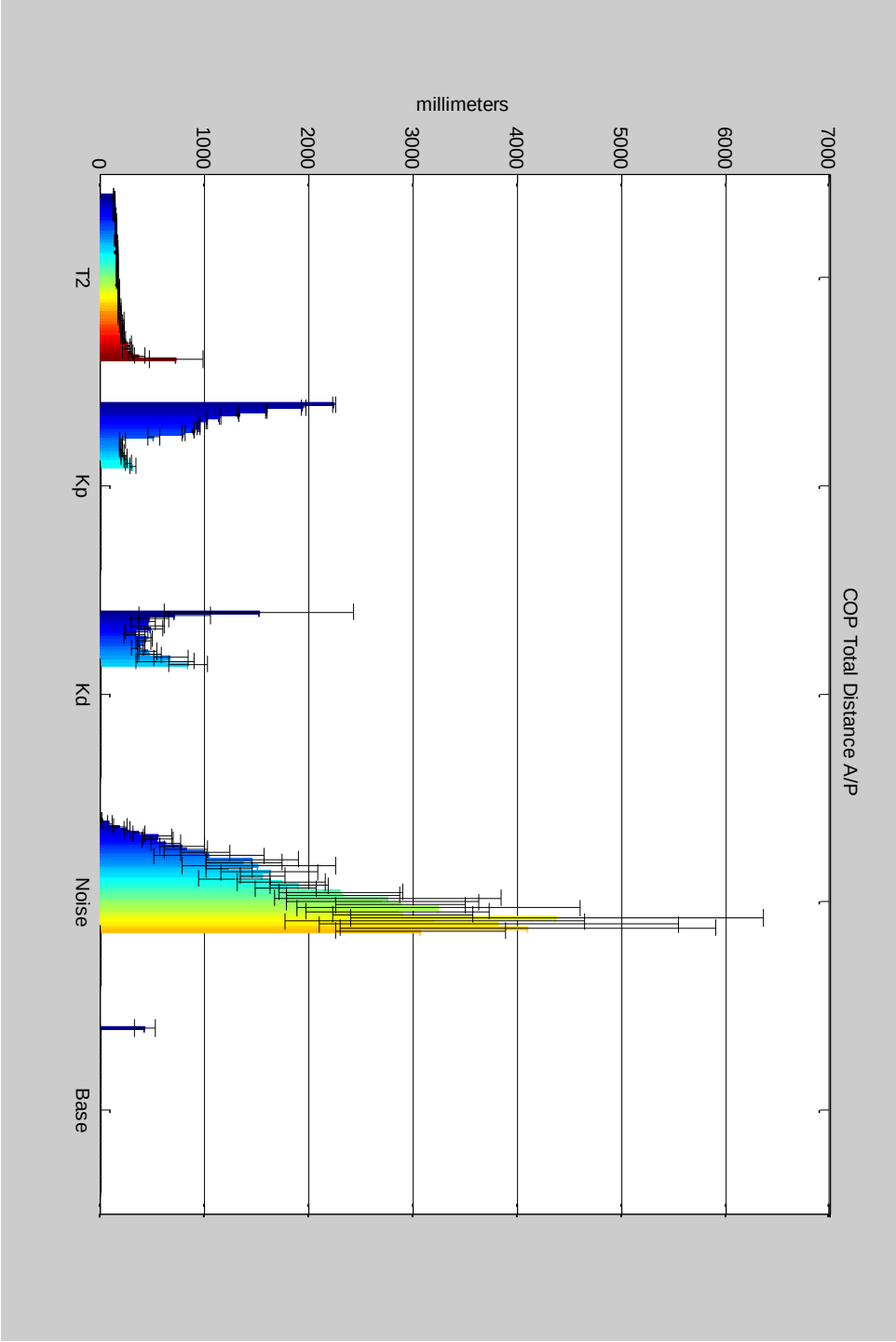

Figure B-12 - Sensitivity Plots for COP Total Distance. Each bar depicts the mean and standard deviation for each test set for model parameter of interest. See figure Table B-2 for the range of test sets show for each model parameter of interest.

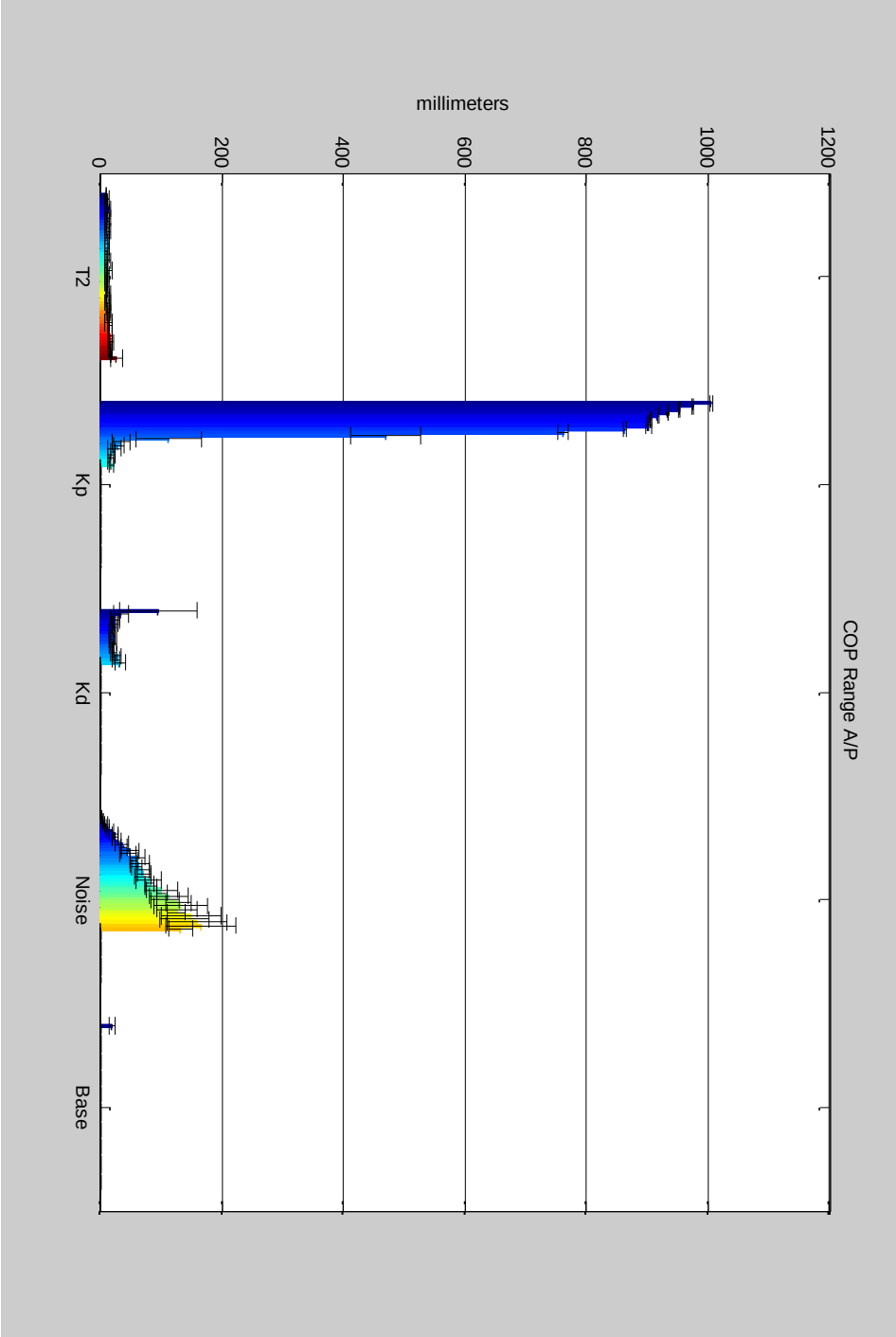

Figure B-13 - Sensitivity Plots for COP AP Range. Each bar depicts the mean and standard deviation for each test set for model parameter of interest. See figure Table B 2 for the range of test sets show for each model parameter of interest.

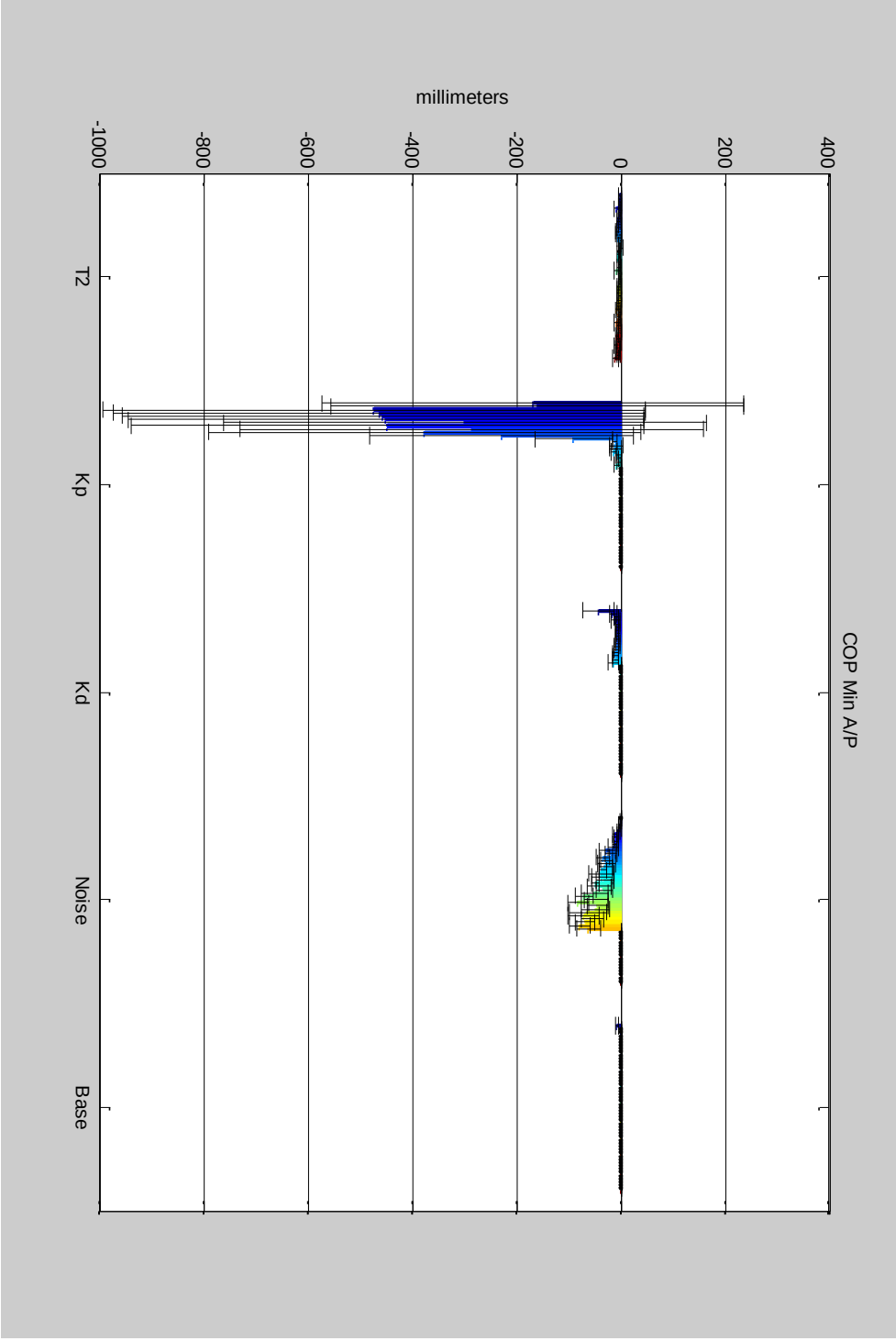

Figure B-14 - Sensitivity Plots for COP MIN AP. Each bar depicts the mean and standard deviation for each test set for model parameter of interest. See figure Table B 2 for the range of test sets show for each model parameter of interest.

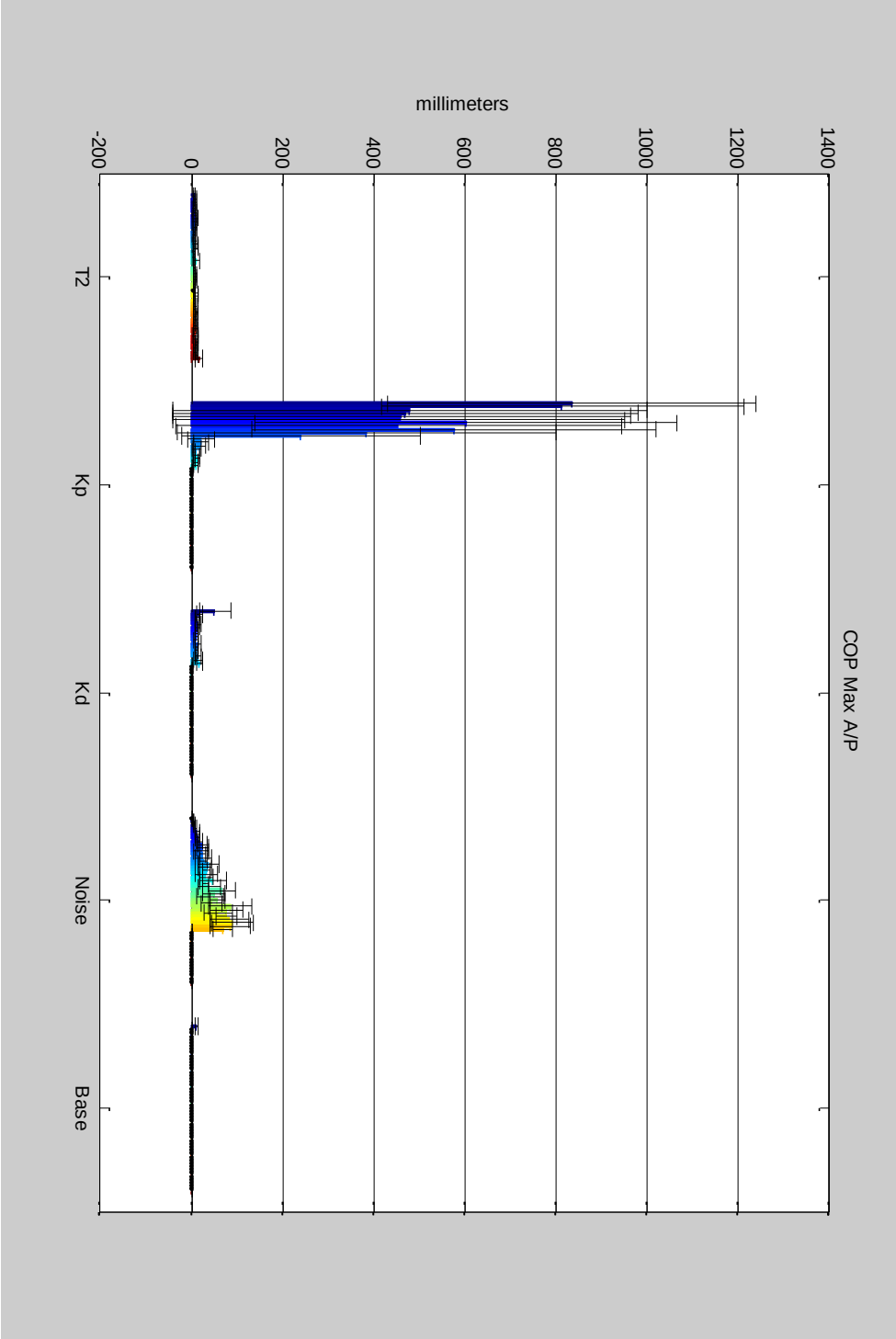

Figure B-15 - Sensitivity Plots for COP Max AP. Each bar depicts the mean and standard deviation for each test set for model parameter of interest. See figure Table B 2 for the range of test sets show for each model parameter of interest.

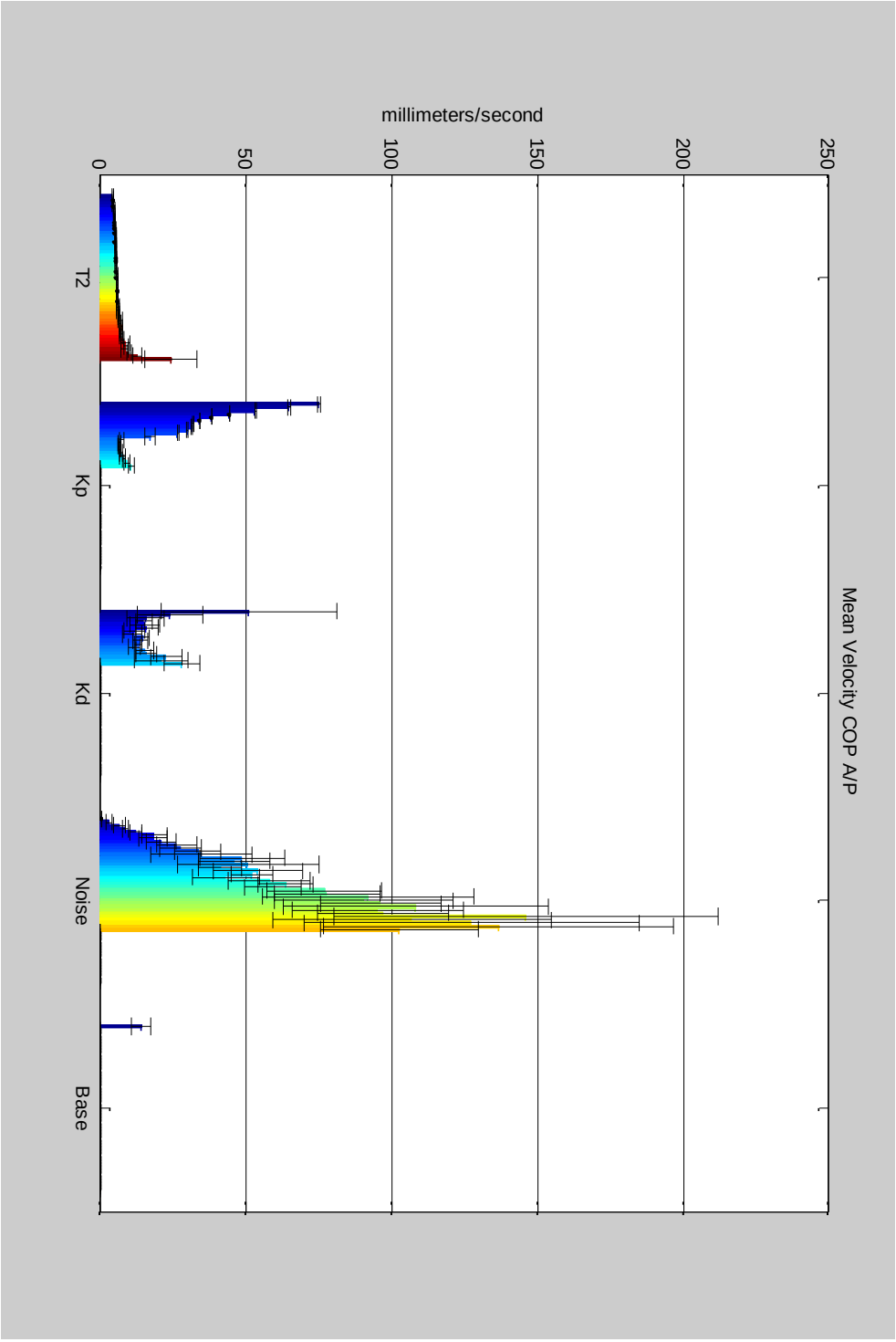

Figure B-16 - Sensitivity Plots for Mean Velocity AP. Each bar depicts the mean and standard deviation for each test set for model parameter of interest. See figure Table B 2 for the range of test sets show for each model parameter of interest.

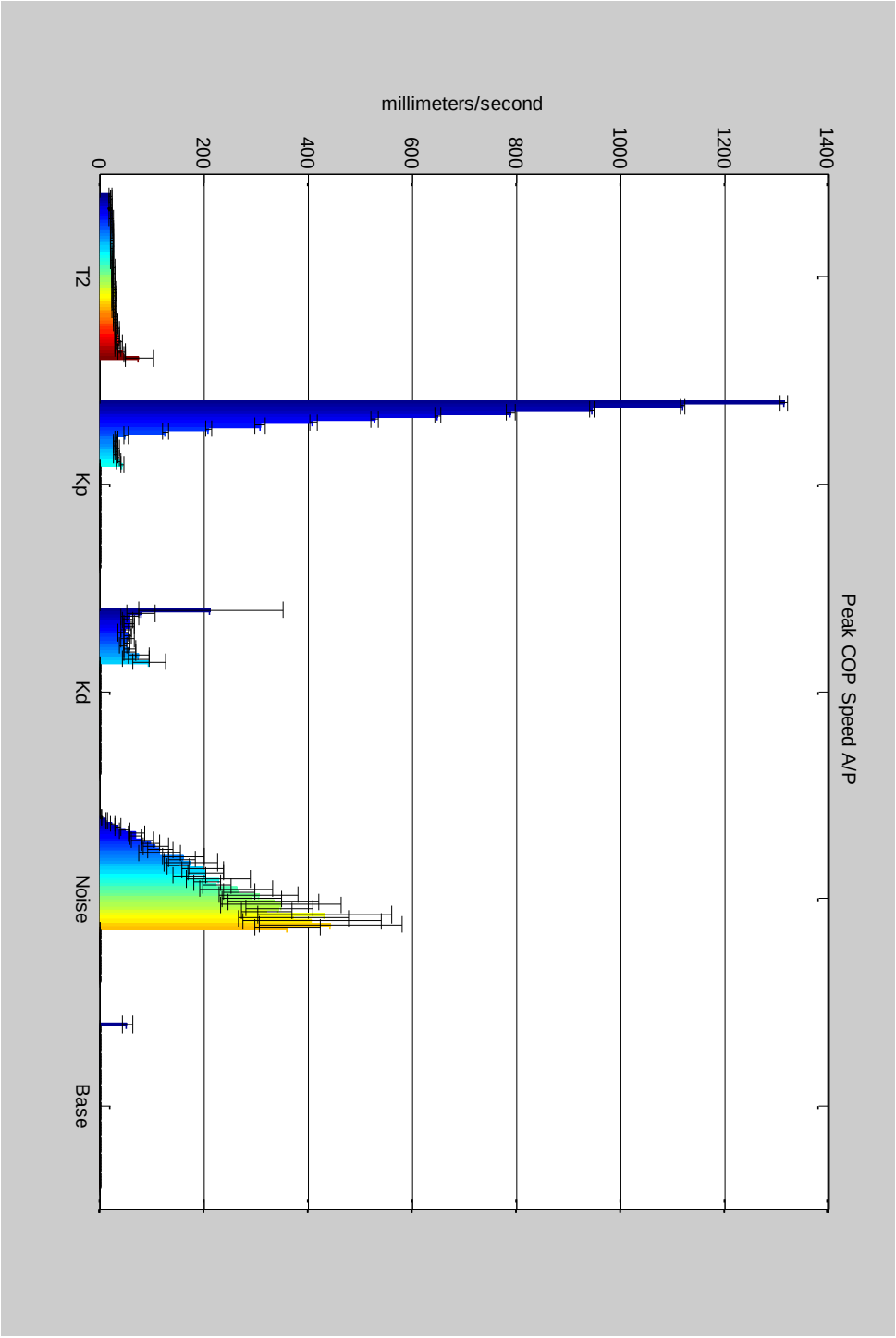

Figure B-17 - Sensitivity Plots for Peak COP Speed AP. Each bar depicts the mean and standard deviation for each test set for model parameter of interest. See figure Table B 2 for the range of test sets show for each model parameter of interest.

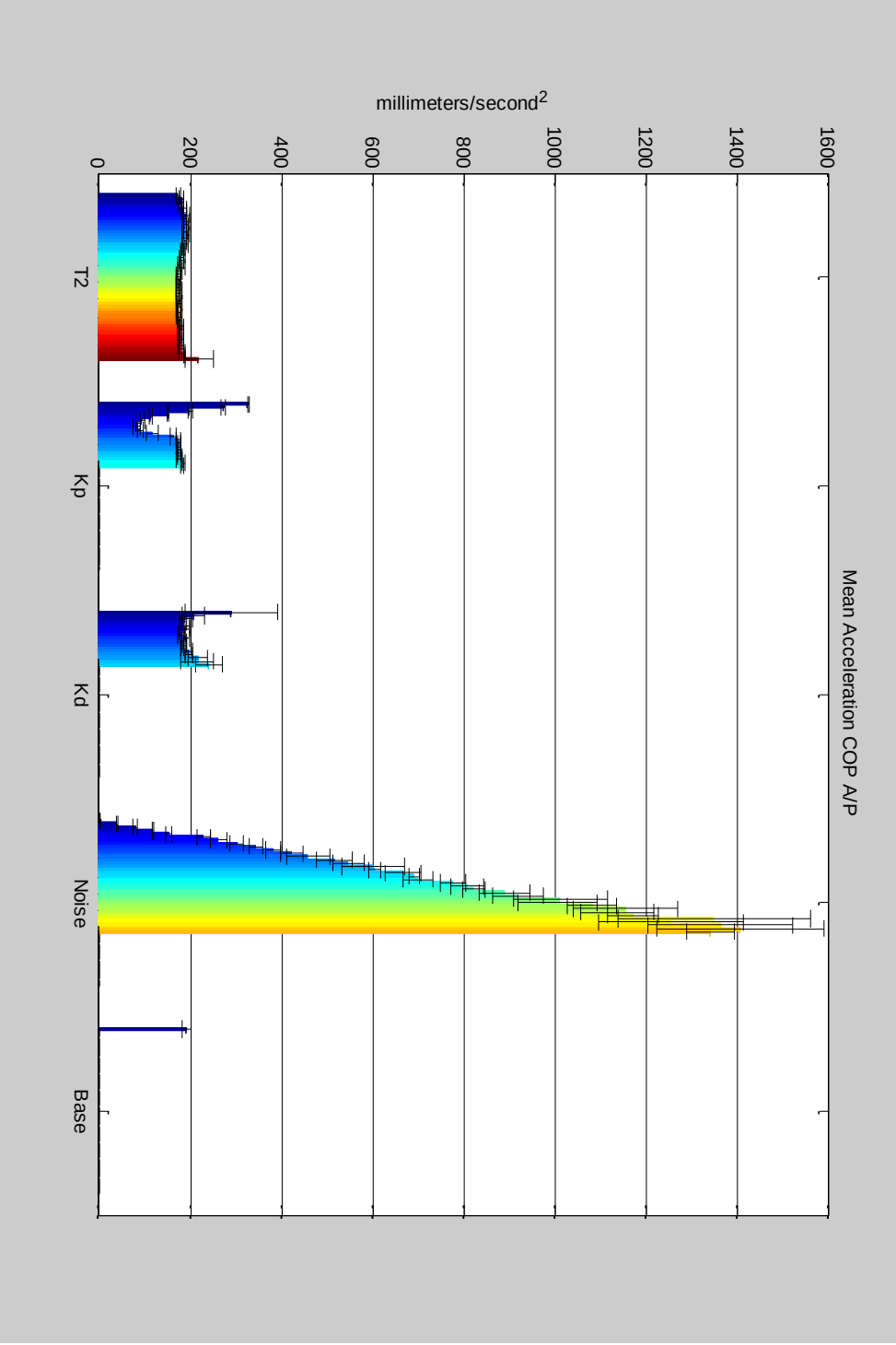

Figure B-18 - Sensitivity Plots for Mean Acceleration AP. Each bar depicts the mean and standard deviation for each test set for model parameter of interest. See figure Table B 2 for the range of test sets show for each model parameter of interest.

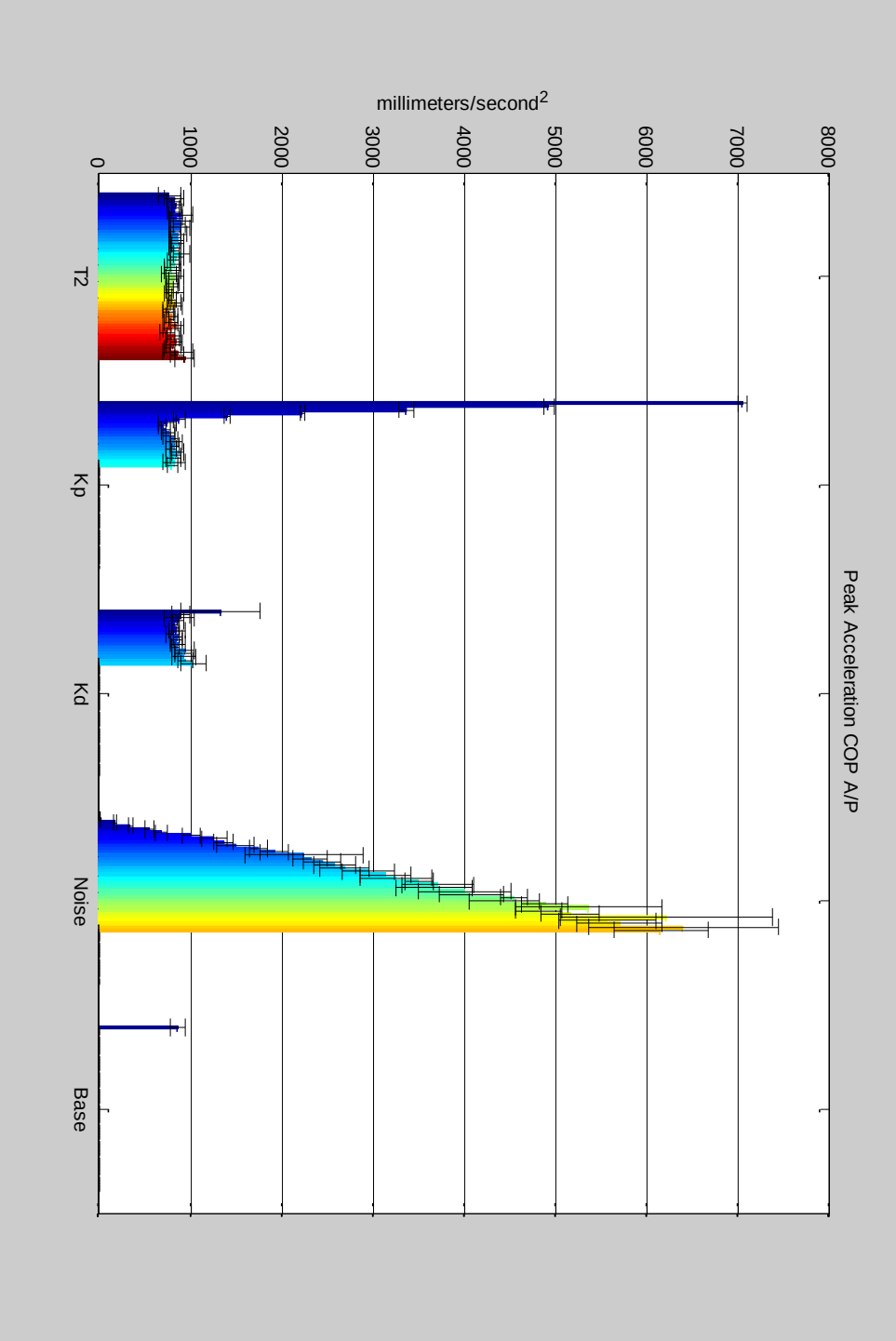

Figure B-19 - Sensitivity Plots for Peak Acceleration COP AP. Each bar depicts the mean and standard deviation for each test set for model parameter of interest. See figure Table B 2 for the range of test sets show for each model parameter of interest.

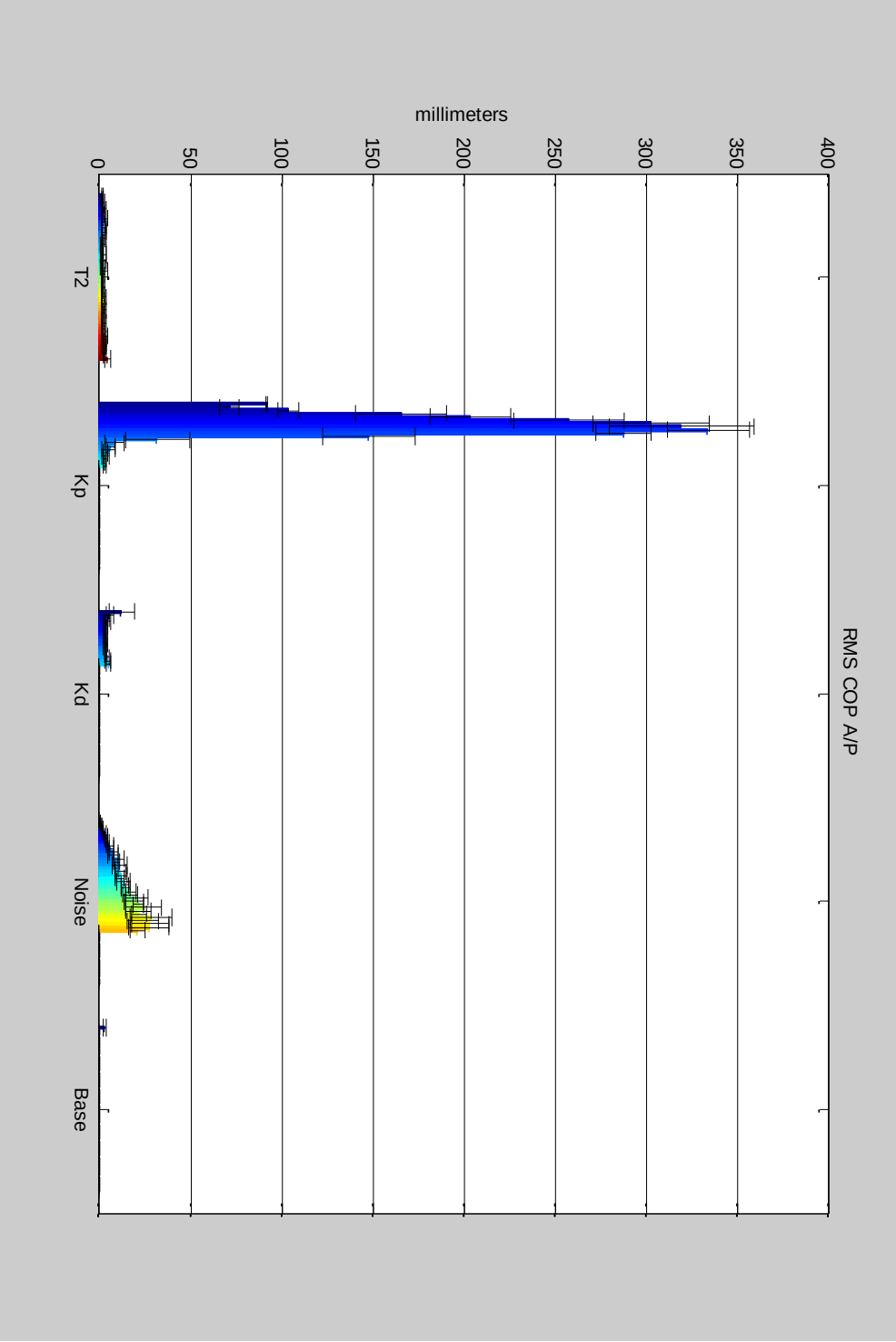

Figure B-20 - Sensitivity Plots for RMS COP AP. Each bar depicts the mean and standard deviation for each test set for model parameter of interest. See figure Table B 2 for the range of test sets show for each model parameter of interest.

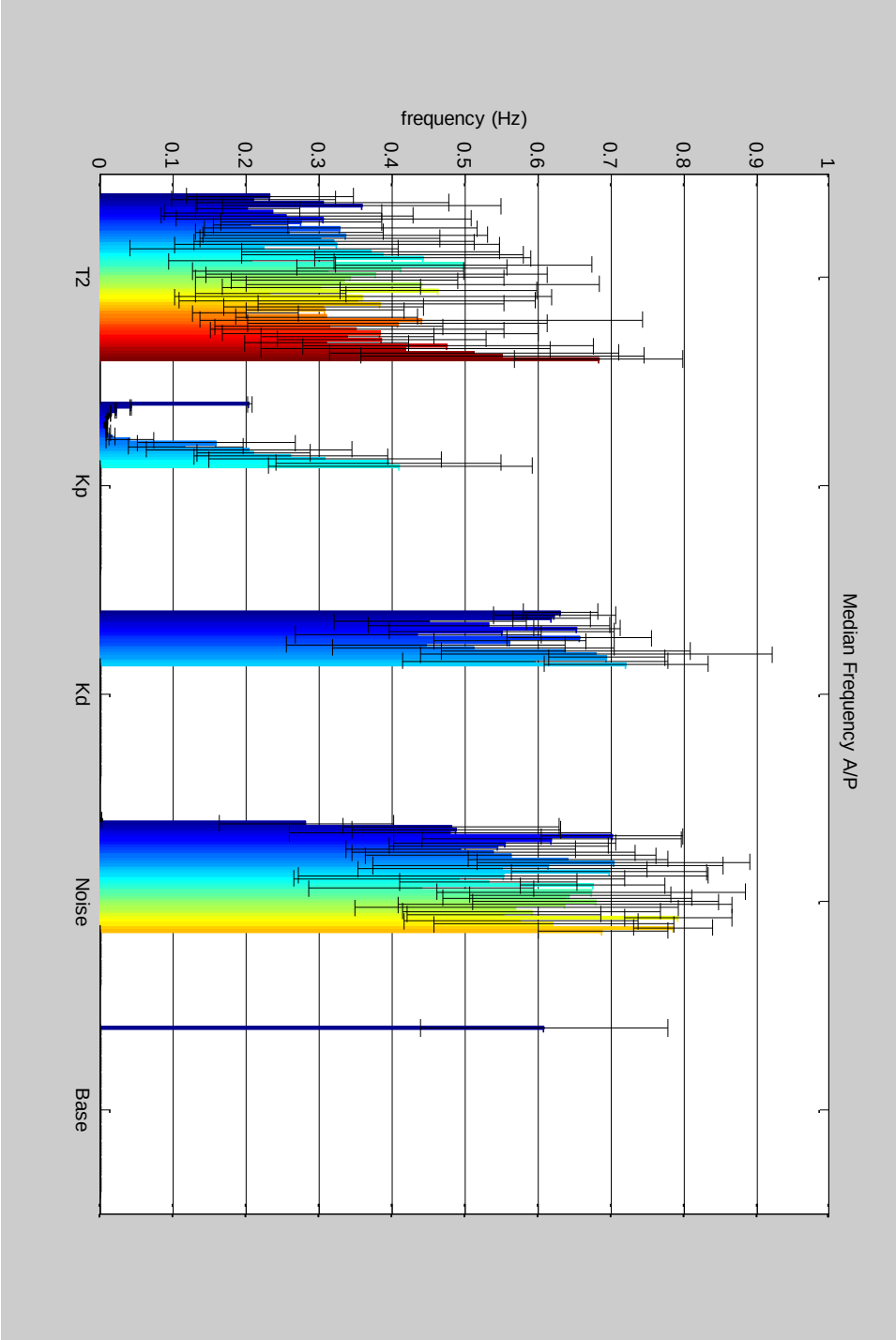

Figure B-21 - Sensitivity Plots for Median Frequency COP AP. Each bar depicts the mean and standard deviation for each test set for model parameter of interest. See figure Table B 2 for the range of test sets show for each model parameter of interest.

	Model Parameters											
	T2			Kp			Kd			Kn		
COP Variables A/P	R^2	Slope	Intercept	R^2	Slope	Intercept	R^2	Slope	Intercept	R^2	Slope	Intercept
Total Distance	0.609	562.773	1,998.909	0.461	114,126.866	793,953.934	0.608	19.058	449.481	0.968	3.703	419.334
Maximum Displacement	0.533	24.599	80.012	0.510	12,614.806	89,677.680	0.092	0.171	11.634	0.832	0.083	11.544
Minimum Displacement	0.511	-24.031	-75.219	0.409	-17,155.696	-116,373.134	0.621	-0.357	-8.607	0.808	-0.083	-7.059
Range	0.522	48.629	155.230	0.451	29,770.502	206,050.814	0.456	0.528	20.242	0.958	0.165	18.603
Peak Velocity	0.503	163.283	504.831	0.475	1,428,768.077	9,996,655.070	0.543	1.641	54.021	0.971	0.471	52.517
Mean Velocity	0.608	18.778	66.692	0.468	2,941.814	20,527.080	0.608	0.635	14.990	0.968	0.124	13.985
Peak Acceleration	0.500	723.955	2,882.138	0.460	519,902,868.960	3,613,378,343.222	0.737	8.285	881.502	0.994	8.566	864.323
Mean Acceleration	0.562	96.094	463.751	0.459	923,142.875	6,411,123.863	0.708	2.295	192.675	0.999	1.848	189.382
RMS	0.586	3.566	13.161	0.514	37.702	271.551	0.307	0.071	3.301	0.916	0.025	2.999
Median Frequency	0.981	0.033	0.631	0.608	0.391	3.324	0.647	0.018	0.600	0.337	0.001	0.570

Table B-3 - Linear Regression Data Table

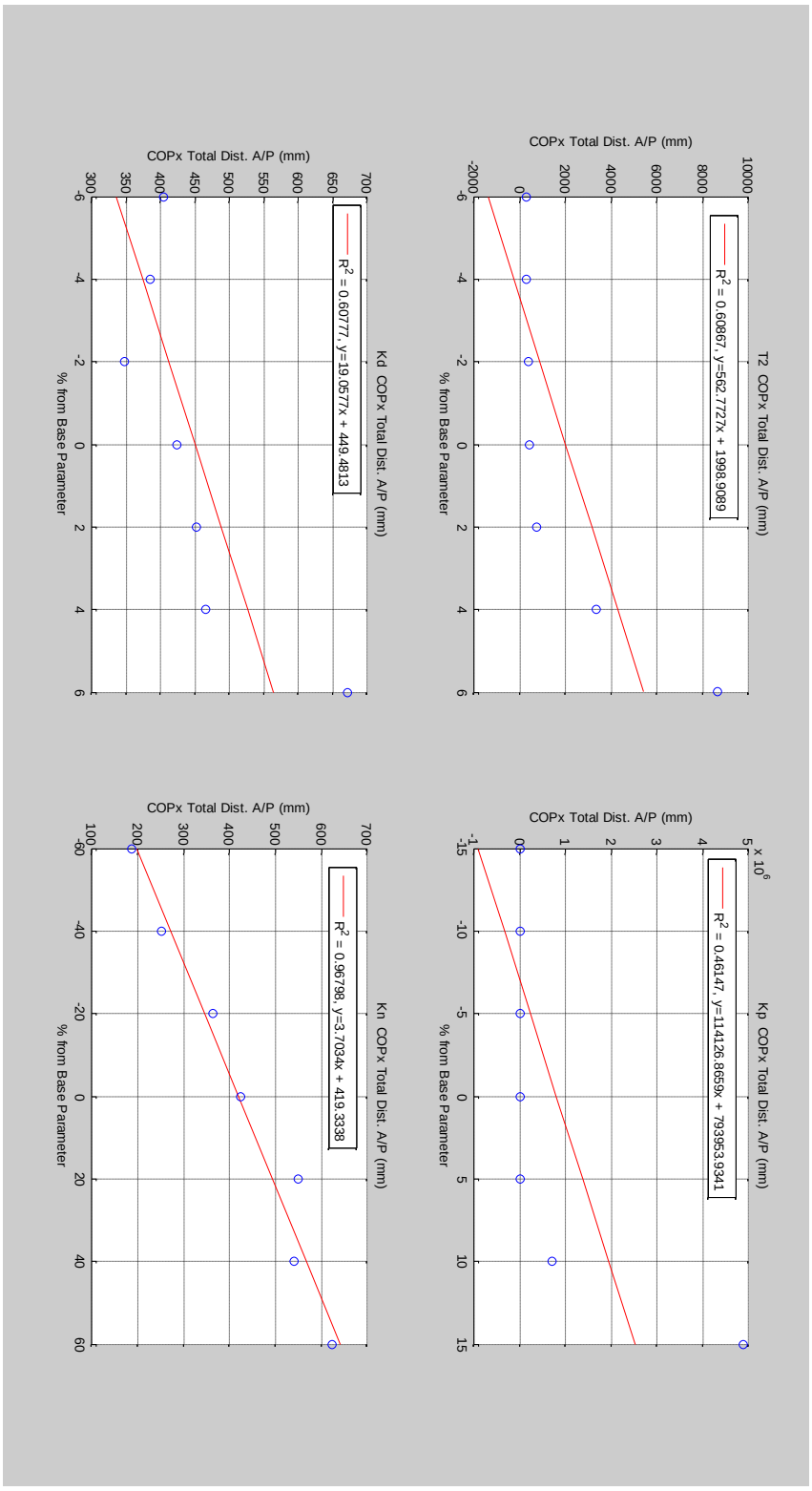

Figure B-22 - Linear Regression Plots COP Total Distance AP

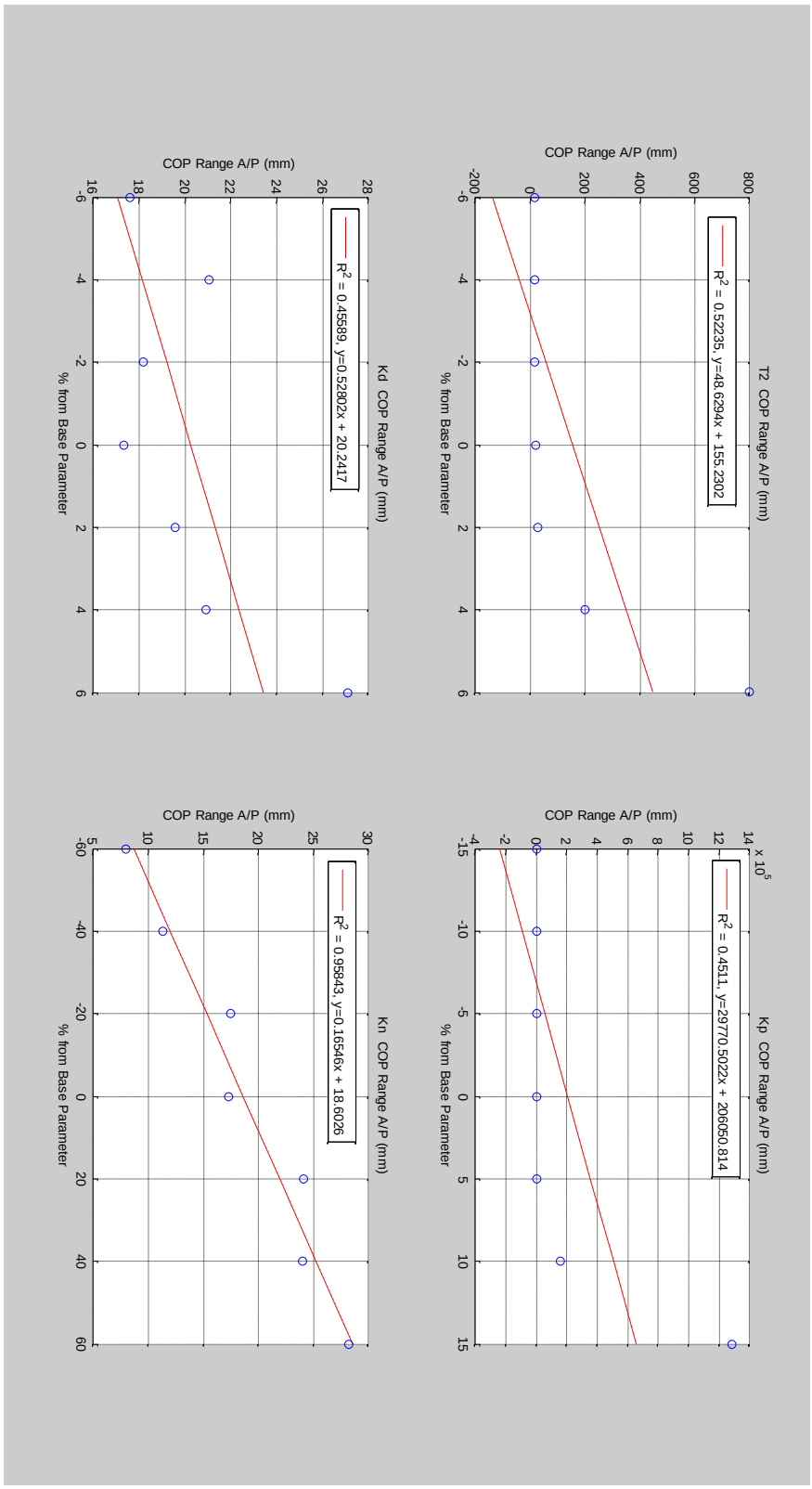

Figure B-23 - Linear Regression Plots COP Range AP

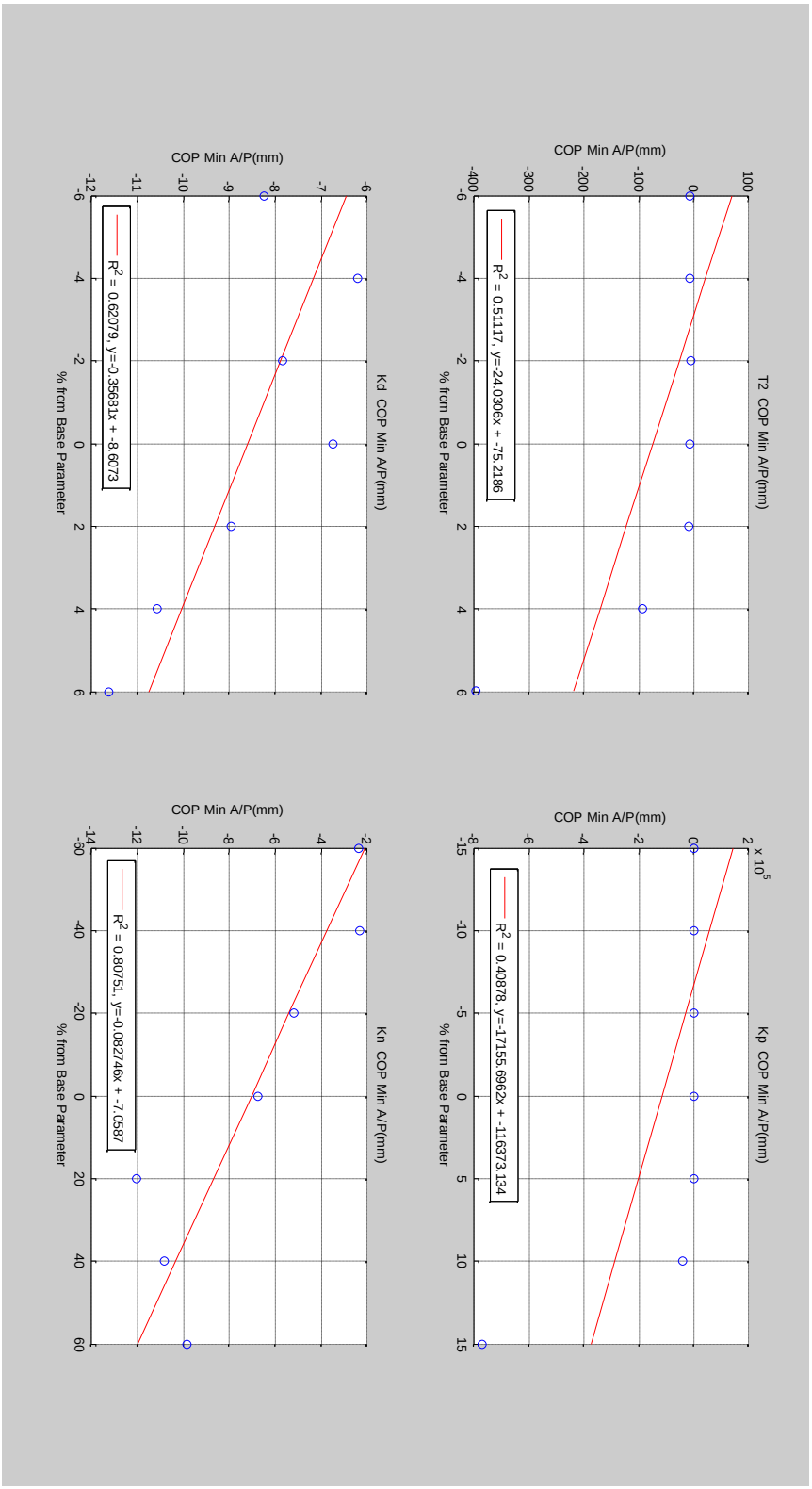

Figure B-24 - Linear Regression Plots COP MIN AP

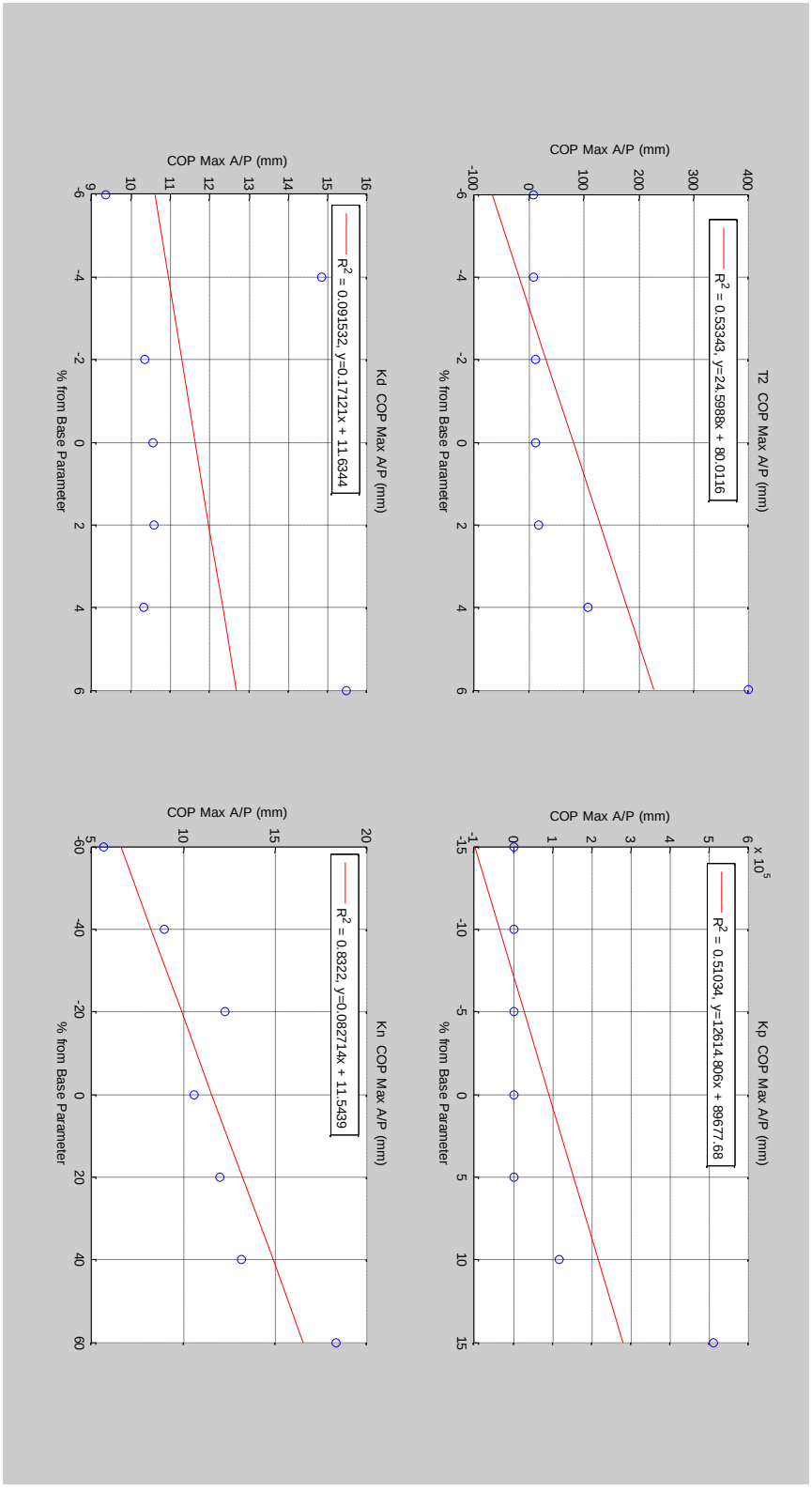

Figure B-25 - Linear Regression Plots COP MAX AP

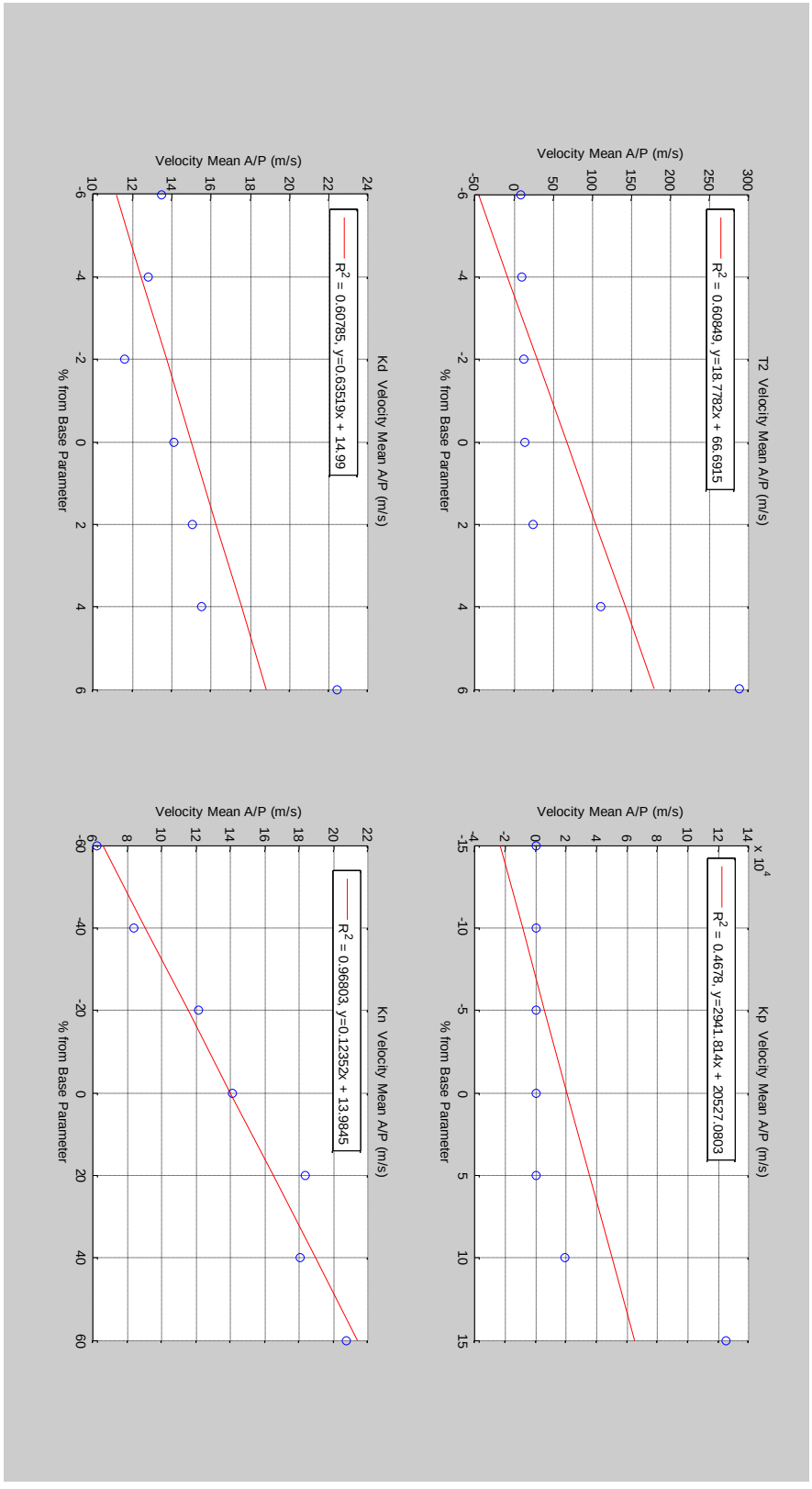

Figure B-26 - Linear Regression Plots Velocity Mean AP

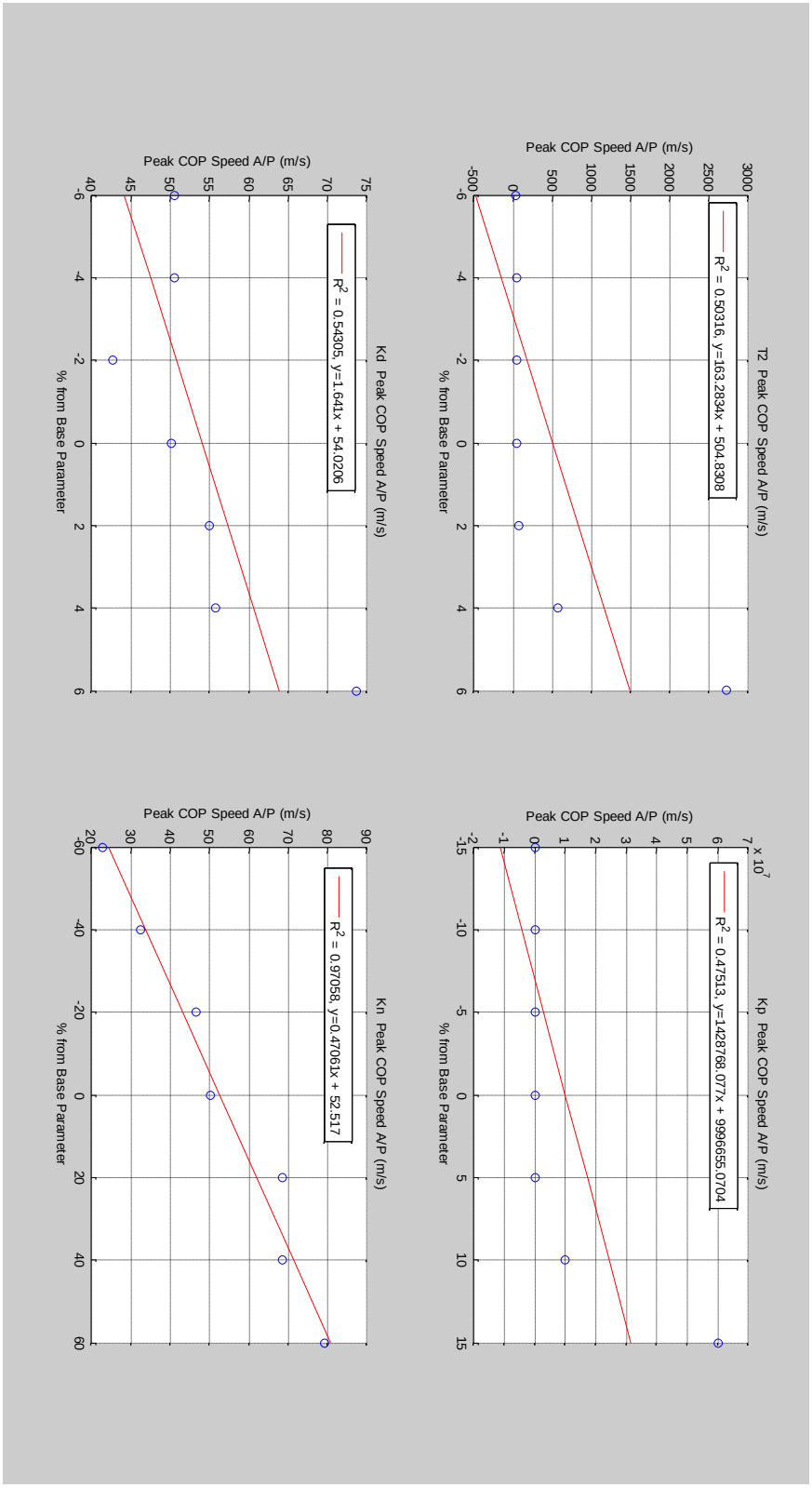

Figure B-27 - Linear Regression Plots Peak Speed AP

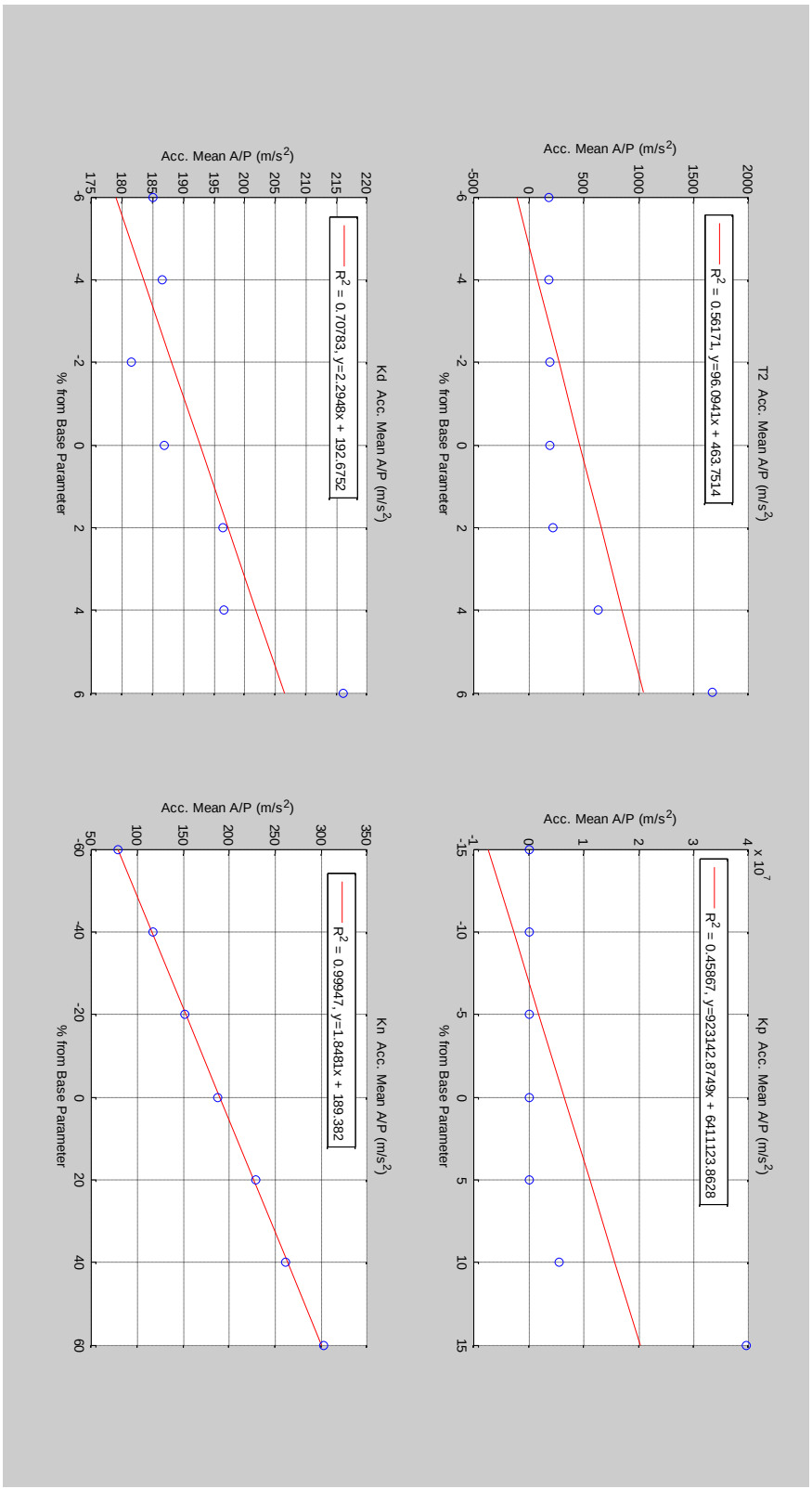

Figure B-28 - Linear Regression Plots Acceleration Mean AP

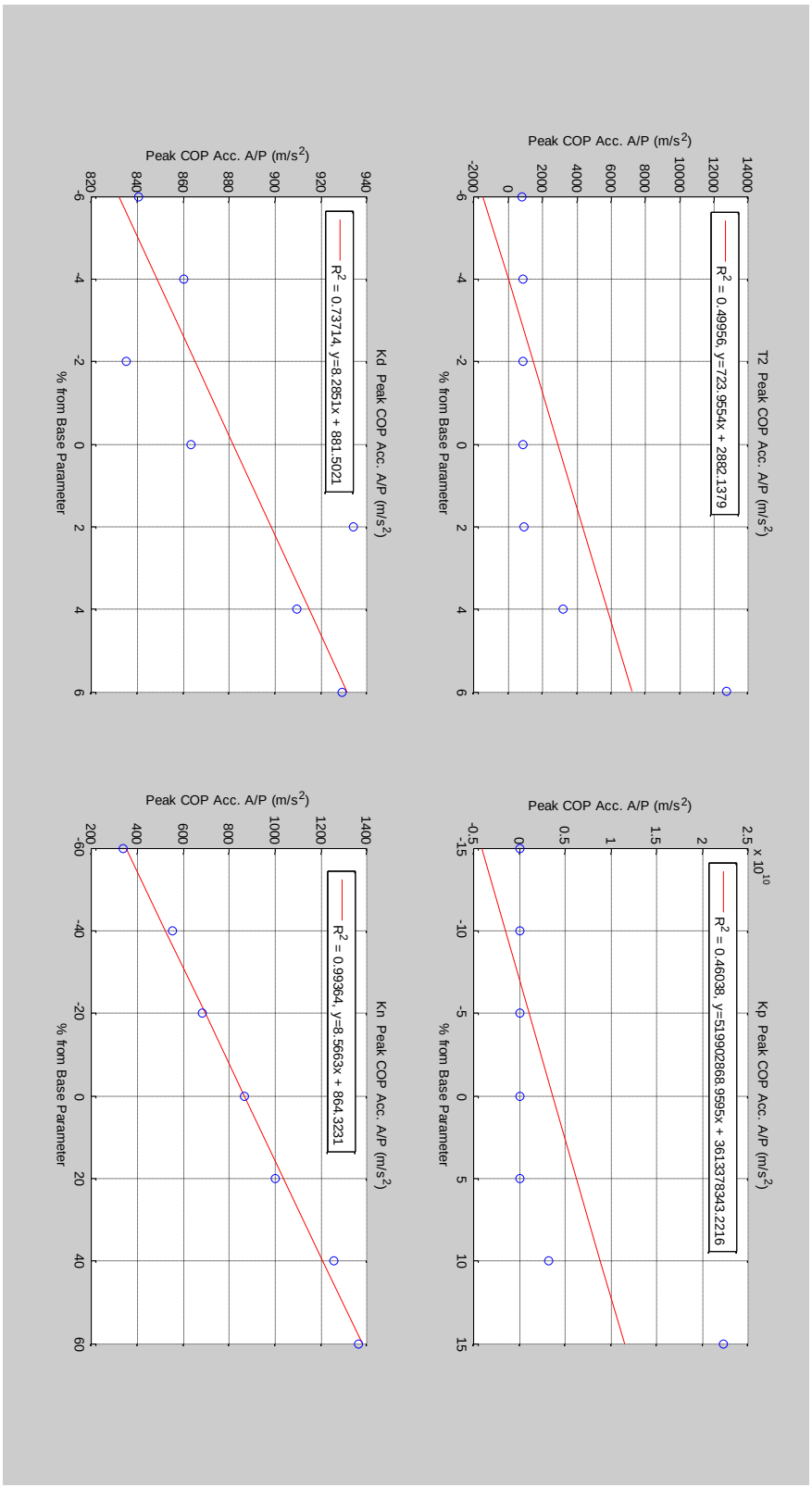

Figure B-29 - Linear Regression Plots Peak Acceleration AP

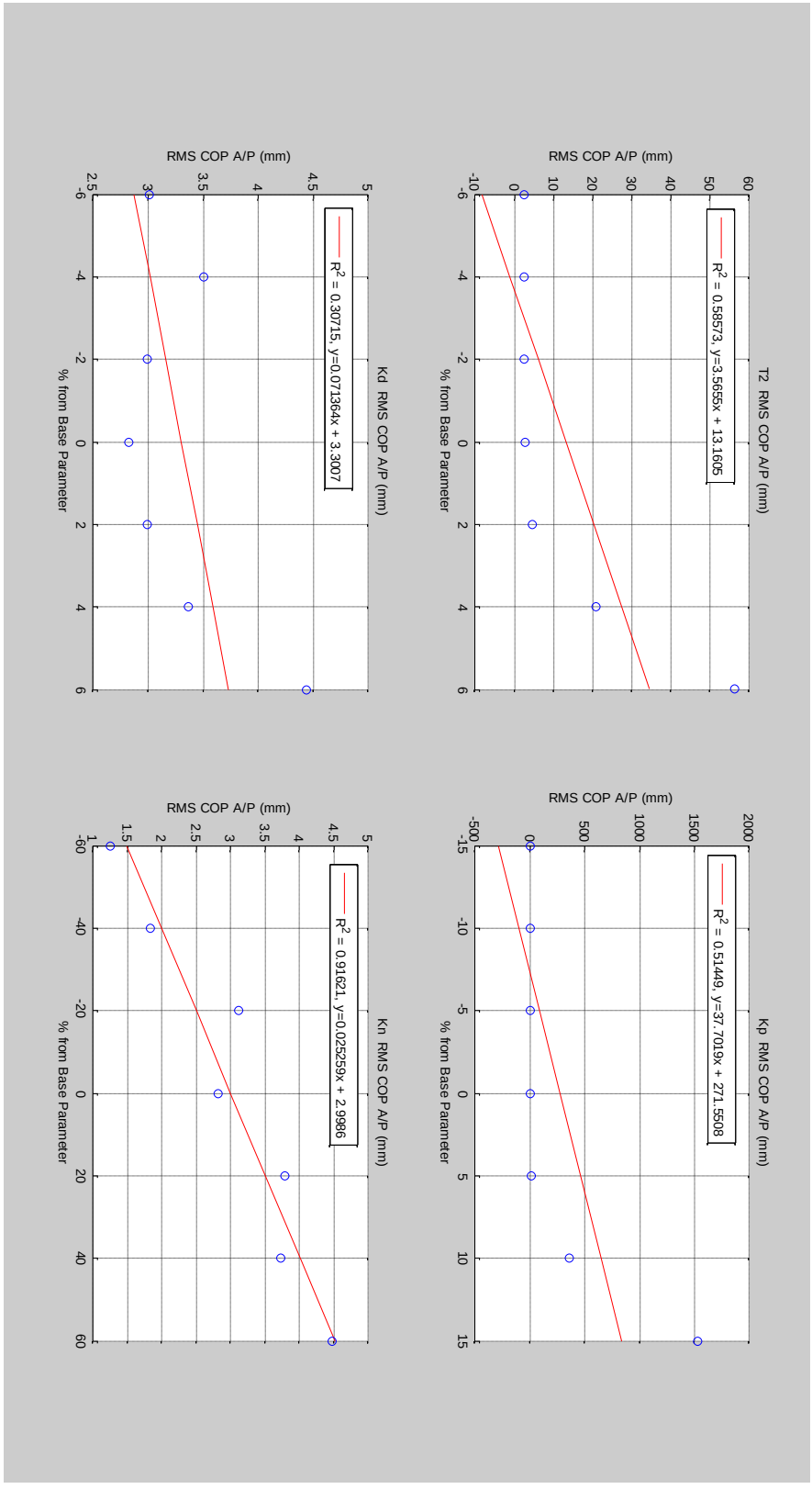

Figure B-30 - Linear Regression Plots RMS AP

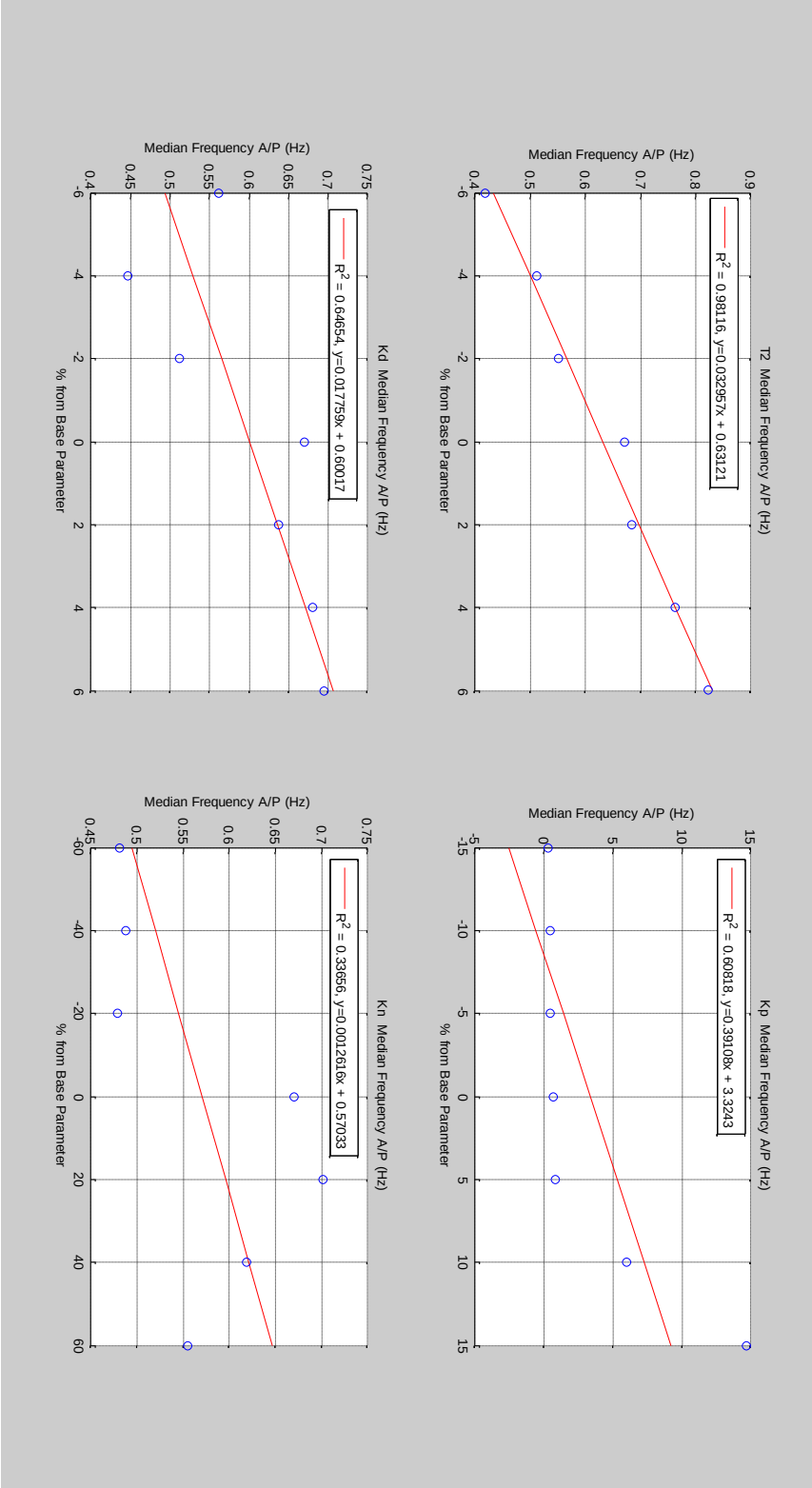

Figure B-31 - Linear Regression Plots Median Frequency

Trials	COP parameter Response to each Trial											Factorial Design Levels			
	COPx_tot_dist	COPx_max	COPx_min	COP_range_AP	vel_mean_x	peak_COP_speed_x	acc_mean_x	peak_COP_acc_x	RMS_COP_x	MedFREQ		T2	Kp	Kd	Kn
1	81.25505065	4.483919593	-1.310294899	5.794214492	2.71433272	12.5047695	71.47057301	337.8629341	1.063970719	0.285554354		137.5523	158.4304	914.5516	4.663977
2	95.36700397	5.509034144	-0.709295599	6.218329744	3.183171071	12.85061683	71.37194308	314.2638553	1.125716018	0.234196859		12.85062	158.4304	914.5516	4.663977
3	736.7120267	28.39699224	-21.85110888	50.24800104	24.56770381	137.5523048	158.4304156	914.5516208	4.663977022	0.727656664		137.5523	71.37194	914.5516	4.663977
4	6124132.491	299329.0778	-141287.371	1711616.449	15495.4488	100147715.2	50973635.25	37009504606	1750.773978	16.78902623		12.85062	71.37194	914.5516	4.663977
5	87.14884429	4.445746987	-0.839793729	5.285540716	2.909553752	11.1720917	69.37828601	324.9816607	0.892756345	0.275115837		137.5523	158.4304	314.2639	4.663977
6	124.1542622	5.352284803	-4.309780266	9.662065069	4.141635439	15.98578726	73.51163139	345.6121033	1.67116527	0.286454562		12.85062	158.4304	314.2639	4.663977
7	2055.512013	89.84264676	-93.72537791	183.568047	68.53983313	553.5306618	431.8798167	3410.701073	11.88216611	0.791183149		137.5523	71.37194	314.2639	4.663977
8	3808359.957	280112.3093	-595994.7643	876107.0736	95045.95955	5001458.5.9	3207488.5.62	1860589.4854	1127.821951	15.19384262		12.85062	71.37194	314.2639	4.663977
9	317.1824883	15.15258677	-14.81519831	29.96778508	10.59415796	46.91941103	280.2158242	1242.916146	6.275514419	0.251495526		137.5523	158.4304	914.5516	1.125716
10	390.5452912	12.41319853	-18.75018591	31.16338445	13.03518077	58.96154054	286.3914734	1330.039565	5.855345016	0.283934399		12.85062	158.4304	914.5516	1.125716
11	5987.159769	275.7151258	-259.1580898	534.8732156	199.6838635	1640.584798	1184.485829	8173.645564	37.99569206	0.829414732		137.5523	71.37194	914.5516	1.125716
12	4744630.955	49968.6009	-47350?.8536	97347?.4545	11651?.5203	5028146?.81	3975094?.96	1885279?.208	1265.87020?	15.90254774		12.85062	71.37194	914.5516	1.125716
13	355.9721186	14.62930831	-14.92247873	29.55178683	11.8837663	45.83802366	284.9955309	1264.502891	5.652171493	0.276800105		137.5523	158.4304	314.2639	1.125716
14	451.8706979	12.91733474	-17.9978022	30.91513694	15.07416602	65.47120012	295.0095719	1378.90018	5.507940919	0.401132751		12.85062	158.4304	314.2639	1.125716
15	57900.20449	3742.62143	-9344.554248	13087.17568	1659.907716	670721.0073	318744.8563	24211706?.2	111.9501569	1.412987008		137.5523	71.37194	314.2639	1.125716
16	801619.4513	84004.48289	-80527.20606	164531.689	19735.18416	8492332.946	6678622.784	318248673?	238.8052512	3.184469455		12.85062	71.37194	314.2639	1.125716

Table B-4 - Design of Experiments Response Data and Factorial Level Design

Figure B-32 - Design of Experiment Two Way Interaction and ANOVA - COP total distance

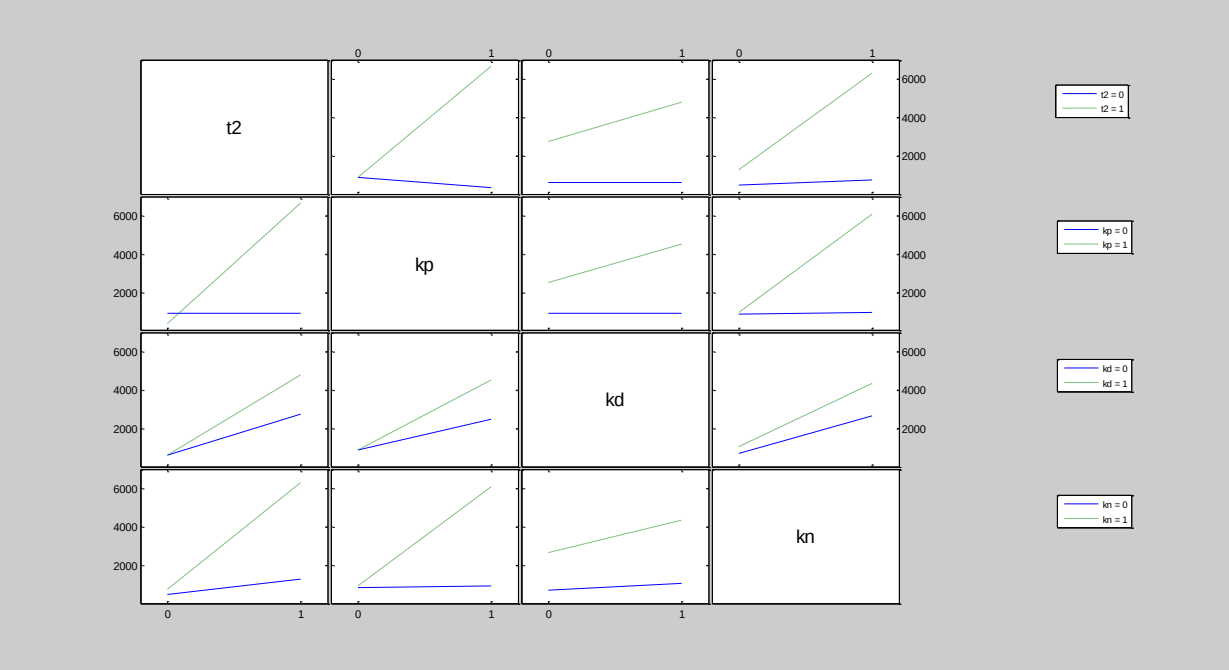

Analysis of Variance

Source	Sum Sq.	d.f.	Mean Sq.	F	Prob>F
t2	4.04295e+07	1	4.04295e+07	6.5	0.0513
Kp	2.7209e+07	1	2.7209e+07	4.38	0.0907
Kd	4.24106e+06	1	4.24106e+06	0.68	0.4465
Kn	2.75823e+07	1	2.75823e+07	4.44	0.089
t2*Kp	4.00547e+07	1	4.00547e+07	6.44	0.052
t2*Kd	4.14474e+06	1	4.14474e+06	0.67	0.4514
t2*Kn	2.22831e+07	1	2.22831e+07	3.58	0.1169
Kp*Kd	4.11315e+06	1	4.11315e+06	0.66	0.453
Kp*Kn	2.59576e+07	1	2.59576e+07	4.17	0.0965
Kd*Kn	1.69488e+06	1	1.69488e+06	0.27	0.6239
Error	3.10886e+07	5	6.21772e+06		
Total	2.28799e+08	15			

Constrained (Type III) sums of squares.

Figure B-33 - Design of Experiments Two Way Interaction and ANOVA - COP maximum displacement

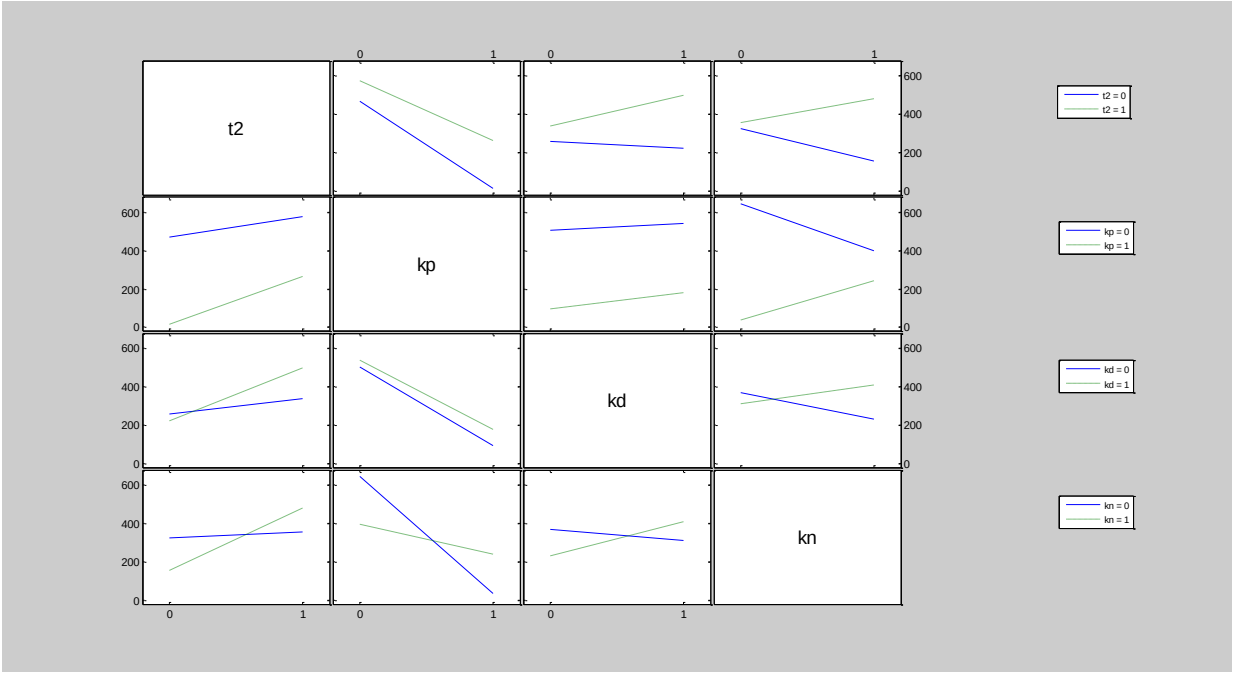

Analysis of Variance

Source	Sum Sq.	d.f.	Mean Sq.	F	Prob>F
t2	127935.2	1	127935.2	12.36	0.017
Kp	592457.5	1	592457.5	57.26	0.0006
Kd	14770.7	1	14770.7	1.43	0.2857
Kn	1884	1	1884	0.18	0.6873
t2*Kp	20387.9	1	20387.9	1.97	0.2194
t2*Kd	38133.3	1	38133.3	3.69	0.113
t2*Kn	88551.3	1	88551.3	8.56	0.0328
Kp*Kd	2472.8	1	2472.8	0.24	0.6456
Kp*Kn	207410.8	1	207410.8	20.05	0.0065
Kd*Kn	54425.8	1	54425.8	5.26	0.0703
Error	51733.4	5	10346.7		
Total	1200162.8	15			

Constrained (Type III) sums of squares.

Figure B-34 - Design of Experiments Two Way Interaction and ANOVA - COP minimum displacement

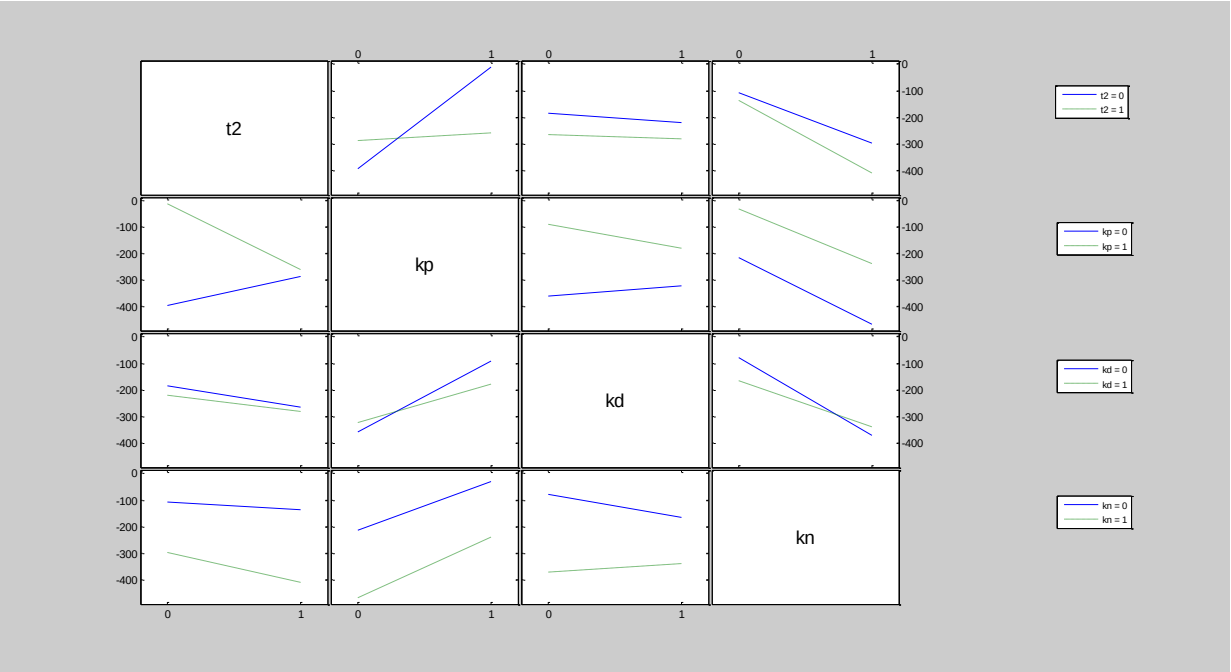

Analysis of Variance

Source	Sum Sq.	d.f.	Mean Sq.	F	Prob>F
t2	20271.6	1	20271.6	0.47	0.525
Kp	169945	1	169945	3.91	0.1049
Kd	2815.5	1	2815.5	0.06	0.8092
Kn	214414.8	1	214414.8	4.93	0.077
t2*Kp	127076	1	127076	2.92	0.148
t2*Kd	491.5	1	491.5	0.01	0.9195
t2*Kn	7105.3	1	7105.3	0.16	0.7027
Kp*Kd	15986.5	1	15986.5	0.37	0.5707
Kp*Kn	2185.2	1	2185.2	0.05	0.8315
Kd*Kn	13864.6	1	13864.6	0.32	0.5966
Error	217341.4	5	43468.3		
Total	791497.5	15			

Constrained (Type III) sums of squares.

Figure B-35 - Design of Experiments Two Way Interaction and ANOVA- COP range

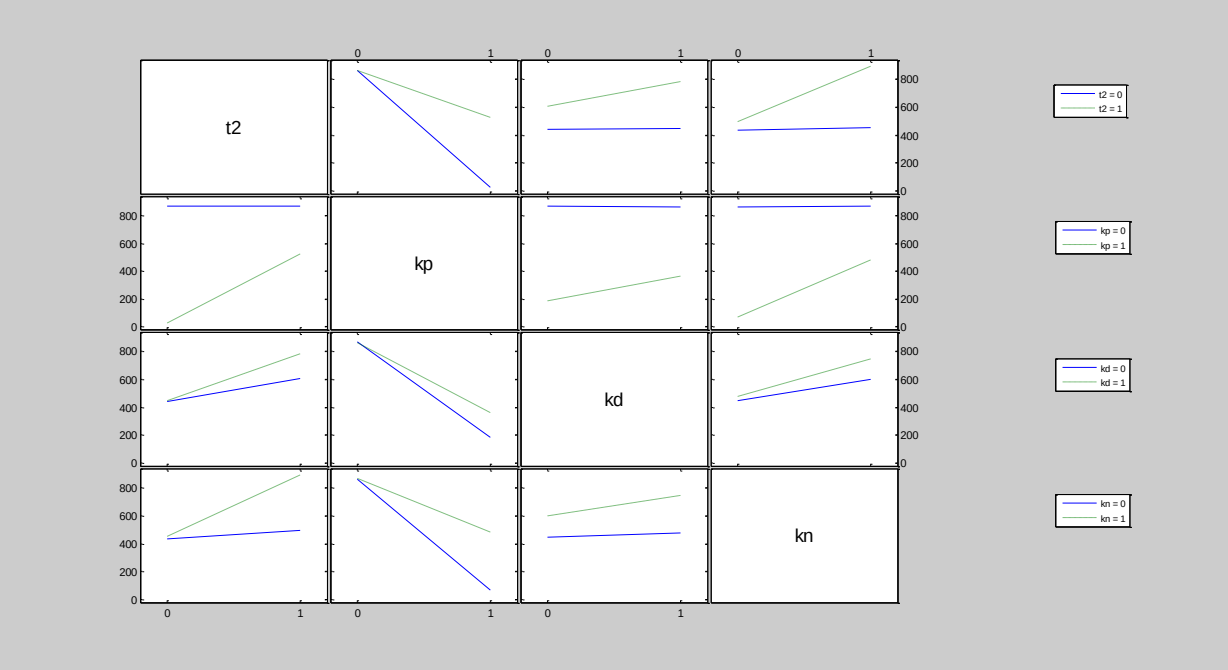

Analysis of Variance

Source	Sum Sq.	d.f.	Mean Sq.	F	Prob>F
t2	250058.7	1	250058.7	5.71	0.0624
Kp	1397021.1	1	1397021.1	31.92	0.0024
Kd	30483.9	1	30483.9	0.7	0.442
Kn	176101.3	1	176101.3	4.02	0.1012
t2*Kp	249264	1	249264	5.7	0.0627
t2*Kd	29966.7	1	29966.7	0.68	0.4456
t2*Kn	145823.4	1	145823.4	3.33	0.1275
Kp*Kd	31034.1	1	31034.1	0.71	0.4381
Kp*Kn	167017.1	1	167017.1	3.82	0.1082
Kd*Kn	13350.7	1	13350.7	0.31	0.6045
Error	218819.6	5	43763.9		
Total	2708940.6	15			

Constrained (Type III) sums of squares.

Figure B-36 - Design of Experiments Two Way Interaction and ANOVA- Velocity Mean

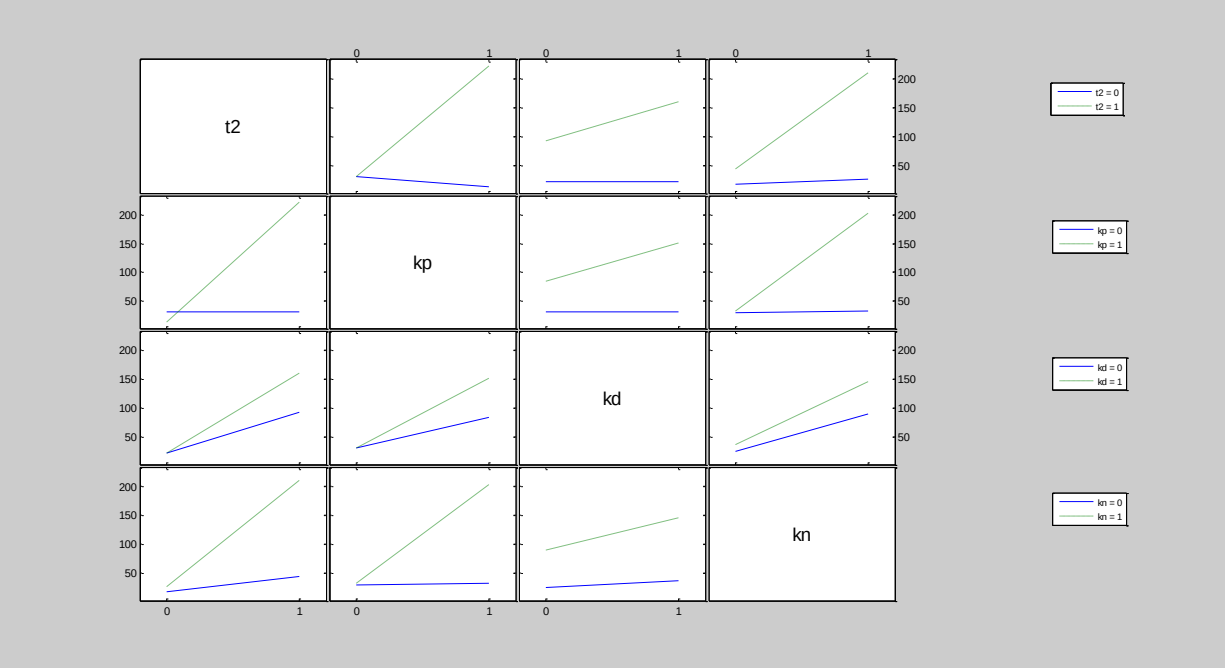

Analysis of Variance

Source	Sum Sq.	d.f.	Mean Sq.	F	Prob>F
t2	44962.6	1	44962.6	6.5	0.0513
Kp	30282.1	1	30282.1	4.38	0.0906
Kd	4722.8	1	4722.8	0.68	0.4462
Kn	30681.3	1	30681.3	4.44	0.0891
t2*Kp	44545.7	1	44545.7	6.44	0.052
t2*Kd	4615.5	1	4615.5	0.67	0.4511
t2*Kn	24777.9	1	24777.9	3.58	0.117
Kp*Kd	4580	1	4580	0.66	0.4528
Kp*Kn	28868.6	1	28868.6	4.17	0.0965
Kd*Kn	1887.4	1	1887.4	0.27	0.6237
Error	34583.8	5	6916.8		
Total	254507.8	15			

Constrained (Type III) sums of squares.

Figure B-37 - Design of Experiments Two Way Interaction and ANOVA - Peak Speed

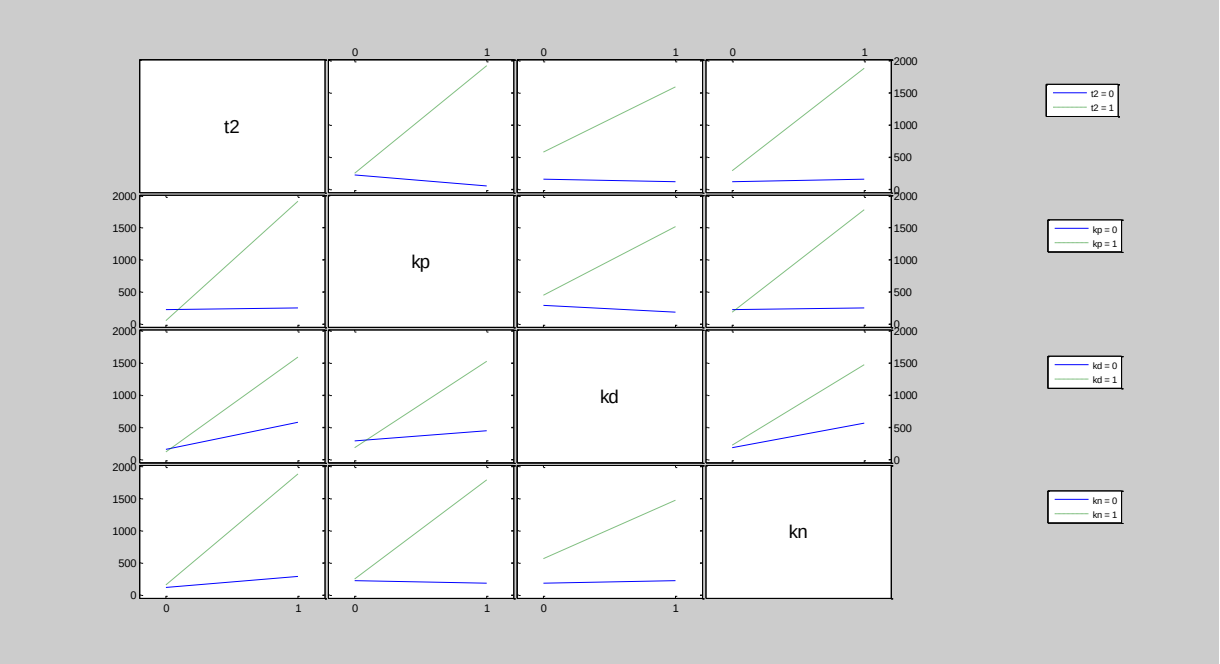

Analysis of Variance

Source	Sum Sq.	d.f.	Mean Sq.	F	Prob>F
t2	3584445.9	1	3584445.9	3.11	0.1383
Kp	2223053	1	2223053	1.93	0.2239
Kd	926285.5	1	926285.5	0.8	0.4114
Kn	2637616.8	1	2637616.8	2.29	0.191
t2*Kp	3419936.5	1	3419936.5	2.96	0.1458
t2*Kd	1107908.3	1	1107908.3	0.96	0.3722
t2*Kn	2352386.5	1	2352386.5	2.04	0.2128
Kp*Kd	1375773.3	1	1375773.3	1.19	0.3247
Kp*Kn	2464017.4	1	2464017.4	2.13	0.2038
Kd*Kn	744821	1	744821	0.65	0.4583
Error	5771004.6	5	1154200.9		
Total	26607248.8	15			

Constrained (Type III) sums of squares.

Figure B-38 - Design of Experiments Two Way Interaction and ANOVA- Acceleration Mean

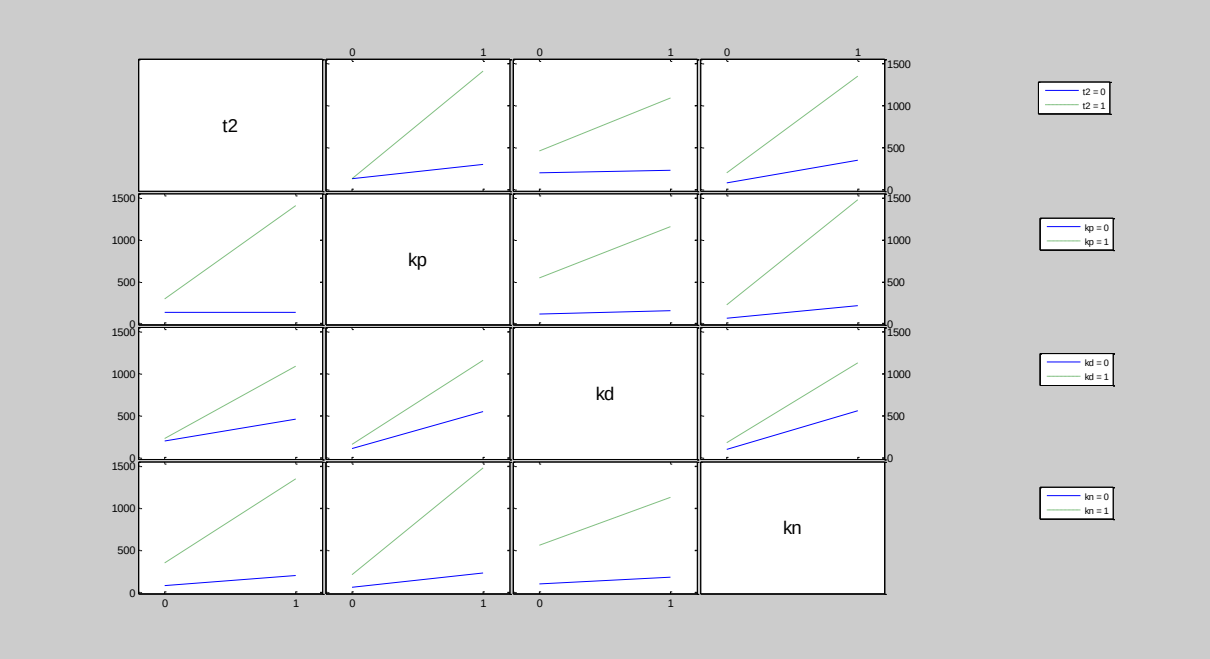

Analysis of Variance

Source	Sum Sq.	d.f.	Mean Sq.	F	Prob>F
t2	1250626.9	1	1250626.9	3.73	0.1114
Kp	2078065.7	1	2078065.7	6.2	0.0552
Kd	430249.6	1	430249.6	1.28	0.3088
Kn	1992602.9	1	1992602.9	5.94	0.0589
t2*Kp	1242559.4	1	1242559.4	3.7	0.1123
t2*Kd	374452.3	1	374452.3	1.12	0.3391
t2*Kn	760937.7	1	760937.7	2.27	0.1924
Kp*Kd	326249.3	1	326249.3	0.97	0.3693
Kp*Kn	1214210.9	1	1214210.9	3.62	0.1155
Kd*Kn	232070.3	1	232070.3	0.69	0.4434
Error	1677208	5	335441.6		
Total	11579233.1	15			

Constrained (Type III) sums of squares.

Figure B-39 - Design of Experiments Two Way Interaction and ANOVA - Peak Acceleration

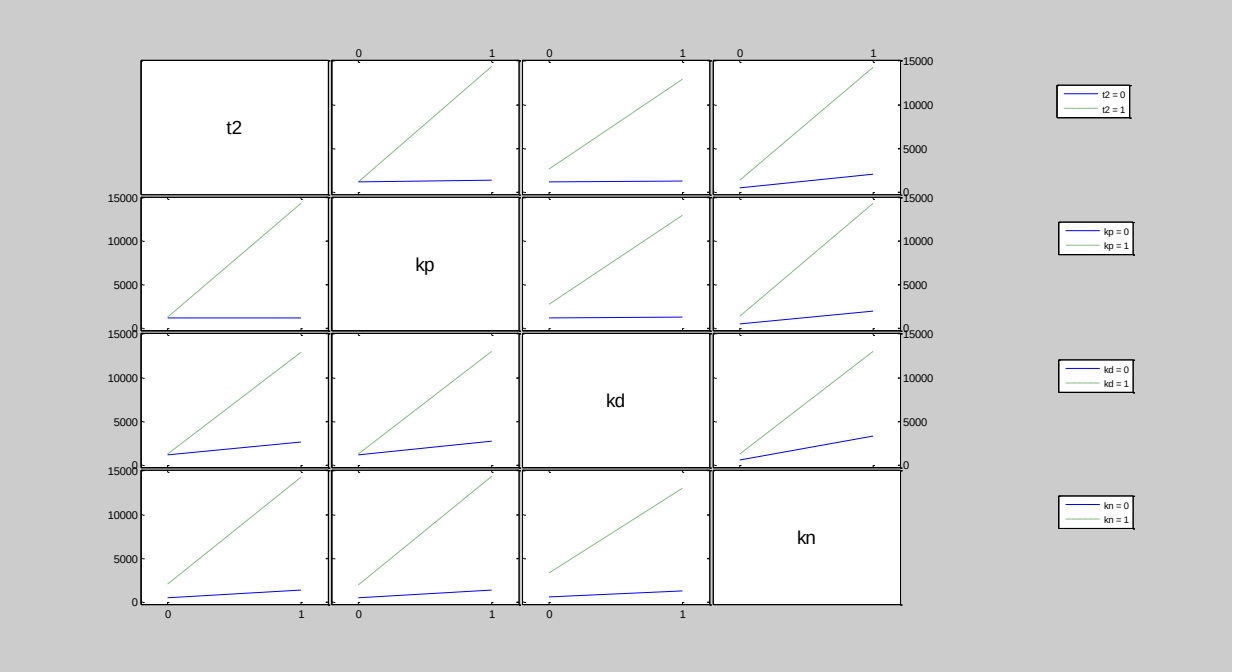

Analysis of Variance

Source	Sum Sq.	d.f.	Mean Sq.	F	Prob>F
t2	1.71097e+08	1	1.71097e+08	1.81	0.2361
Kp	1.77465e+08	1	1.77465e+08	1.88	0.2287
Kd	1.06794e+08	1	1.06794e+08	1.13	0.3362
Kn	2.1137e+08	1	2.1137e+08	2.24	0.1949
t2*Kp	1.70827e+08	1	1.70827e+08	1.81	0.2364
t2*Kd	1.03224e+08	1	1.03224e+08	1.09	0.3437
t2*Kn	1.29188e+08	1	1.29188e+08	1.37	0.2948
Kp*Kd	1.02501e+08	1	1.02501e+08	1.09	0.3452
Kp*Kn	1.33674e+08	1	1.33674e+08	1.42	0.2875
Kd*Kn	8.07042e+07	1	8.07042e+07	0.85	0.3976
Error	4.72118e+08	5	9.44236e+07		
Total	1.85896e+09	15			

Constrained (Type III) sums of squares.

Figure B-40 - Design of Experiments Two Way Interaction and ANOVA – RMS

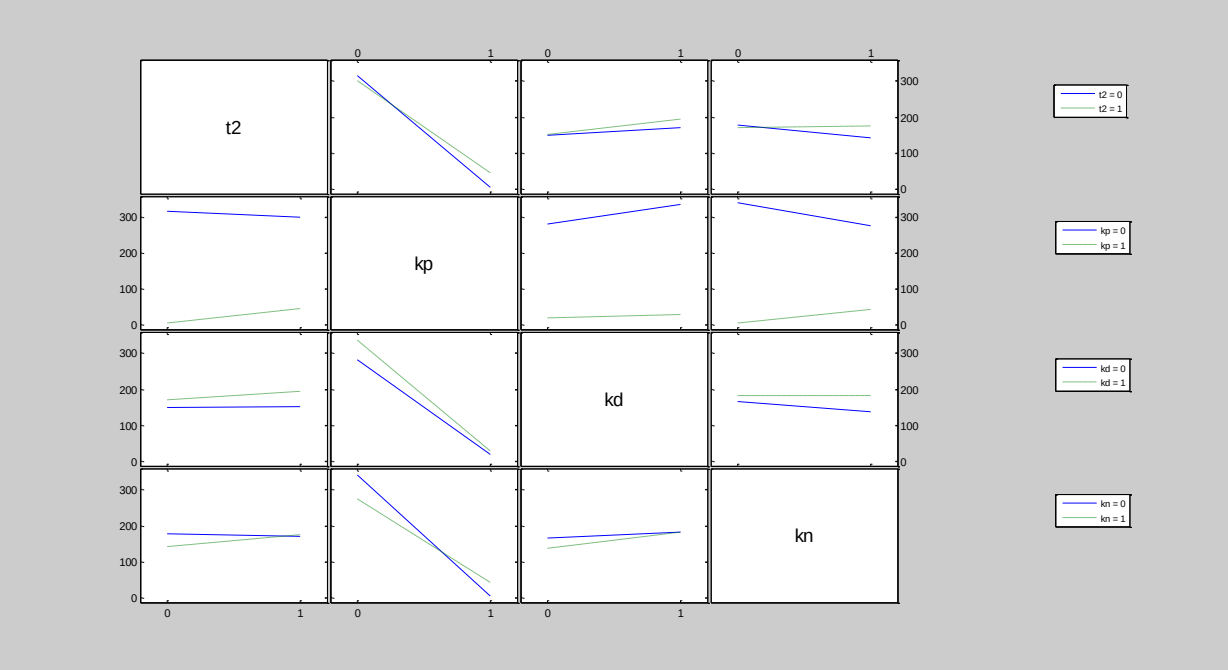

Analysis of Variance

Source	Sum Sq.	d.f.	Mean Sq.	F	Prob>F
t2	649.9	1	649.9	3.24	0.1319
Kp	322972.4	1	322972.4	1608.95	0
Kd	3908.8	1	3908.8	19.47	0.0069
Kn	870.4	1	870.4	4.34	0.0918
t2*Kp	3029.5	1	3029.5	15.09	0.0116
t2*Kd	420.4	1	420.4	2.09	0.2075
t2*Kn	1420.5	1	1420.5	7.08	0.0449
Kp*Kd	2180.2	1	2180.2	10.86	0.0216
Kp*Kn	10563.8	1	10563.8	52.63	0.0008
Kd*Kn	814.6	1	814.6	4.06	0.1001
Error	1003.7	5	200.7		
Total	347834.3	15			

Constrained (Type III) sums of squares.

Figure B-41 - Design of Experiments Two Way Interaction and ANOVA - Median Frequency

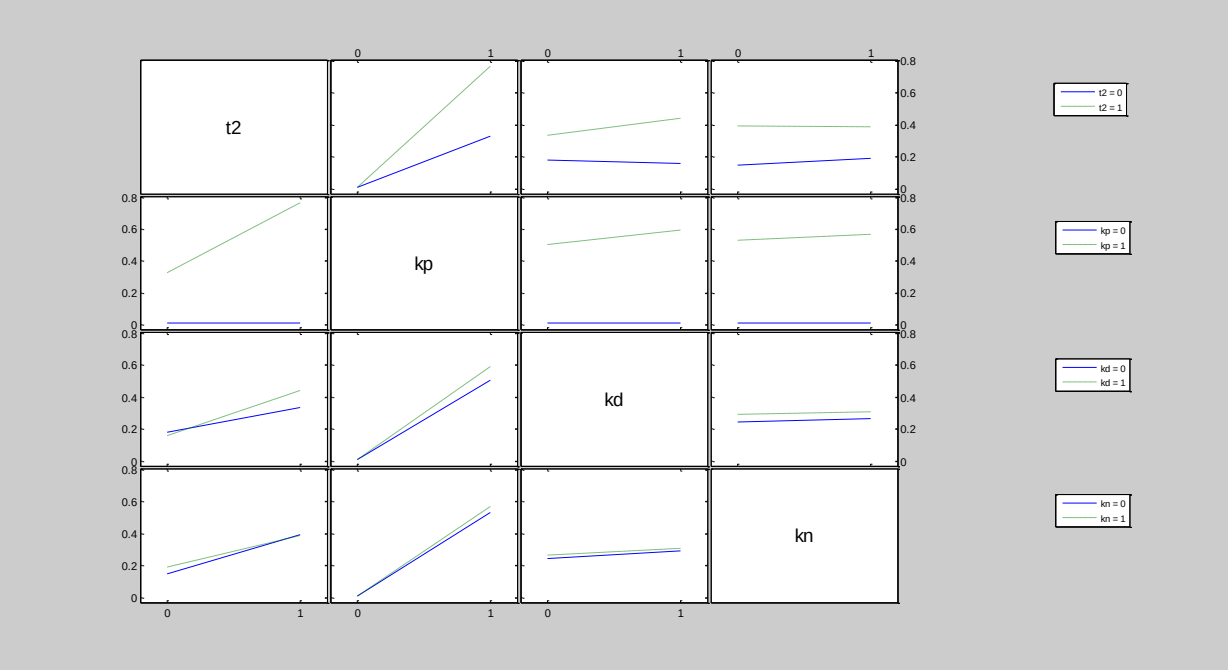

Analysis of Variance

Source	Sum Sq.	d.f.	Mean Sq.	F	Prob>F
t2	0.19345	1	0.19345	52.61	0.0008
Kp	1.16945	1	1.16945	318.01	0
Kd	0.00814	1	0.00814	2.21	0.197
Kn	0.00133	1	0.00133	0.36	0.5733
t2*Kp	0.19349	1	0.19349	52.62	0.0008
t2*Kd	0.01635	1	0.01635	4.45	0.0888
t2*Kn	0.0021	1	0.0021	0.57	0.4835
Kp*Kd	0.00757	1	0.00757	2.06	0.2108
Kp*Kn	0.00143	1	0.00143	0.39	0.5599
Kd*Kn	0.00005	1	0.00005	0.01	0.9135
Error	0.01839	5	0.00368		
Total	1.61176	15			

Constrained (Type III) sums of squares.

Table B-5 - Pearson Correlation Experimental Data

Simple Statistics						
Variable	N	Mean	Std Dev	Sum	Minimum	Maximum
COPx_tot_dist	21	335.27903	129.3022	7041	192.72509	685.84465
COPx_max	21	-26.23904	47.23038	-551.01974	-119.01983	55.33674
COPx_min	21	-52.68668	46.42976	-1106	-138.28983	37.28125
COP_range_AP	21	26.44765	8.58197	555.40056	14.06401	43.03448
vel_mean_x	21	11.1934	4.3137	235.06136	6.44478	22.87773
peak_COP_speed_x	21	65.42324	23.76267	1374	30.7014	126.37068
acc_mean_x	21	227.81889	71.63565	4784	124.97204	430.3234
peak_COP_acc_x	21	1635	760.6892	34343	648.29998	3176
RMS_COP_x	21	4.26063	1.57265	89.47318	2.27418	7.67118
MedFREQ	21	0.45315	0.1393	9.51614	0.16586	0.80081

Pearson Correlation Coefficients, N = 21										
	COPx_tot_dist	COPx_max	COPx_min	COP_range_AP	vel_mean_x	peak_COP_speed_x	acc_mean_x	peak_COP_acc_x	RMS_COP_x	MedFREQ
COPx_tot_dist	1	0.12725	0.01634	0.61191	1	0.89009	0.73462	0.43628	0.39964	0.63993
		0.5826	0.944	0.0032	<.0001	<.0001	0.0001	0.048	0.0727	0.0018
COPx_max	0.12725	1	0.98335	0.18335	0.12647	0.19028	-0.14839	0.22552	0.18718	-0.13389
	0.5826		<.0001	0.4263	0.5849	0.4087	0.5209	0.3256	0.4165	0.5629
COPx_min	0.01634	0.98335	1	0.00168	0.01558	0.08952	-0.23839	0.14969	0.023	-0.10515
	0.944	<.0001		0.9942	0.9466	0.6996	0.298	0.5172	0.9212	0.6501
COP_range_AP	0.61191	0.18335	0.00168	1	0.61173	0.56288	0.47311	0.43128	0.90571	-0.16796
	0.0032	0.4263	0.9942		0.0032	0.0079	0.0303	0.0509	<.0001	0.4668
vel_mean_x	1	0.12647	0.01558	0.61173	1	0.89008	0.7359	0.43721	0.3996	0.6401
	<.0001	0.5849	0.9466	0.0032		<.0001	0.0001	0.0475	0.0727	0.0018
peak_COP_speed_x	0.89009	0.19028	0.08952	0.56288	0.89008	1	0.65448	0.54413	0.3616	0.55335
	<.0001	0.4087	0.6996	0.0079	<.0001		0.0013	0.0108	0.1073	0.0093
acc_mean_x	0.73462	-0.14839	-0.23839	0.47311	0.7359	0.65448	1	0.65265	0.37374	0.4456
	0.0001	0.5209	0.298	0.0303	0.0001	0.0013		0.0013	0.0951	0.0429
peak_COP_acc_x	0.43628	0.22552	0.14969	0.43128	0.43721	0.54413	0.65265	1	0.52262	0.05041
	0.048	0.3256	0.5172	0.0509	0.0475	0.0108	0.0013		0.0151	0.8282
RMS_COP_x	0.39964	0.18718	0.023	0.90571	0.3996	0.3616	0.37374	0.52262	1	-0.40064
	0.0727	0.4165	0.9212	<.0001	0.0727	0.1073	0.0951	0.0151		0.0719
MedFREQ	0.63993	-0.13389	-0.10515	-0.16796	0.6401	0.55335	0.4456	0.05041	-0.40064	1
	0.0018	0.5629	0.6501	0.4668	0.0018	0.0093	0.0429	0.8282	0.0719	

Table B-6 - Pearson Correlation Model Base Set Data

Simple Statistics						
Variable	N	Mean	Std Dev	Sum	Minimum	Maximum
COPx_tot_dist	21	430.49746	108.86464	9040	319.13501	775.0856
COPx_max	21	12.33966	3.6048	259.1329	6.5051	22.1573
COPx_min	21	-7.00203	3.69745	-147.04266	-12.59497	-0.00361
COP_range_AP	21	19.34169	3.33174	406.17556	14.28069	27.98317
vel_mean_x	21	14.35772	3.62669	301.51203	10.64863	25.83811
peak_COP_speed_x	21	51.36944	11.34146	1079	36.53758	79.52939
acc_mean_x	21	193.02083	10.64192	4053	181.96785	228.09103
peak_COP_acc_x	21	883.79897	89.11377	18560	767.77411	1144
RMS_COP_x	21	3.10393	0.58968	65.18251	2.38201	4.73958
MedFREQ	21	0.57043	0.15732	11.97901	0.2706	0.84191

Pearson Correlation Coefficients, N = 21										
	COPx_tot_dist	COPx_max	COPx_min	COP_range_AP	vel_mean_x	peak_COP_speed_x	acc_mean_x	peak_COP_acc_x	RMS_COP_x	MedFREQ
COPx_tot_dist	1	0.34033	-0.36561	0.77396	1	0.78842	0.91049	0.31459	0.86575	0.46804
		0.1312	0.1031	<.0001	<.0001	<.0001	<.0001	0.1649	<.0001	0.0324
COPx_max	0.34033	1	0.5839	0.43396	0.34061	0.18338	0.29408	-0.10826	0.44025	-0.54433
	0.1312		0.0055	0.0494	0.1308	0.4262	0.1957	0.6404	0.0458	0.0107
COPx_min	-0.36561	0.5839	1	-0.47801	-0.36543	-0.47292	-0.3579	-0.12139	-0.34877	-0.83649
	0.1031	0.0055		0.0284	0.1033	0.0304	0.1112	0.6002	0.1213	<.0001
COP_range_AP	0.77396	0.43396	-0.47801	1	0.77406	0.72324	0.71537	0.01758	0.86338	0.33936
	<.0001	0.0494	0.0284		<.0001	0.0002	0.0003	0.9397	<.0001	0.1323
vel_mean_x	1	0.34061	-0.36543	0.77406	1	0.78878	0.91037	0.31474	0.86579	0.46793
	<.0001	0.1308	0.1033	<.0001		<.0001	<.0001	0.1646	<.0001	0.0324
peak_COP_speed_x	0.78842	0.18338	-0.47292	0.72324	0.78878	1	0.79496	0.46653	0.62643	0.57756
	<.0001	0.4262	0.0304	0.0002	<.0001		<.0001	0.033	0.0024	0.0061
acc_mean_x	0.91049	0.29408	-0.3579	0.71537	0.91037	0.79496	1	0.31017	0.76373	0.43087
	<.0001	0.1957	0.1112	0.0003	<.0001	<.0001		0.1712	<.0001	0.0512
peak_COP_acc_x	0.31459	-0.10826	-0.12139	0.01758	0.31474	0.46653	0.31017	1	0.03444	0.28172
	0.1649	0.6404	0.6002	0.9397	0.1646	0.033	0.1712		0.8822	0.216
RMS_COP_x	0.86575	0.44025	-0.34877	0.86338	0.86579	0.62643	0.76373	0.03444	1	0.31563
	<.0001	0.0458	0.1213	<.0001	<.0001	0.0024	<.0001	0.8822		0.1634
MedFREQ	0.46804	-0.54433	-0.83649	0.33936	0.46793	0.57756	0.43087	0.28172	0.31563	1
	0.0324	0.0107	<.0001	0.1323	0.0324	0.0061	0.0512	0.216	0.1634	

Appendix C : Modelling Parkinson's disease

EYES CLOSED TRIALS	HC (n = 21)		PD (n = 23)	
	mean	std	mean	std
COP Total Distance AP	335.28	129.30	671.01	477.61
COP Range AP	26.45	8.58	40.70	17.55
RMS COP AP	4.26	1.53	6.28	2.47
Med Freq AP	0.45	0.14	0.54	0.20
Peak Speed AP	65.42	23.19	128.42	80.15
Mean Speed AP	11.19	4.21	22.12	15.63

Table C-1 - Experimental Data means and standard deviations.

HCEC Trap Range		
	ECHC Below	ECHC Above
COPx_tot_dist	205.98	464.58
COP_range_AP	17.87	35.03
vel_mean_x	6.98	15.40
peak_COP_speed_x	42.23	88.61
RMS_COP_x	2.73	5.80
MedFREQ	0.32	0.59

Table C-2 - Trap Ranges for Healthy Control Eyes Closed based +/- 1 standard deviation of the mean.

PDEC Trap Range		
	ECPD Below	ECPD Above
COPx_tot_dist	193.40	1148.63
COP_range_AP	23.15	58.25
vel_mean_x	6.49	37.75
peak_COP_speed_x	48.27	208.57
RMS_COP_x	3.80	8.75
MedFREQ	0.34	0.74

Table C-3 Trap ranges for Parkinson's disease eyes closed +/- 1 standard deviation of the mean.

Standard Deviation Cut				
	Actual Value		% change from base value	
	Min	Max	Min	Max
T2	0.12642	0.14994	-14%	2%
Kp	15.652	22.36	-30%	0%
Kd	5.471154	7.71573	-22%	10%
Kn	629.244	1887.732	-20%	140%

Table C-4 - This range was decided by cthe values of interest within 1 std +/- the outer bounds of HC and PD. If 3/5 of the parameters are useful the test set was kept.

Mean Responses - T2									
% Change from Base	-14	-12	-10	-8	-6	-4	-2	0	2
COPx_tot_dist	208.1251	224.5715	253.9983	260.4249	249.7762	288.7569	370.8584	423.1563	722.1128
COP_range_AP	15.13357	13.85478	16.26791	15.29809	14.94051	15.42241	16.20374	17.30562	26.64811
vel_mean_x	6.951156	7.498191	8.477778	8.689972	8.337087	9.633892	12.36862	14.11126	24.07706
peak_COP_speed_x	31.68969	31.90908	35.11235	32.70827	32.92307	40.8459	45.77526	50.16382	73.99716
RMS_COP_x	3.060136	2.518515	2.972054	2.577389	2.554628	2.581164	2.465494	2.818765	4.671869
MedFREQ	0.33893	0.385456	0.309671	0.475774	0.418156	0.511464	0.551112	0.670027	0.6831

Table C-5- Healthy Control standard deviation comparative analysis for T_2. Yellow shows the COP model measures within the HC boundaries.

Mean responses - T2									
% Change from Base	-14	-12	-10	-8	-6	-4	-2	0	2
COPx_tot_dist	208.1251	224.5715	253.9983	260.4249	249.7762	288.7569	370.8584	423.1563	722.1128
COP_range_AP	15.13357	13.85478	16.26791	15.29809	14.94051	15.42241	16.20374	17.30562	26.64811
vel_mean_x	6.951156	7.498191	8.477778	8.689972	8.337087	9.633892	12.36862	14.11126	24.07706
peak_COP_speed_x	31.68969	31.90908	35.11235	32.70827	32.92307	40.8459	45.77526	50.16382	73.99716
RMS_COP_x	3.060136	2.518515	2.972054	2.577389	2.554628	2.581164	2.465494	2.818765	4.671869
MedFREQ	0.33893	0.385456	0.309671	0.475774	0.418156	0.511464	0.551112	0.670027	0.6831

Table C-6- Parkinson's disease standard deviation comparative analysis for T_2. Yellow shows the COP model measures within the PD boundaries.

Mean Responses - Kp							
% Change from Base	-30	-25	-20	-15	-10	-5	0
COPx_tot_dist	196.9182	207.9197	221.4098	237.558	268.9184	310.2241	423.1563
COP_range_AP	22.19892	18.79538	16.82534	15.98013	13.84801	18.00883	17.30562
vel_mean_x	6.577301	6.941394	7.392608	7.930273	8.976166	10.34992	14.11126
peak_COP_speed_x	31.00551	30.94845	29.97112	33.89045	34.86773	40.97956	50.16382
RMS_COP_x	5.000829	3.492239	3.302433	2.80522	2.299126	2.916659	2.818765
MedFREQ	0.204029	0.209657	0.261418	0.307657	0.395423	0.410547	0.670027

Table C-7- Healthy Control standard deviation comparative analysis for K_p. Yellow shows the COP model measures within the HC boundaries.

Mean Responses -Kp							
% Change from Base	-30	-25	-20	-15	-10	-5	0
COPx_tot_dist	196.9182	207.9197	221.4098	237.558	268.9184	310.2241	423.1563
COP_range_AP	22.19892	18.79538	16.82534	15.98013	13.84801	18.00883	17.30562
vel_mean_x	6.577301	6.941394	7.392608	7.930273	8.976166	10.34992	14.11126
peak_COP_speed_x	31.00551	30.94845	29.97112	33.89045	34.86773	40.97956	50.16382
RMS_COP_x	5.000829	3.492239	3.302433	2.80522	2.299126	2.916659	2.818765
MedFREQ	0.204029	0.209657	0.261418	0.307657	0.395423	0.410547	0.670027

Table C-8– Parkinson's disease standard deviation comparative analysis for K_p. Yellow shows the COP model measures within the PD boundaries.

Mean Responses - Kd																	
% Change from Base	-22	-20	-18	-16	-14	-12	-10	-8	-6	-4	-2	0	2	4	6	8	10
COPx_tot_dist	710.6392	462.9235	443.7713	451.6464	473.2519	341.9627	321.9697	431.2593	404.0572	384.209	347.2363	423.1563	451.7099	464.6545	671.3459	619.8931	837.8731
COP_range_AP	33.5716	22.82567	23.71229	22.88474	22.23703	17.30951	17.32457	19.96397	17.59103	21.05666	18.19221	17.30562	19.54866	20.89516	27.10286	24.41521	31.32888
vel_mean_x	23.69286	15.43965	14.79859	15.0589	15.78059	11.40807	10.74015	14.38086	13.47458	12.81678	11.58238	14.11126	15.06377	15.49683	22.38425	20.67236	27.93545
peak_COP_speed_x	77.33103	56.03319	51.84074	54.46686	55.17699	47.74448	43.57515	52.40624	50.56433	50.48444	42.65488	50.16382	54.93463	55.75039	73.59197	66.37702	93.71924
RMS_COP_x	5.720197	3.673234	4.293734	3.679272	3.563977	2.631628	2.877989	3.259366	3.008044	3.506951	2.987007	2.818765	2.986446	3.358773	4.439147	4.550711	5.126685
MedFREQ	0.622712	0.618933	0.451886	0.532632	0.652962	0.550747	0.435194	0.656636	0.560982	0.446301	0.511757	0.670027	0.63709	0.680433	0.694621	0.595423	0.720804

Table C-9- Healthy Control standard deviation comparative analysis for K_d. Yellow shows the COP model measures within the HC boundaries.

Mean Responses - Kd																	
% Change from Base	-22	-20	-18	-16	-14	-12	-10	-8	-6	-4	-2	0	2	4	6	8	10
COPx_tot_dist	710.6392	462.9235	443.7713	451.6464	473.2519	341.9627	321.9697	431.2593	404.0572	384.209	347.2363	423.1563	451.7099	464.6545	671.3459	619.8931	837.8731
COP_range_AP	33.5716	22.82567	23.71229	22.88474	22.23703	17.30951	17.32457	19.96397	17.59103	21.05666	18.19221	17.30562	19.54866	20.89516	27.10286	24.41521	31.32888
vel_mean_x	23.69286	15.43965	14.79859	15.0589	15.78059	11.40807	10.74015	14.38086	13.47458	12.81678	11.58238	14.11126	15.06377	15.49683	22.38425	20.67236	27.93545
peak_COP_speed_x	77.33103	56.03319	51.84074	54.46686	55.17699	47.74448	43.57515	52.40624	50.56433	50.48444	42.65488	50.16382	54.93463	55.75039	73.59197	66.37702	93.71924
RMS_COP_x	5.720197	3.673234	4.293734	3.679272	3.563977	2.631628	2.877989	3.259366	3.008044	3.506951	2.987007	2.818765	2.986446	3.358773	4.439147	4.550711	5.126685
MedFREQ	0.622712	0.618933	0.451886	0.532632	0.652962	0.550747	0.435194	0.656636	0.560982	0.446301	0.511757	0.670027	0.63709	0.680433	0.694621	0.595423	0.720804

Table C-10- Parkinson's disease standard deviation comparative analysis for K_d. Yellow shows the COP model measures within the PD boundaries.

Mean Responses - Kn									
% Change from Base	-20	0	20	40	60	80	100	120	140
COPx_tot_dist	363.2997	423.1563	549.264	540.9071	621.799	778.9071	818.9337	998.3606	1036.325
COP_range_AP	17.41499	17.30562	24.04563	24.00907	28.17428	34.78331	38.31037	47.41199	44.13937
vel_mean_x	12.11514	14.11126	18.31621	18.03672	20.74128	25.9732	27.31583	33.29254	34.5607
peak_COP_speed_x	46.57029	50.16382	68.38665	68.3609	79.17955	95.59689	105.7955	113.6312	113.2787
RMS_COP_x	3.114523	2.818765	3.778058	3.73018	4.474135	5.720114	6.23339	8.001278	7.620637
MedFREQ	0.478722	0.670027	0.701821	0.618097	0.55501	0.545376	0.493926	0.538785	0.562963

Table C-11 - Healthy Control standard deviation comparative analysis for K_n. Yellow shows the COP model measures within the HC boundaries.

Mean Responses - Kn									
% Change	-20	0	20	40	60	80	100	120	140
COPx_tot_dist	363.2997	423.1563	549.264	540.9071	621.799	778.9071	818.9337	998.3606	1036.325
COP_range_AP	17.41499	17.30562	24.04563	24.00907	28.17428	34.78331	38.31037	47.41199	44.13937
vel_mean_x	12.11514	14.11126	18.31621	18.03672	20.74128	25.9732	27.31583	33.29254	34.5607
peak_COP_speed_x	46.57029	50.16382	68.38665	68.3609	79.17955	95.59689	105.7955	113.6312	113.2787
RMS_COP_x	3.114523	2.818765	3.778058	3.73018	4.474135	5.720114	6.23339	8.001278	7.620637
MedFREQ	0.478722	0.670027	0.701821	0.618097	0.55501	0.545376	0.493926	0.538785	0.562963

Table C-12 - Parkinson's standard deviation comparative analysis for K_n. Yellow shows the COP model measures within the PD boundaries.

Mean Responses - T2									
% Change from base	-14	-12	-10	-8	-6	-4	-2	0	2
COPx_tot_dist	208.1251	224.5715	253.9983	260.4249	249.7762	288.7569	370.8584	423.1563	722.1128
COP_range_AP	15.13357	13.85478	16.26791	15.29809	14.94051	15.42241	16.20374	17.30562	26.64811
vel_mean_x	6.951156	7.498191	8.477778	8.689972	8.337087	9.633892	12.36862	14.11126	24.07706
peak_COP_speed_x	31.68969	31.90908	35.11235	32.70827	32.92307	40.8459	45.77526	50.16382	73.99716
RMS_COP_x	3.060136	2.518515	2.972054	2.577389	2.554628	2.581164	2.465494	2.818765	4.671869
MedFREQ	0.33893	0.385456	0.309671	0.475774	0.418156	0.511464	0.551112	0.670027	0.6831

Table C-13- Healthy control ANOVA analysis for T_2. Yellow shows COP model measures not significantly different from the HC group.

Mean Responses - T2									
% Change from base	-14	-12	-10	-8	-6	-4	-2	0	2
COPx_tot_dist	208.1251	224.5715	253.9983	260.4249	249.7762	288.7569	370.8584	423.1563	722.1128
COP_range_AP	15.13357	13.85478	16.26791	15.29809	14.94051	15.42241	16.20374	17.30562	26.64811
vel_mean_x	6.951156	7.498191	8.477778	8.689972	8.337087	9.633892	12.36862	14.11126	24.07706
peak_COP_speed_x	31.68969	31.90908	35.11235	32.70827	32.92307	40.8459	45.77526	50.16382	73.99716
RMS_COP_x	3.060136	2.518515	2.972054	2.577389	2.554628	2.581164	2.465494	2.818765	4.671869
MedFREQ	0.33893	0.385456	0.309671	0.475774	0.418156	0.511464	0.551112	0.670027	0.6831

Table C-14– Parkinson's disease ANOVA analysis for T_2. Yellow shows COP model measures not significantly different from the PD group.

Mean Responses - Kp							
% Change	-30	-25	-20	-15	-10	-5	0
COPx_tot	196.9182	207.9197	221.4098	237.558	268.9184	310.2241	423.1563
COP_rang	22.19892	18.79538	16.82534	15.98013	13.84801	18.00883	17.30562
vel_mean	6.577301	6.941394	7.392608	7.930273	8.976166	10.34992	14.11126
peak_COP	31.00551	30.94845	29.97112	33.89045	34.86773	40.97956	50.16382
RMS_COP	5.000829	3.492239	3.302433	2.80522	2.299126	2.916659	2.818765
MedFREQ	0.204029	0.209657	0.261418	0.307657	0.395423	0.410547	0.670027

Table C-15 - Healthy control ANOVA analysis for K_p. Yellow shows COP model measures not significantly different from the HC group.

Mean Responses - Kp							
% Change	-30	-25	-20	-15	-10	-5	0
COPx_tot	196.9182	207.9197	221.4098	237.558	268.9184	310.2241	423.1563
COP_rang	22.19892	18.79538	16.82534	15.98013	13.84801	18.00883	17.30562
vel_mean	6.577301	6.941394	7.392608	7.930273	8.976166	10.34992	14.11126
peak_COP	31.00551	30.94845	29.97112	33.89045	34.86773	40.97956	50.16382
RMS_COP	5.000829	3.492239	3.302433	2.80522	2.299126	2.916659	2.818765
MedFREQ	0.204029	0.209657	0.261418	0.307657	0.395423	0.410547	0.670027

Table C-16- Parkinson's disease ANOVA analysis for K_p. Yellow shows COP model measures not significantly different from the PD group.

Mean Responses - Kd																	
% Change frome Base	-22	-20	-18	-16	-14	-12	-10	-8	-6	-4	-2	0	2	4	6	8	10
COPx_tot_dist	710.6392	462.9235	443.7713	451.6464	473.2519	341.9627	321.9697	431.2593	404.0572	384.209	347.2363	423.1563	451.7099	464.6545	671.3459	619.8931	837.8731
COP_range_AP	33.5716	22.82567	23.71229	22.88474	22.23703	17.30951	17.32457	19.96397	17.59103	21.05666	18.19221	17.30562	19.54866	20.89516	27.10286	24.41521	31.32888
vel_mean_x	23.69286	15.43965	14.79859	15.0589	15.78059	11.40807	10.74015	14.38086	13.47458	12.81678	11.58238	14.11126	15.06377	15.49683	22.38425	20.67236	27.93545
peak_COP_speed_x	77.33103	56.03319	51.84074	54.46686	55.17699	47.74448	43.57515	52.40624	50.56433	50.48444	42.65488	50.16382	54.93463	55.75039	73.59197	66.37702	93.71924
RMS_COP_x	5.720197	3.673234	4.293734	3.679272	3.563977	2.631628	2.877989	3.259366	3.008044	3.506951	2.987007	2.818765	2.986446	3.358773	4.439147	4.550711	5.126685
MedFREQ	0.622712	0.618933	0.451886	0.532632	0.652962	0.550747	0.435194	0.656636	0.560982	0.446301	0.511757	0.670027	0.63709	0.680433	0.694621	0.595423	0.720804

Table C-17- Healthy control ANOVA analysis for K_d. Yellow shows COP model measures not significantly different from the HC group.

Mean Responses - Kd																	
% Change from base	-22	-20	-18	-16	-14	-12	-10	-8	-6	-4	-2	0	2	4	6	8	10
COPx_tot_dist	710.6392	462.9235	443.7713	451.6464	473.2519	341.9627	321.9697	431.2593	404.0572	384.209	347.2363	423.1563	451.7099	464.6545	671.3459	619.8931	837.8731
COP_range_AP	33.5716	22.82567	23.71229	22.88474	22.23703	17.30951	17.32457	19.96397	17.59103	21.05666	18.19221	17.30562	19.54866	20.89516	27.10286	24.41521	31.32888
vel_mean_x	23.69286	15.43965	14.79859	15.0589	15.78059	11.40807	10.74015	14.38086	13.47458	12.81678	11.58238	14.11126	15.06377	15.49683	22.38425	20.67236	27.93545
peak_COP_speed_x	77.33103	56.03319	51.84074	54.46686	55.17699	47.74448	43.57515	52.40624	50.56433	50.48444	42.65488	50.16382	54.93463	55.75039	73.59197	66.37702	93.71924
RMS_COP_x	5.720197	3.673234	4.293734	3.679272	3.563977	2.631628	2.877989	3.259366	3.008044	3.506951	2.987007	2.818765	2.986446	3.358773	4.439147	4.550711	5.126685
MedFREQ	0.622712	0.618933	0.451886	0.532632	0.652962	0.550747	0.435194	0.656636	0.560982	0.446301	0.511757	0.670027	0.63709	0.680433	0.694621	0.595423	0.720804

Table C-18- Parkinson's disease ANOVA analysis for K_d. Yellow shows COP model measures not significantly different from the PD group.

Mean Responses - Kn									
% Change from Base	-20	0	20	40	60	80	100	120	140
COPx_tot_dist	363.2997	423.1563	549.264	540.9071	621.799	778.9071	818.9337	998.3606	1036.325
COP_range_AP	17.41499	17.30562	24.04563	24.00907	28.17428	34.78331	38.31037	47.41199	44.13937
vel_mean_x	12.11514	14.11126	18.31621	18.03672	20.74128	25.9732	27.31583	33.29254	34.5607
peak_COP_speed_x	46.57029	50.16382	68.38665	68.3609	79.17955	95.59689	105.7955	113.6312	113.2787
RMS_COP_x	3.114523	2.818765	3.778058	3.73018	4.474135	5.720114	6.23339	8.001278	7.620637
MedFREQ	0.478722	0.670027	0.701821	0.618097	0.55501	0.545376	0.493926	0.538785	0.562963

Table C-19- Healthy control ANOVA analysis for K_n. Yellow shows COP model measures not significantly different from the HC group.

Mean Responses - Kn									
% Change from Base	-20	0	20	40	60	80	100	120	140
COPx_tot_dist	363.2997	423.1563	549.264	540.9071	621.799	778.9071	818.9337	998.3606	1036.325
COP_range_AP	17.41499	17.30562	24.04563	24.00907	28.17428	34.78331	38.31037	47.41199	44.13937
vel_mean_x	12.11514	14.11126	18.31621	18.03672	20.74128	25.9732	27.31583	33.29254	34.5607
peak_COP_speed_x	46.57029	50.16382	68.38665	68.3609	79.17955	95.59689	105.7955	113.6312	113.2787
RMS_COP_x	3.114523	2.818765	3.778058	3.73018	4.474135	5.720114	6.23339	8.001278	7.620637
MedFREQ	0.478722	0.670027	0.701821	0.618097	0.55501	0.545376	0.493926	0.538785	0.562963

Table C-20- Parkinson's disease ANOVA analysis for K_n. Yellow shows COP model measures not significantly different from the PD group.